THE PETROLOGY, DIAGENESIS AND DEPOSITIONAL ENVIRONMENT OF THE BARTLESVILLE SANDSTONE IN THE CUSHING OIL FIELD, CREEK COUNTY, OKLAHOMA

By

ERIK PAUL MASON

Bachelor of Arts

Principia College

Elsah, Illinois

1976

Submitted to the Faculty of the Graduate College
of the Oklahoma State University
in partial fulfillment of the requirements
for the Degree of
MASTER OF SCIENCE
December, 1982

OKLAHOMA STATE UNIVERSITY

THE PETROLOGY, DIAGENESIS AND DEPOSITIONAL ENVIRONMENT OF THE BARTLESVILLE SANDSTONE IN THE CUSHING OIL FIELD, CREEK COUNTY, OKLAHOMA

Thesis Approved:

Zuhair al-Shaieb
Thesis Adviser

Gary F. Stewart

Nowell Donovan

Norman N. Durham
Dean of the Graduate College

ACKNOWLEDGMENTS

I would like to extend my genuine thanks to the following individuals and companies for their support of this study: Dr. Zuhair Al-Shaieb, my adviser, who was the originator of the topic and was a tremendous support throughout the study--always energetic, enthusiastic, and full of ideas. Drs. Gary Stewart and Nowell Donovan made numerous helpful suggestions as to the depositional environment and the construction of the subsurface maps. Dr. John Shelton provided constructive advice about depositional-environment interpretation. Rick May edited the manuscript. Phillips Petroleum Company and Ketal Oil and Production Company permitted the use of their electric-log libraries. The Institute for Energy Analysis (I.E.A.) (and its chairman, Dr. Joe Mize) funded the project. Heinz Hall photographed the cores; ARCO provided the opportunity to describe and sample several of their cores. Grayce Wynd patiently typed the manuscript. A special thanks to Dr. Gary Stewart, who patiently edited the thesis. Laurie Crow gave valuable moral support. Finally, my parents could not have been more helpful, positive and supportive; this study is dedicated to them.

TABLE OF CONTENTS

LIST OF TABLES

LIST OF FIGURES

LIST OF PLATES

ABSTRACT

The Bartlesville Sandstone has been one of the most oil productive sandstones in Oklahoma. In the Cushing Field it has produced more than 350 million barrels of oil since the Bartlesville discovery well was drilled in December, 1913. The emphasis of the study is the diagenetic history of the Bartlesville but the local depositional environments and regional and local tectonic history have been studied in some detail in order to understand better how and when the diagenetic processes took place.

In the study area, the Bartlesville Sandstone was deposited in distributary and alluvial stream channels. Four sand bodies were identified through the use of cores, electric-log signatures and the construction of a suite of subsurface maps. Deposition was influenced by structural geology; the stream channels avoided the crests of the domes that were topographic highs during early Desmoinesian time.

The anticline grew primarily in Early to Middle Pennsylvanian time. Growth may have been related to strike-slip movement (as well as the well documented dip-slip movement) along the Wilzetta Fault, a northeast- to southwest-trending fault that bounds the east side of the field. Thickening of section on the downthrown eastern block has been documented in this study; thus the Wilzetta Fault can also be shown to have "grown," a fact that indicates again, geomorphic influence upon sedimentation of the Bartlesville.

The Bartlesville is subarkosic to arkosic. Potassic feldspar and plagioclase as well as detrital matrix were identified. Authigenic minerals are clays (kaolinite, illite and chlorite), quartz, calcite, siderite, hematite, leucoxene, pyrite, and galena.

To a large degree, the morphology and mineralogic composition of the Bartlesville Sandstone in the Cushing Field have been determined by diagenetic processes. Four general groups of diagenetic features have been recognized and documented by thin-section analysis and scanning-electron microscopy: dissolution features, precipitates, alteration products and replacement features.

Secondary porosity, dominant in this reservoir, is mainly grain molds, oversized pores, and "honeycombed" pores. Micropores and fractures are also present. Primary porosity is relatively rare. Dissolution of feldspars accounted for most of the secondary porosity; evidence of dissolution is most abundant in the coarser-grained facies. This indicates that depositional environments probably had strong influence upon diagenetic processes.

Based on vitrinite reflectance of organic matter contained in the Bartlesville in the Cushing Field, maximal depth of burial is estimated to be nearly 7,000 feet. Organic material indicates that metamorphism was great enough to generate hydrocarbons. The hydrocarbons migrated from west and south, finally accumulating in the Cushing anticline. Generation of hydrocarbons from Pennsylvanian sediments produced CO_2 gas which mixed with pore waters to create carbonic acid and cause the pore fluids to become acidic enough to leach feldspars and precipitate quartz and kaolinite.

CHAPTER I

INTRODUCTION

Location

The subject of this investigation is the Bartlesville Sandstone (Boggy Formation, Desmoinesian Series, Pennsylvanian System) in the Cushing Oil Field, Townships 16, 17, 18 and 19 North; Range 7 East, Creek County, Oklahoma (Figure 1).

Purpose

The purpose of the study was to develop evidence that might explain the complex diagenetic relationships and origins of porosity in the Bartlesville Sandstone of the Cushing Field, and to describe a paragenetic history of the Bartlesville in this area. The Cushing Oil Field was chosen because the Bartlesville has been tremendously productive here but very little work has been done on its reservoir characteristics.

Method of Study

In order to develop evidence that would lead to an understanding of paragenetic history of the reservoir, it was believed that as much as possible had to be known about the sandstone (its petrology and depositional environment), regional and local tectonic history, geometry of the structure (the Cushing anticline) and about the thermal history of

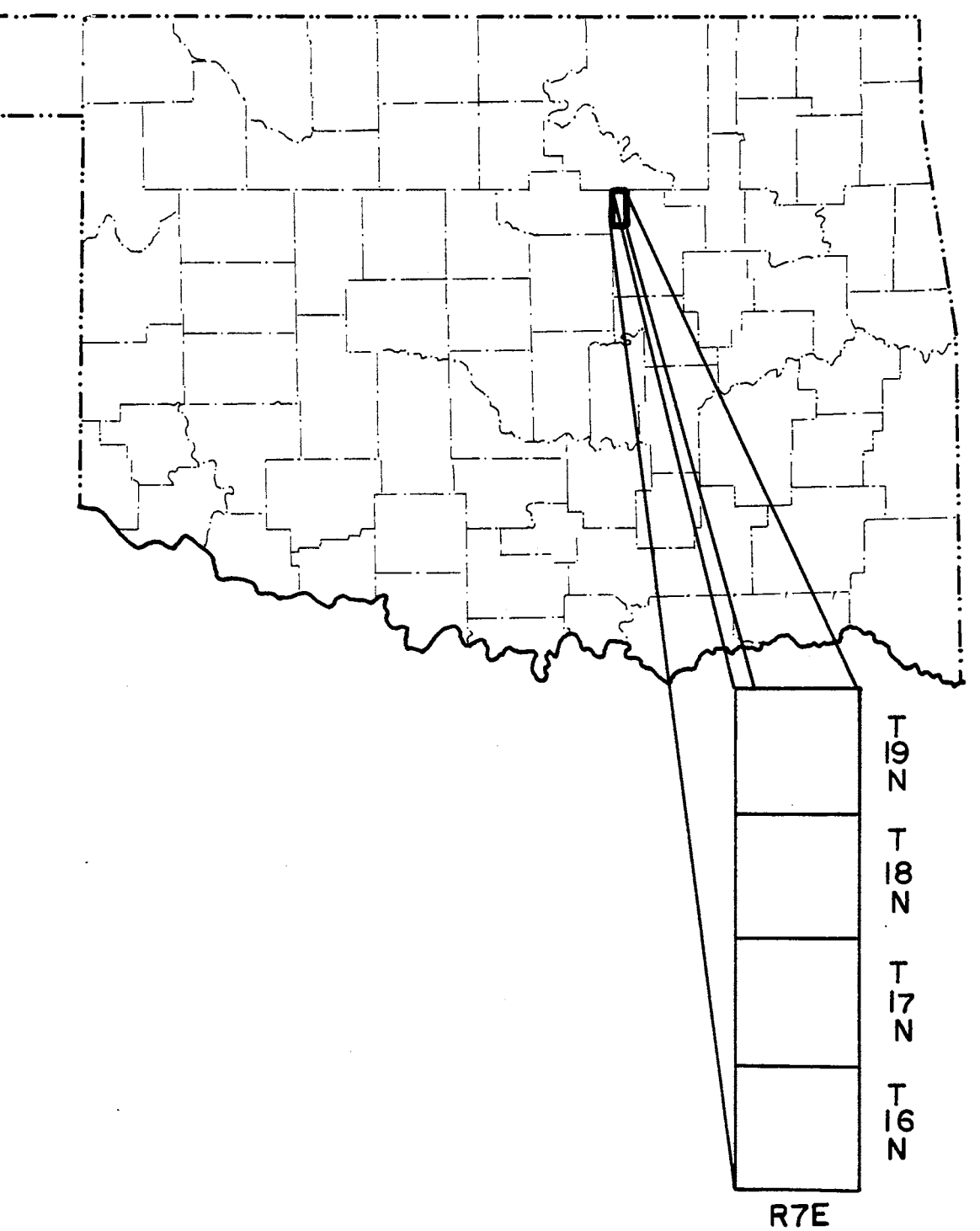

Figure 1. Map Showing Location of the Study Area

the Cherokee Group (which includes the Bartlesville). The methods included:

1. A thorough review of the literature on the Bartlesville Sandstone.

2. Construction of a suite of subsurface maps and cross-sections to define accurately and precisely the structural geology and depositional environment of the Bartlesville in the study area.

3. Description and sampling of nine Bartlesville cores from the Cushing Field.

4. Routine thin-section examination, x-ray diffraction and scanning electron microscopy (equipped with an energy dispersive x-ray analyzer) to document quantitatively the petrology and diagenetic features existing in the reservoir.

5. Compilation of vitrinite reflectance data of organic matter contained within the Bartlesville, to determine the degree of maturation and hydrocarbon generation potential, as well as approximate maximal depth of burial.

6. Sulphur-isotope analysis from pyrite in the Bartlesville, to determine if a hydrocarbon-induced diagenetic aureole exists.

CHAPTER II

HISTORY OF THE CUSHING OIL FIELD

The Cushing Oil Field has a colorful and somewhat extraordinary history. Details of the rapid development of the field and the effects of that development are well-documented in studies by Smith (1913), Buttram (1914), Beal (1917), Bosworth (1920), Wardwell (1927), Bullard (1928), Weirich (1929), and Merritt (1930). Also, an exhaustive study of the southern and central parts of the field was completed by Riggs and others at the U. S. Bureau of Mines in 1958, the purpose being to aid operators in increasing oil recovery from the field. A brief summary of the history of development will be recited here, all of the data having been taken from these reports.

March 10, 1912 was the date of discovery of the Cushing Oil Field; production initially was from an upper zone in the Oswego (Wheeler) Limestone (Desmoinesian Series, Pennsylvanian System). Initial production from these early wells was as much as 2,000 barrels of oil per day (BOPD). A more important discovery however, the first Bartlesville Sand (Desmoinesian Series, Pennsylvanian System) completion, took place in December, 1913. The Bartlesville quickly became the largest producer of oil in the field. At one time, 160 Bartlesville wells yielded 160,000 BOPD. Figure 2 indicates how tremendously productive this sand was. Note the direct relationship between large initial production rates and structural highs.

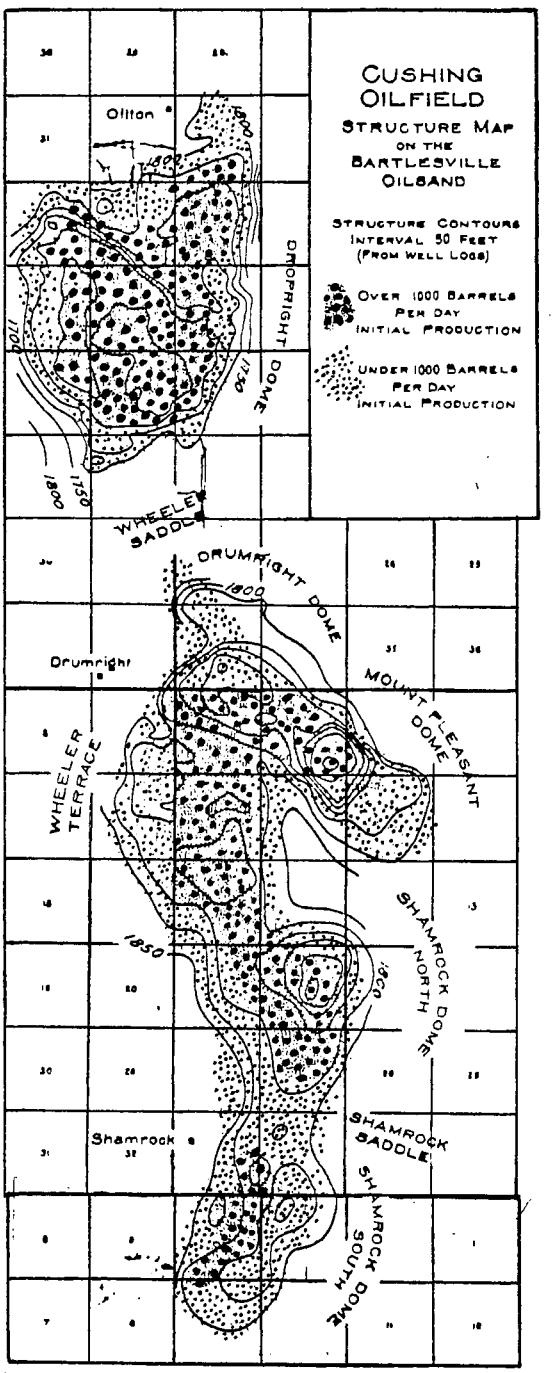

Figure 2. Combined Structure and Initial Production Map on the Bartlesville Sand (from C. Beal, 1917)

Peak production from all of the zones in the field occurred in 1915 at a phenomenal rate of more than 300,000 BOPD (Wardwell, 1927). So great was the amount of production from the field that the oil market was broken and, according to Riggs (1958, p. 9), "a drop in price from $1.05 in February, 1914 to a low of $.40 per barrel in the summer of 1915" resulted. Eleven producing formations ultimately were discovered: the Arbuckle Dolomite, Simpson Sands, Misener Sand, Bartlesville Sand, Red Fork Sand, Skinner Sand, Prue Sand, Oswego (Wheeler) Limestone, Cleveland Sand, Jones Sand, and Layton Sand.

In addition to oil, natural gas also was abundant. For a short period of time in 1916, many millions of cubic feet of gas were produced daily. Enormous quantities of gas were wasted, especially during 1913 and 1914 when hundreds of millions of cubic feet of gas were flared. Operators invariably were interested in reaching the big oil pay in the Bartlesville, because there was just no market for natural gas. This huge amount of gas wastage eventually resulted in the passage of a law by the state legislature requiring that "all wells in the state that produced over two million cubic feet of gas daily be capped until a market was available for the gas" (Riggs, 1958, p. 10). This tremendous amount of gas escapage also led to experimentation by the Bureau of Mines Engineers in the use of "mud" in the annulus of a hole in order to keep the fluids and gas in their respective formations. These experiments in the Cushing Field proved successful and the practice of "mudding-up the string" became commonplace.

Surely one of the most colorful portrayals of the history of the Cushing Field is contained in a film entitled, "How Millionaires Are Made." Filmed to encourage investors to support drilling in the area,

the movie depicts the rapid development and tremendous numbers of wells that had already been drilled up to 1915. Copies of this film were sent to various people within Oklahoma and throughout the country.

Zones of Production

At one time or another oil and/or gas has been produced from eleven different zones in the Cushing Field. To date, cumulative production is more than 500 million barrels of oil and an unknown but large amount of natural gas.

The Bartlesville has yielded nearly 400 million barrels of oil, with production by way of water flooding, continuing until today (Figure 3). Other major producing zones in the field are the Layton Sandstone (Coffeyville Formation, Skiatook Group, Missourian Series Pennsylvanian System), Simpson Sands (Ordovician System), and Oswego (or Wheeler) Limestone (Marmaton Group, Desmoinesian Series, Pennsylvanian System). Production from these zones accounts for more than 95 percent of the oil produced from the field. The remaining five percent came from seven zones ranging from Cambro-Ordovician to mid-Pennsylvanian (Figure 4).

As might be expected, several of the zones in the Cushing Field have been waterflooded extensively. The history and success of waterflooding in the field up until 1955 have been reviewed by Riggs and others (1958). Waterflooding continues to the present date; ARCO, Getty, Mobil, and Union Oil Companies are major operators of the floods.

Regional Tectonic Setting

The area of study is located on the Central Oklahoma or "Cherokee" Platform (Figure 5). To the west is the Nemaha Ridge, to the east

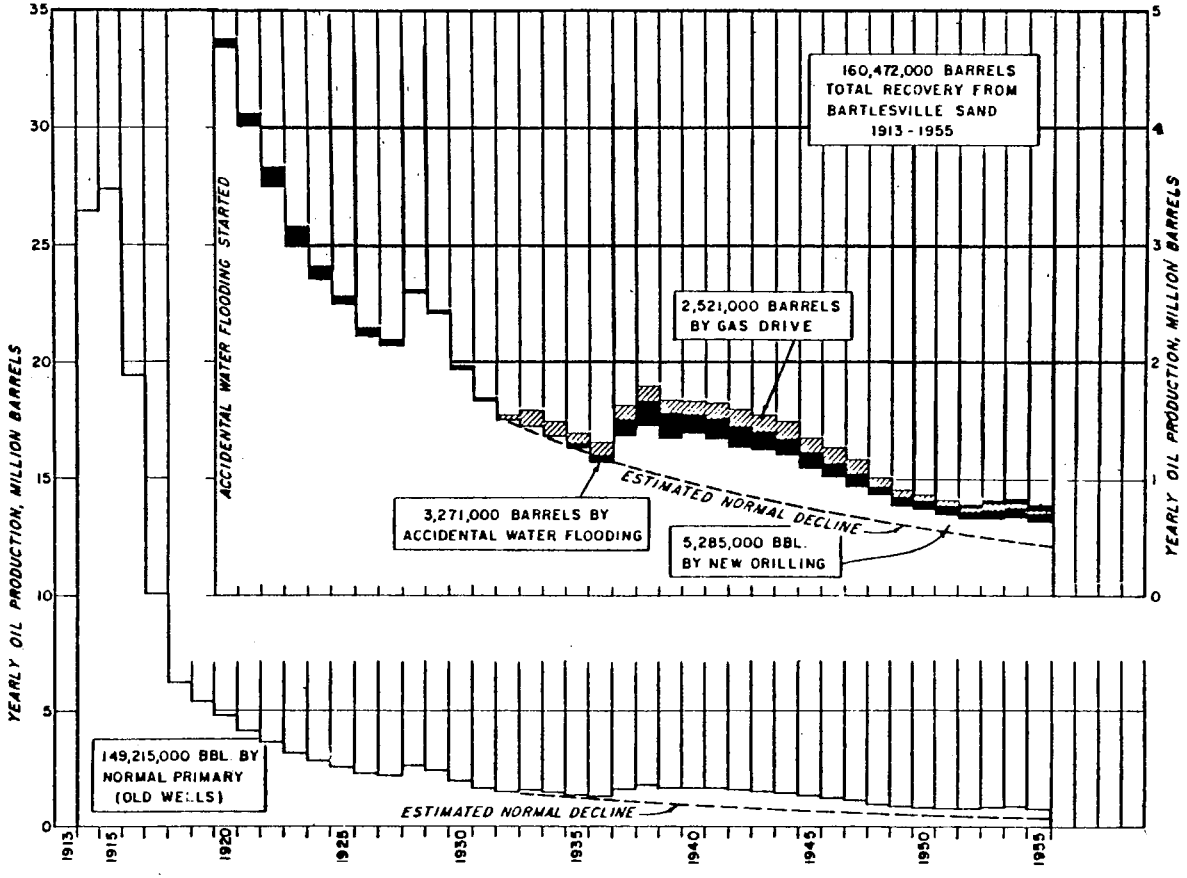

Figure 3. Total Yearly Production from the Bartlesville Sand in the Cushing Oil Field up to 1956 (modified from Riggs et al., 1958)

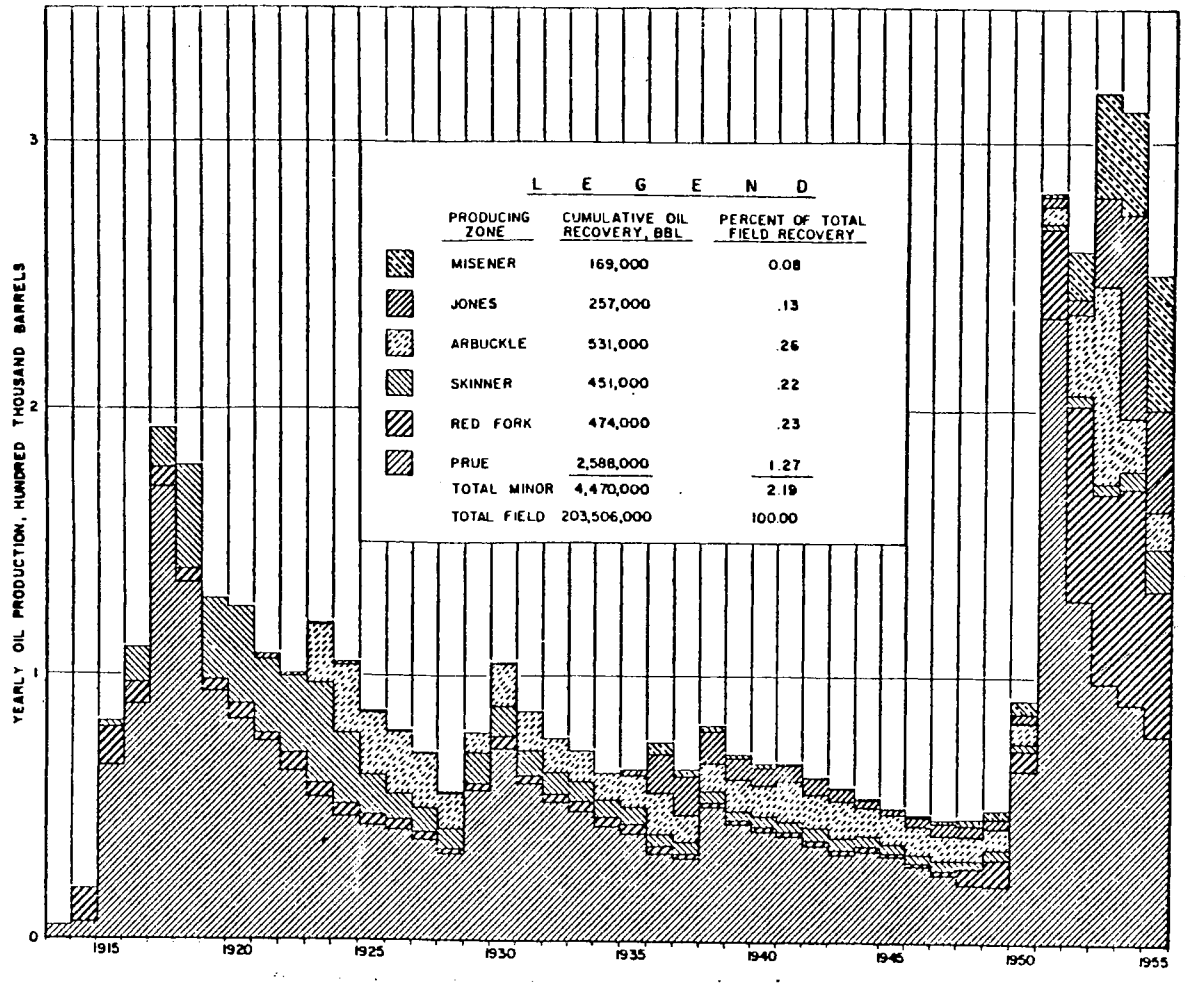

Figure 4. Minor Producing Zones in Cushing Oil Field up to 1956 (from Riggs et al., 1958)

the Ozark Dome, the Arkoma (or McAlester) basin is to the southeast.

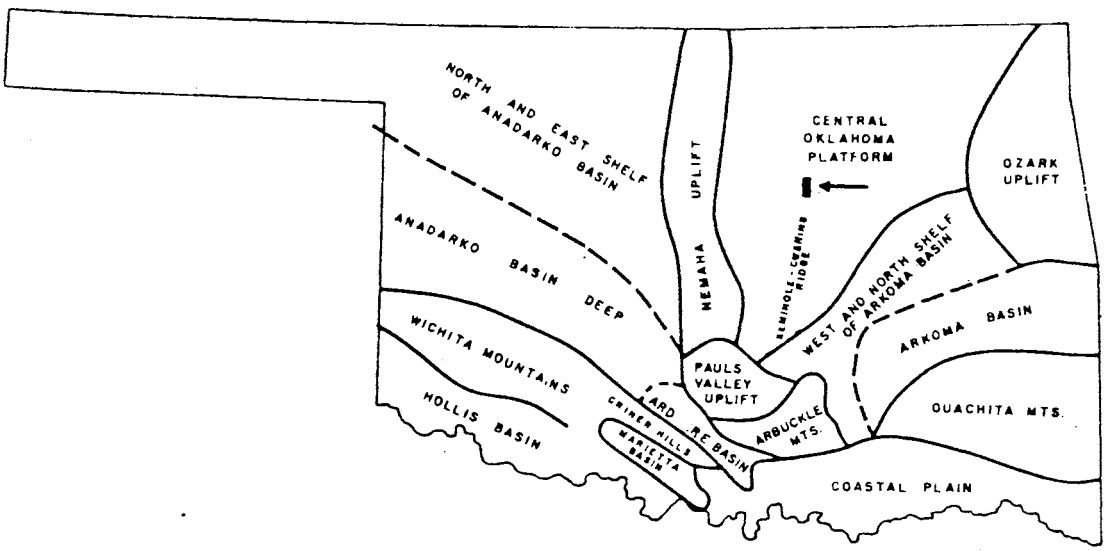

Figure 5. Tectonic Map of Oklahoma (modified from Koff, 1979)

The Central Oklahoma Platform, a generally stable area, is continuous with the Cherokee basin of Kansas. The Cherokee strata of the platform have a largely homoclinal dip of 25 to 80 feet per mile (Dalton, 1960; Hanke, 1967; Saitta, 1968; Phares, 1969). Numerous local structures interrupt this homoclinal dip along the platform, one of which is the Cushing anticline.

To the west of the platform, the Nemaha Ridge is a north-trending zone of highly fractured, faulted and uplifted features (Koff, 1978; Luza and Lawson, 1981) extending from Nebraska to a southern terminus at the Oklahoma City Uplift. These crustal blocks are generally three to five miles long and five to twenty miles wide; they generally are bounded by faults on the east side that are downthrown to the east

(Luza and Lawson, 1981, p. 16). Depths to crystalline basement rock range from 200 feet in Kansas to nearly 7,000 feet in the area of the Oklahoma City Uplift (Koff, 1979). In Kansas and northern Oklahoma, Pennsylvanian Desmoinesian sediments directly overlie Precambrian crystalline rocks along the axis of the ridge.

South of the Central Oklahoma Platform is the Arkoma Basin, the site of a thick Pennsylvanian section of rocks (more than 20,000 feet of sediment). Along the original basin axis Pennsylvanian rocks of Morrowan age conformably overlie Mississippian Chesterian aged rocks. This sedimentary section thins abruptly northward until the "hinge line" separating the steep basin slope from the gently dipping Central Oklahoma Platform is reached. This hinge line trends northeastward from the Pauls Valley Uplift to the Ozark Uplift along the line separating the west and north shelf of the Arkoma Basin from the Central Oklahoma Platform (Figure 5). North of the hinge line the sedimentary section thins more gradually.

East of the Central Oklahoma Platform, the Ozark Dome or Oklahoma Geanticline is present as a very large, broad positive element in Northeast Oklahoma, southeast Kansas, and western Missouri.

CHAPTER IV

GEOLOGIC HISTORY OF REGION

Precambrian

The Precambrian surface throughout most of Oklahoma (including the Central Oklahoma Platform) is characterized by a rugged hilly topography (Dille, 1956). It was upon this surface that all younger sediments were unconformably deposited. During Precambrian time a large, broad geosyncline (aulacogen) extended across southern Oklahoma into Arkansas in what Briggs and Wickham describe as a zone of crustal weakness (Briggs and Wickham, 1976, after Koff, 1979). The Nemaha Ridge was perhaps only a marginal high (Koff, 1979). In the study area (Figure 6), drilling data indicate that a Precambrian granite topographic high, perhaps a truncated fold (Weirich, 1929), existed at the present site of the Shamrock Dome (Dille, 1956). Evidence to support this is that the overlying Arbuckle sediments are much thinner here than in other nearby localities (Dille, 1956).

Cambrian

Early and Middle Cambrian time were quiescent on the platform while to the south, the geosyncline was being filled with as much as 20,000 feet of graywackes and basalt and rhyolite flows. Cambrian time marked deposition of the Reagan Sandstone and Arbuckle carbonates, the first

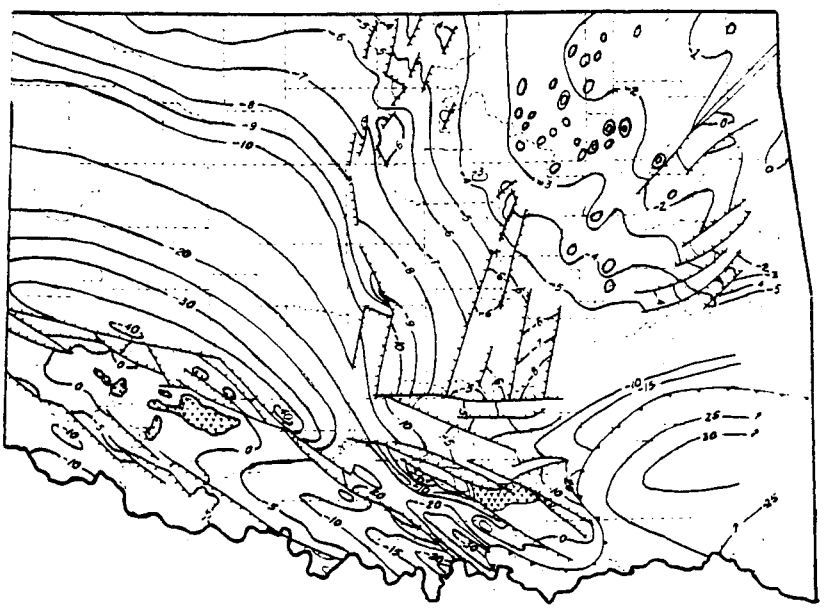

Figure 6. Contour Map of Oklahoma Basement Rocks and Faults Extending to Basement. Contour Interval: 1,000 - 5,000 feet (from Jordan, 1967)

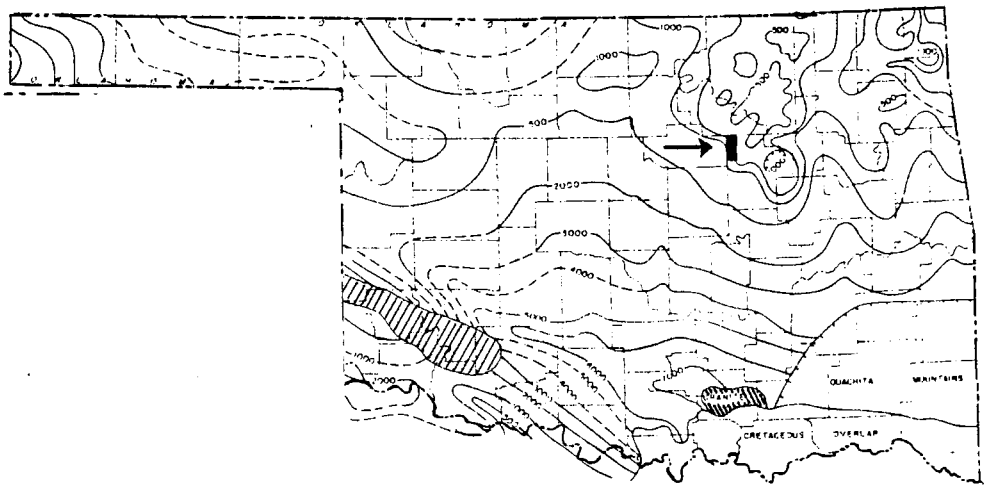

Figure 7. Isopach Map - Arbuckle Group (based on Roth, Ireland, Lee, Merriam, Bartram, McCoy, Herndon Map Service; from Huffman, 1959)

preserved Paleozoic sedimentary rocks on the platform (Figure 7). Deposition of the Arbuckle limestone and dolomite by a northward transgressing sea continued into Early Ordovician (Sartin, 1958; Dalton, 1960; Jordan, 1967; Koff, 1979). Arbuckle limestone is present over the entire study area where it unconformably overlies Precambrian granite.

Ordovician

Following Arbuckle deposition, sands of the Simpson Group were conformably deposited over the Arbuckle carbonates. In southern Oklahoma where the Simpson Group is quite thick, six different units are recognized. On the platform, Simpson sands are thinner and only two units are recognized, the "Wilcox" and Burgen-Tyner sands (Figure 9). The Ozark Dome was uplifted during Ordovician and was a minor sediment source for the Simpson Group on the platform (Dalton, 1960).

Onlapping the Simpson sands was the Viola Limestone, the Fernvale Limestone (Figure 10) and the Sylvan Shale (Figure 8)(Dalton, 1960). Minor episodes of erosion supposedly separated each of these depositional events (Weirich, 1929; Sartin, 1958; Jordan, 1967). These units were all deposited over the study area though perhaps more thinly over the area of the Shamrock Dome, still probably a submarine topographic high at the beginning of deposition of the Viola Limestone.

Silurian-Devonian

According to Weirich (1929), Sartin (1958), Dalton (1960), Pulling (1979), and Koff (1979), the entire aulocogen and nearly all of the north and Central Oklahoma Platform (including the study area) was

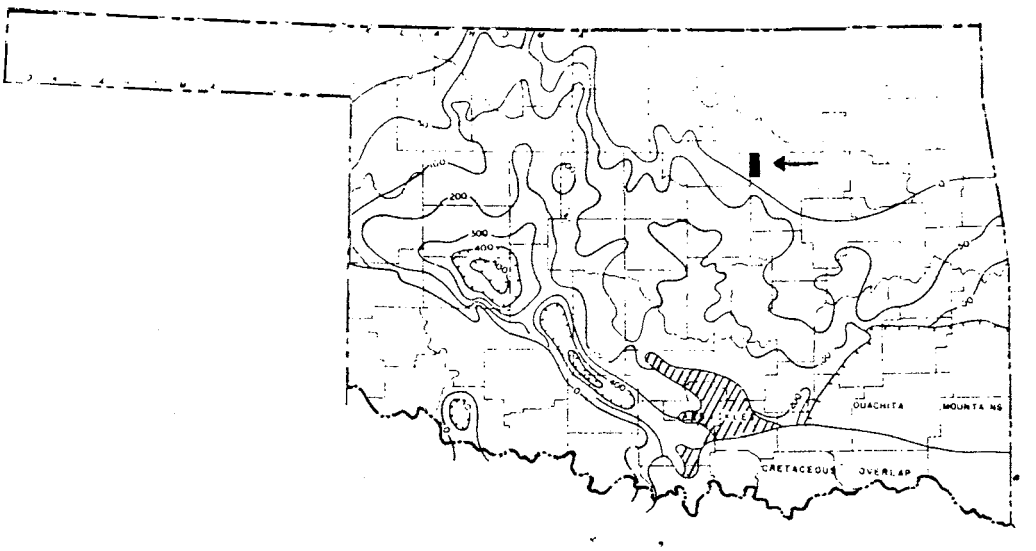

Figure 8. Isopach Map - Sylvan Shale (based on Taylor, Lee, Ackerman, Herndon Map Service; from Huffman, 1959)

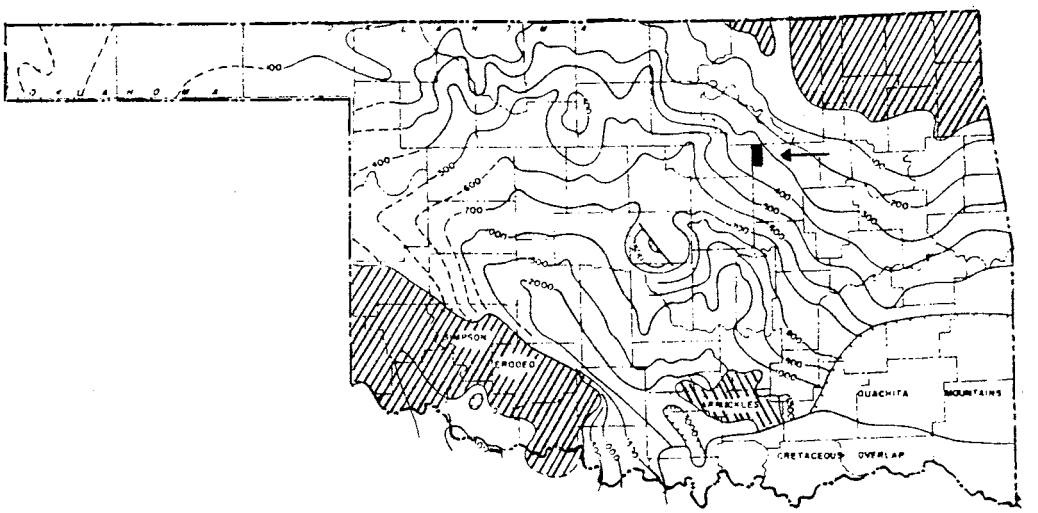

Figure 9. Isopach Map - Simpson Group (based on Roth, Lee, McCoy, Disney and Cronewett, and Herndon Map Service; from Huffman, 1959)

inundated during Silurian-Devonian time and Hunton carbonate sediments were deposited (Figure 11). These carbonates were thickest in the geosyncline, thinning gradually northward across the platform. Southwestward tilting of the platform following Hunton deposition resulted in erosion and truncation, leaving the Hunton absent over some of the platform.

A second explanation proposed by Sartin (1959) and Dalton (1960) invokes a broad uplift of the shelf following deposition of the Ordovician Sylvan Shale. This uplift left the shelf largely exposed during Silurian-Devonian times and resulted in the non-deposition of the Hunton Group over northern and northeastern Oklahoma, including the thesis area. This uplift also caused regional tilt to the southwest.

Pulling (1979) described a major post-Hunton, Middle to Late Devonian epeirogeny as apparently the cause of some faulting and folding in Pottawatomie County. Presumably, during this epeirogeny the Wilzetta Fault, which extends northward and bounds the east side of the Cushing anticline (Plate 1), first showed activity along the area of the Seminole-Cushing Ridge (Pulling, 1979; Figures 5-9). A thinned Hunton section over the Seminole-Cushing Ridge in Pottawatomie County may be evidence that the fault was active during this time (Pulling, 1979). This activity may have reached into the thesis area.

Devonian-Mississippian

Late Devonian-Early Mississippian time was marked by relative tectonic stability throughout the geosynclinal and shelf areas of Oklahoma (Sartin, 1958; Koff, 1979). Transgression of Devonian seas over the shelf area resulted in the unconformable deposition of the thin

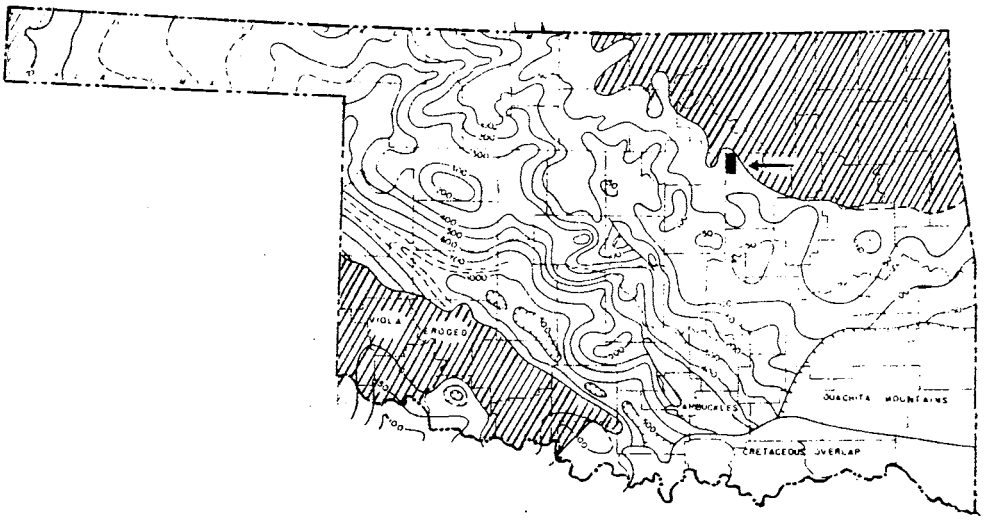

Figure 10. Isopach Map - Viola/Ferndale Limestone (based on Taylor, Lee, Wangerd, Maher, Collins, and Herndon Map Service; from Huffman, 1959)

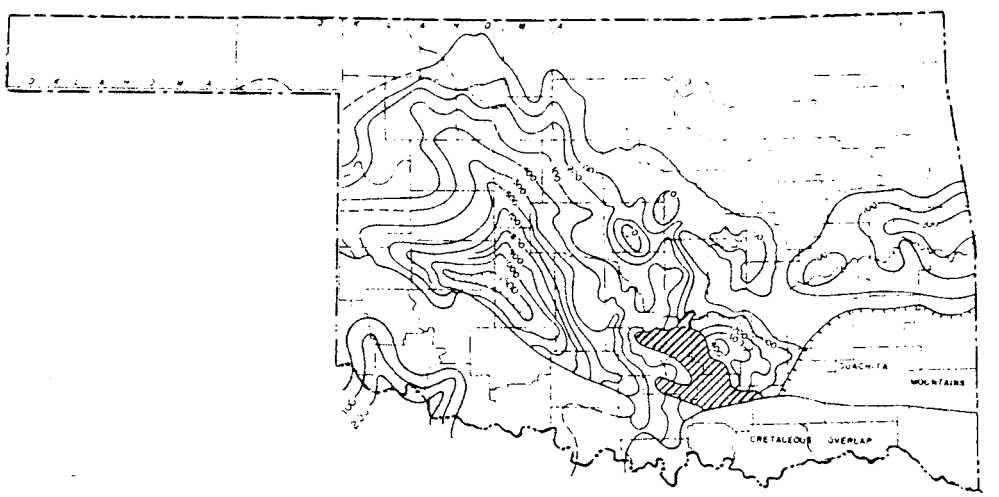

Figure 11. Isopach Map - Hunton Group (based on Roth, Tarr, Lee, Taylor, Herdon Map Service; from Huffman, 1959

Misener Sandstone. Deposited conformably over the Misener was the Woodford Shale (Figure 12). The Woodford thickens southwestward, as is the case with all of the underlying units. Osagean, Meramecian ("Mississippi Limestone") and Chesterian (Hindsville, Fayetteville and Pitkins Formations) were deposited on the Woodford Shale over the platform (Figure 13). An angular unconformity also exists between Osagean and Meramecian units suggesting uplift, exposure and erosion in post-Osage/pre-Meramec times (Jordan, 1959). All of these units were deposited over the study area.

Pennsylvanian

Tectonic History

In southern Oklahoma, Pennsylvanian time was marked by two major orogenies (Jordan, 1967), and perhaps as many as six episodes of tectonism. The two major orogenies were pre-Desmoinesian (Late Mississippian through Atokan, called the Wichita Orogeny) and post-Missourian, pre-Vanoss (called the Arbuckle Orogeny). Ouachita deformation probably took place during the late Atokan, though the exact time is not determined (Jordan, 1967). The climax of the Wichita Orogeny occurred in Morrowan time and resulted in the uplift of the Wichita Mountains in southwest Oklahoma. This subsequently caused the transformation of the southern part of the broad geosyncline into a narrow elongated basin that became the site of more than 40,000 feet of Pennsylvanian sediment (Ham, Dennison, and Merritt, 1964).

A second major result of this orogeny was the "clear separation of the Anadarko Basin from the Central Oklahoma Platform" (Koff, 1979, pp.

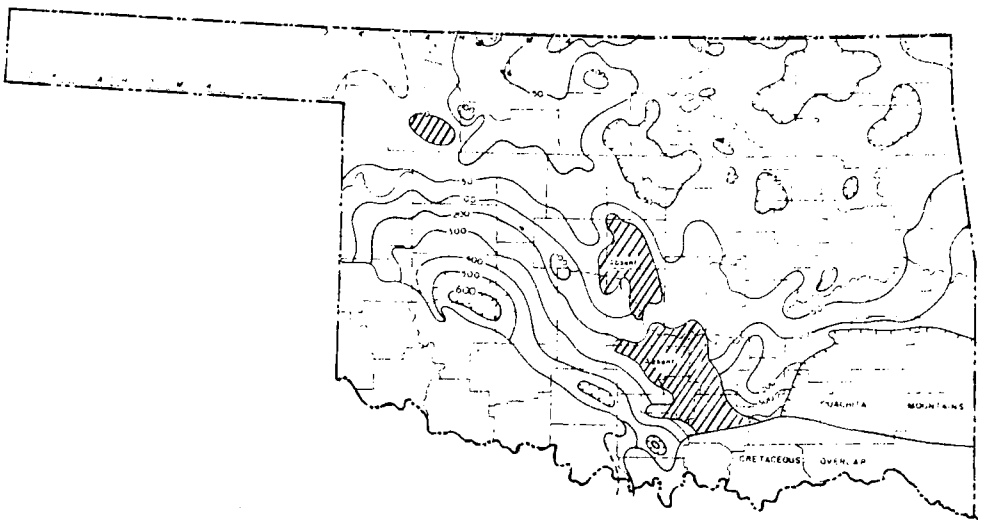

Figure 12. Isopach Map - Chattanooga/Woodford Shale (based on Lee, Herndon Map Service; from Huffman, 1959)

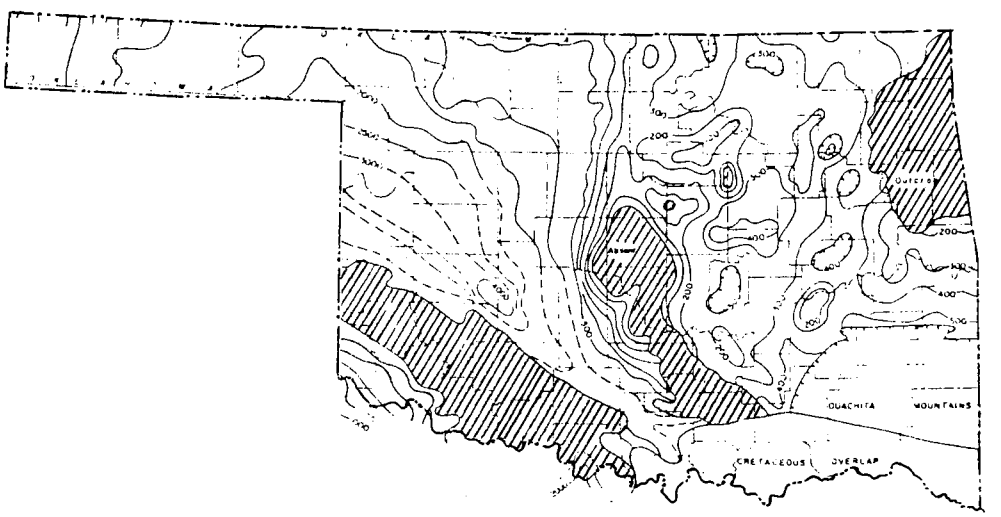

Figure 13. Isopach Map - Mississippian System (based on Roth, Totten, Lee, Maker and Collins, and Herndon Map Service; from Huffman (1959)

32-33). This was accomplished through the uplift of the north-trending Nemaha Ridge. The Nemaha Ridge also separates the Arkoma and Anadarko Basins.

During this pre-Desmoninesian orogeny, faults along the Seminole-Cushing uplift (including the Wilzetta Fault) were re-activated, and significant folding occurred (Pulling, 1979). Because of nondeposition of Morrowan and Atokan strata in the area of this study, activity along the Wilzetta Fault during these epochs cannot be documented.

Overthrusting of the Ouachita system in Morrowan-Atokan time led to formation of the trough-like Arkoma basin (Jordan, 1967). As the Ouachitas were uplifted, the basin axis and basin hingeline shifted northward. This shift coincided with northward transgression of early Pennsylvanian "Cherokee" seas.

Depositional History

Whereas the Early and Middle Pennsylvanian orogenic history is complex, the depositional history is less complicated, being characterized by a general northward transgression of the Cherokee sea, interrupted by periods of regression or southeastward delta progradation. This process has been referred to previously as cyclic sedimentation. The source area of most of the sediments is thought to have been in northeastern Kansas and western Missouri (Weirich, 1953). Morrowan, Atokan, and Desmoinesian (Figure 14) units thicken gradually southward over the platform and then thicken abruptly down the slope into the Arkoma Basin (Weirich, 1953; Visher, 1968; Phares, 1969; Bennison, 1979). As the sea moved northward, younger sediments onlapped older sediments, i.e., Atokan units onlapped Morrowan units, then Desmoinesian sediments

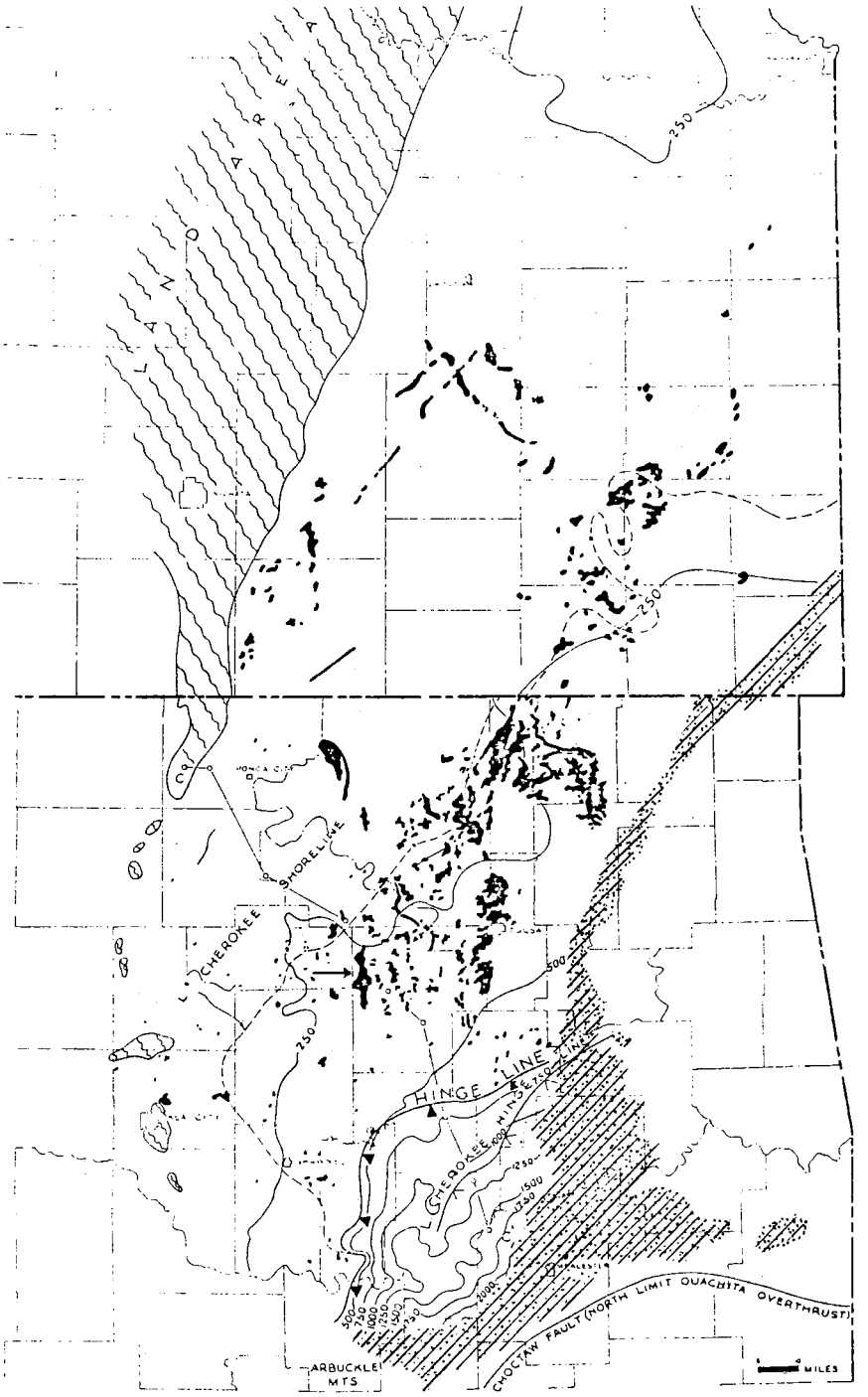

Figure 14. Isopach Map - Middle Cherokee Unit (including the Bartlesville) (oil fields shown in black. Oil fields producing from Red Fork and Bartlesville Sands are confined to the shelf; from Weirich, 1953)

onlapped Atokan rocks. Regional investigations describing this onlapping nature of early Pennsylvanian sediments have been completed by Weirich (1953), Branson (1954), Visher (1968), Visher, Saitta and Phares (1971) and most recently Bennison (1979) and Moore (1979). Desmoinesian sediments of the Krebs Group were the first of Pennsylvanian age to be deposited over the Cushing Field. Figure 15 from the study done by Visher, Saitta and Phares also clearly depicts this onlap, showing how younger Pennsylvanian sediments were deposited progressively northward.

Deposition of the Marmaton Group marked reversal in paleoslope from north to south. By the end of Desmoinesian time, transportation from the northern sediment source had stopped and the southern source (Ouachita Mountains) had become prominent. This paleoslope reversal is well documented by Krumme (1975) and Bennison (1979) (Figure 16). By this time the Arkoma Basin had become completely filled with sediment and the sea had transgressed up into Kansas. The Nemaha Ridge also had been inundated by the sea and covered with sediments, eliminating it as a source of clastic material. Deposition of the "Big Lime" and "Oswego Limestone" over most of the northern part of the shelf (that part of the shelf not affected by terrigenous clastics input from the Ouachita Mountains) ensued.

Depositional events that occurred during Missourian and Virgilian time will not be discussed, as they are not germane to this study.

Post-Pennsylvanian

An epeirogenic tilt westward averaging 40 to 50 feet per mile in Late Permian through Early Jurassic was the last major event to affect the region (Figure 17) (Jordan, 1967, p. 227).

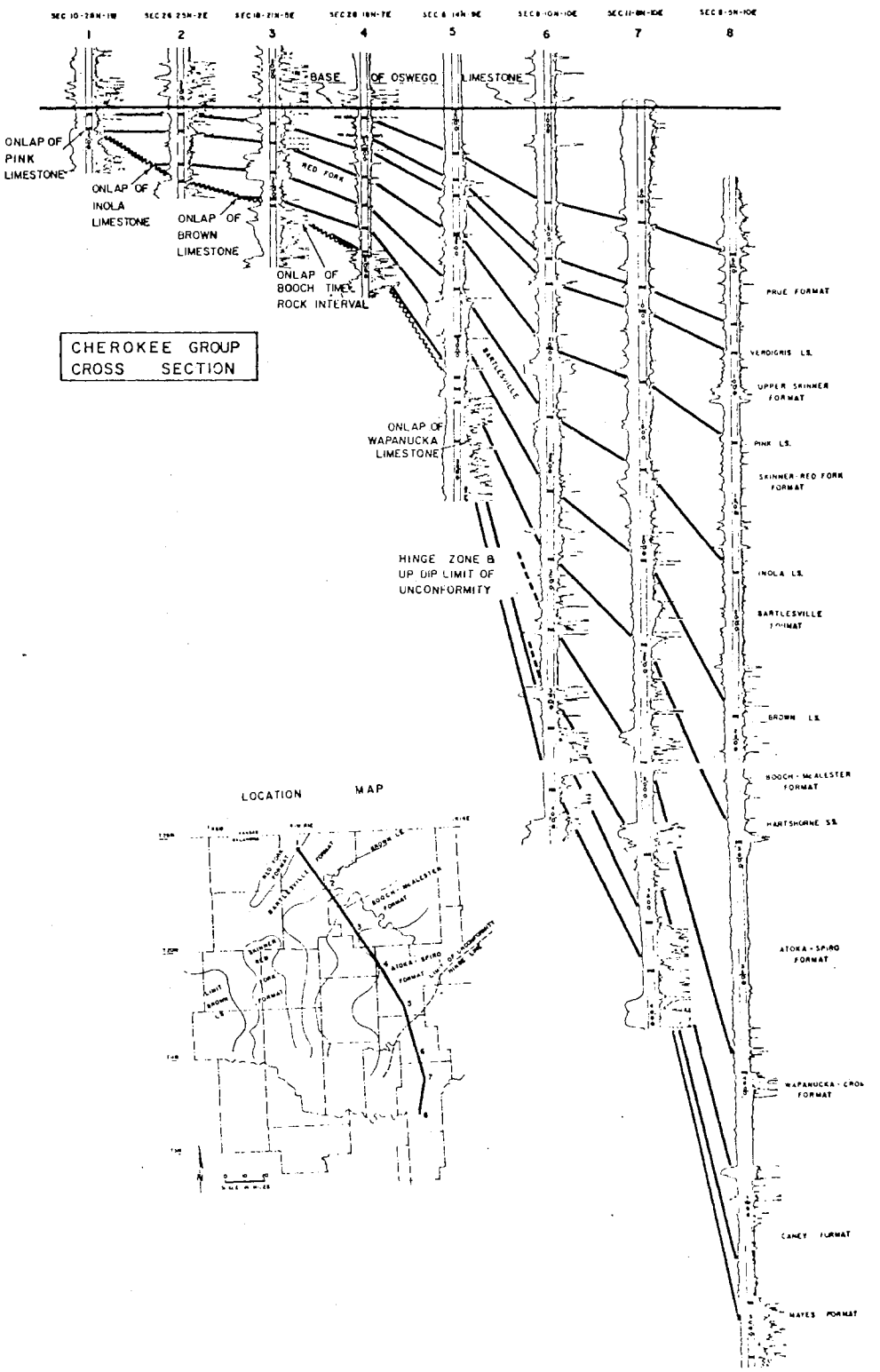

Figure 15. Cross-section Showing Basinward Thickening of the Lower Pennsylvanian Sediments (from Visher, Saitta and Phares, 1971)

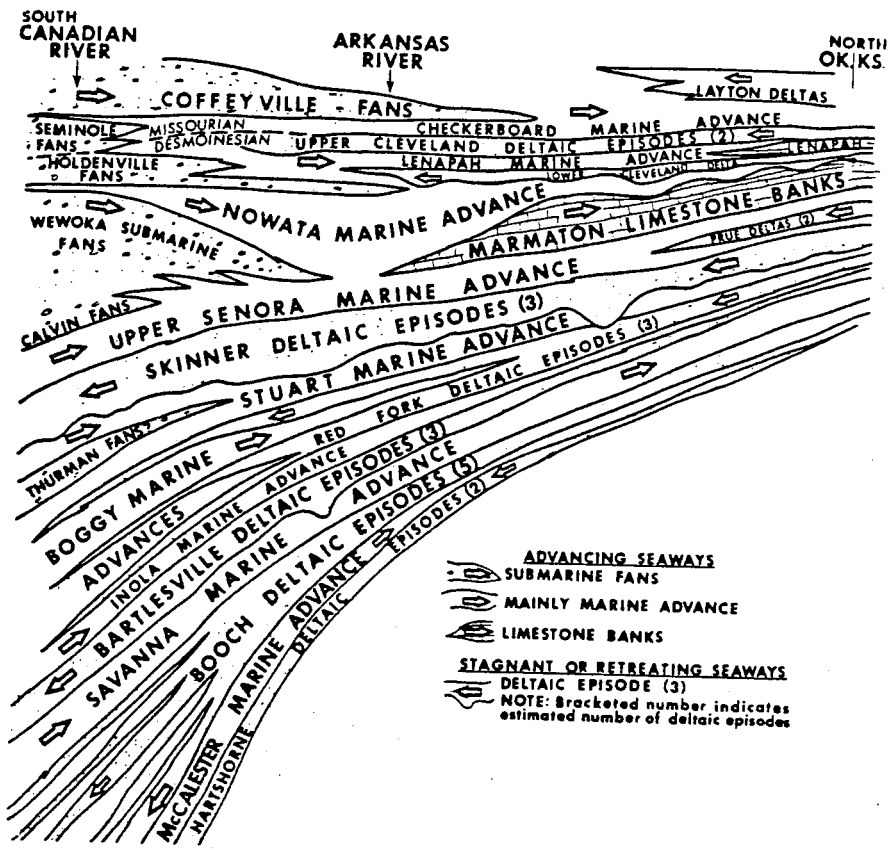

Figure 16. Cross-section Showing Paleo-environmental Patterns in Northeastern Oklahoma During Desmoinesian and Missourian Time (from Bennison, 1979)

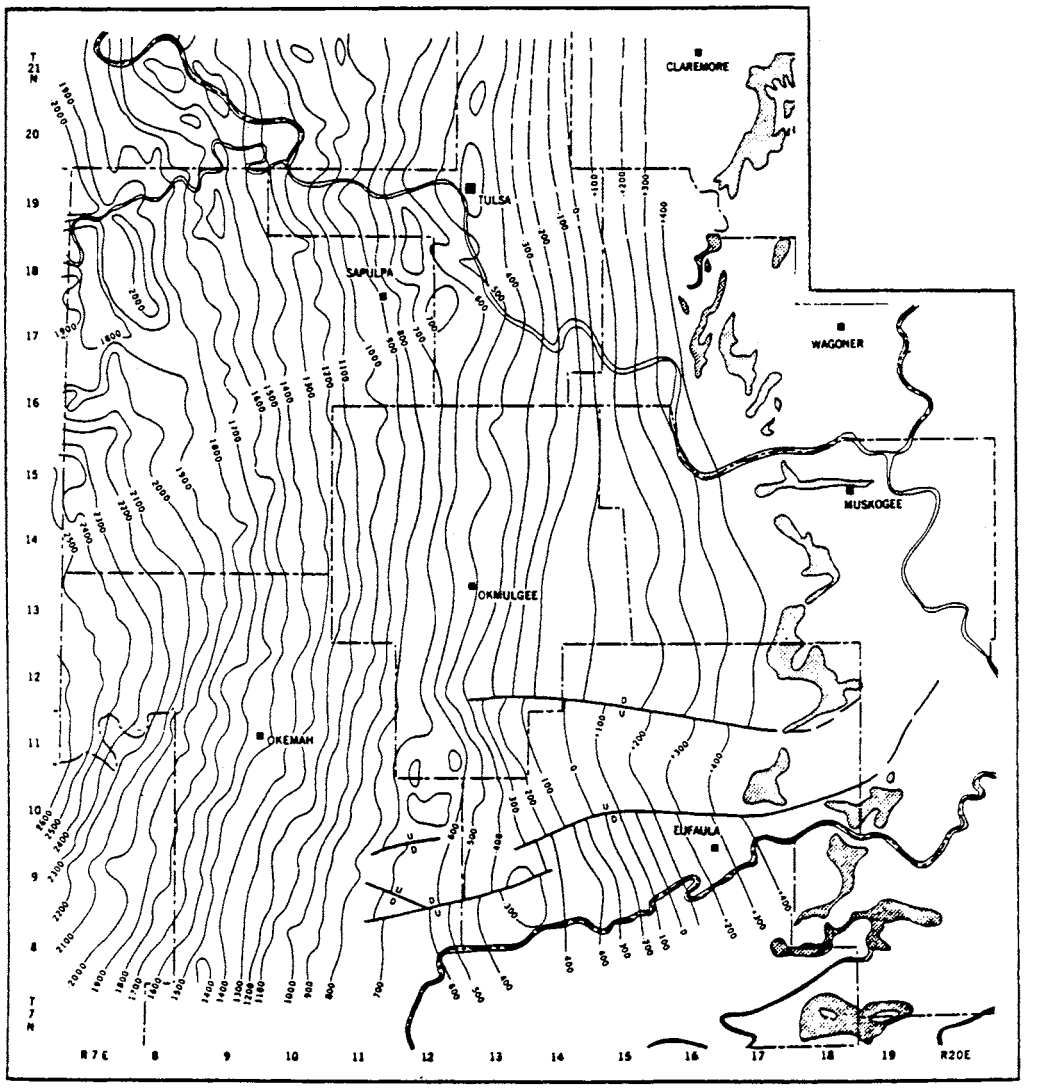

Figure 17. Structural Map of Bluejacket (Bartlesville) Formation in Part of Northeast Oklahoma (from Saitta, 1968), Showing Gently Westward Dip of Strata

CHAPTER V

LOCAL STRUCTURAL GEOLOGY

The structural complexities of the Cushing Field have been reported by several investigators, especially Buttram (1914), Beal (1917), Bosworth (1920), Weirich (1929), Merritt (1930), and Oakes (1959). Structural studies of the surrounding region were conducted by Foley (1920), Fath (1929), and Dille (1956).

The general structure of the Cushing Field is that of an anticline with a north-trending axis. This structure produces a distinct reversal of the approximate 40-50 feet per mile westward regional dip. The fold is about three miles wide and 20 miles long. The field is bounded on its east flank by the Wilzetta Fault, which dips eastward with a throw in the Desmoinesian section of approximately 100 feet. This fault may have originated as a strike-slip fault and it probably has shown significant strike-slip movement at various times during its history.

More precisely, the anticline is composed of four distinct domes. From north to south these are the Dropright, Drumright, Mt. Pleasant, and Shamrock Domes (Plate 1). The surface structure, mapped on the upper surface of the Pawhuska Limestone (Figure 18) clearly indicates the presence of an anticline with three distinct domes, the Dropright, Mt. Pleasant, and Shamrock Domes. The Drumright Dome is much less pronounced at the surface. Maximum amount of closure exhibited by any of the individual domes is about 100 feet and not more than 125 feet. Comparison of the

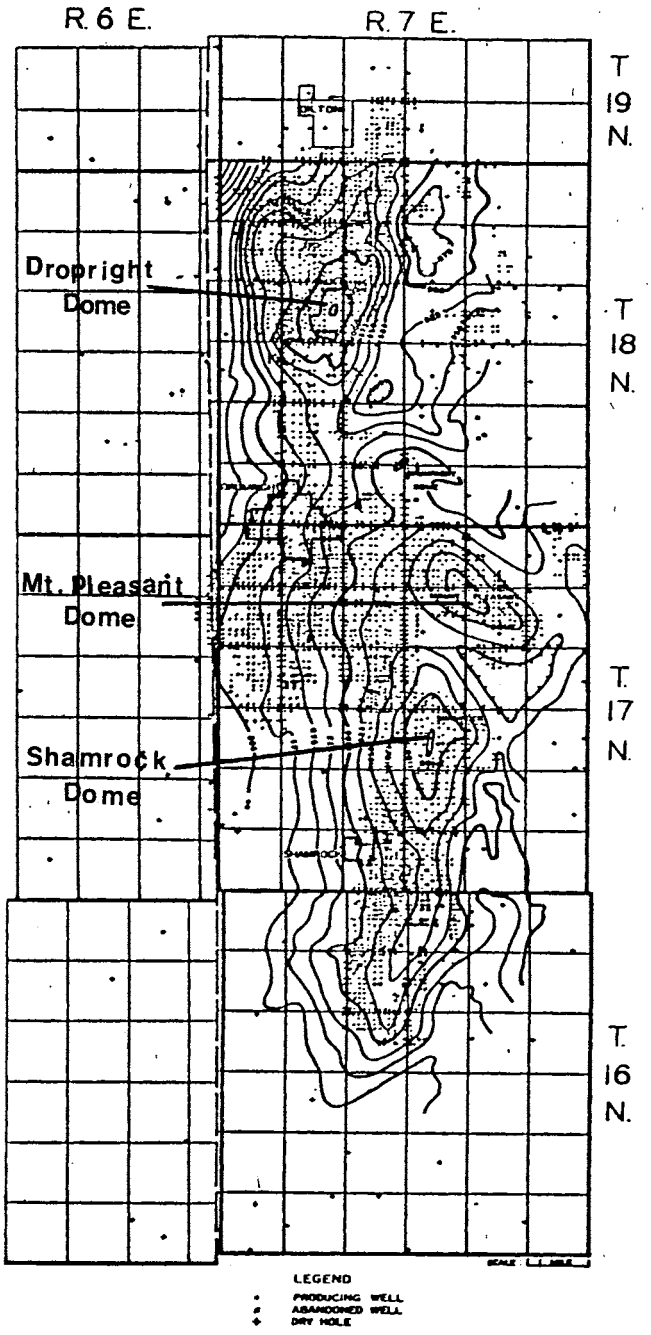

Figure 18. Surface Structure of the Cushing Anticline as Mapped on the Pawhuska Limestone (from Beal, 1917)

surface structure (Figure 18) with the structure shown on the Inola Limestone (Plate 1) clearly shows that the amount of closure increases with depth to an average of about 170 feet. The most distinct and sharply folded are the Mt. Pleasant and Dropright Domes.

The Wilzetta Fault which bounds the field on the east is a major fault that extends approximately 100 miles from southern Osage County down into southwestern Pottawatomie County (Figure 19). This fault may extend into Kansas. According to Jordan (1967) (Figure 6), this fault is deep-seated, originating in the basement. As indicated on Figure 19, the Wilzetta Fault has been mapped as a "scissor fault" with a hinge in northwest Lincoln County, T14N-R6E. The eastern block is downthrown north of the hinge and upthrown south of the hinge.

Another significant feature of the Wilzetta Fault is that it is a growth fault along part and perhaps all of its length. Pulling (1979, Figure 6) documented thickened Pennsylvanian section on the downthrown western block in Pottawatomie County. Verish (1979, pp. 224-226, Figure 6) identified "reciprocal sedimentation" across the fault in Lincoln County. Stewart (personal communication, 1982) has detected growth characteristics on the eastern downthrown block of this fault zone in Pawnee County. Examination of the east-west stratigraphic cross-sections that cross the fault in the Cushing Field (Plates 2a, 2b), clearly indicate thickened Desmoinesian sections on the downthrown eastern block. Average amount of thickening of the Oswego-Brown Limestone section is more than 100 feet. The conclusion is that the fault was active during Desmoinesian deposition and that the geomorphic expression of the fault caused increased deposition on the downthrown block.

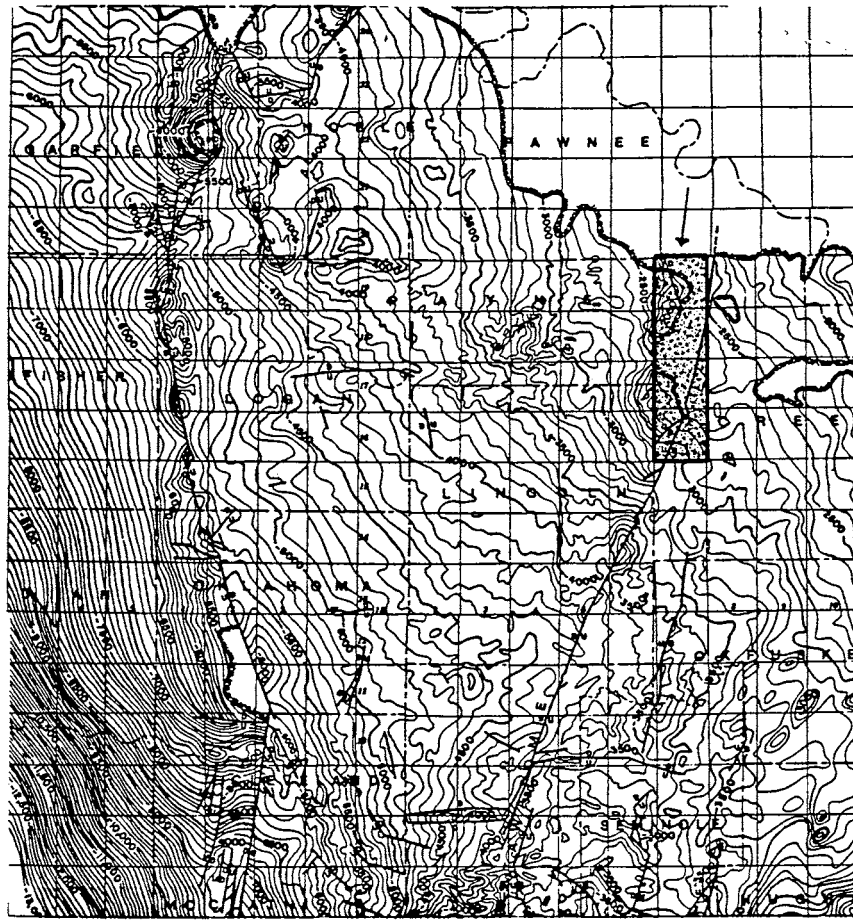

Figure 19. Structure Contour Map - Top of Viola Formation (compiled by Hagengast, Koff and Axtmann, from Luza and Lawson, 1981)

The Cushing Anticline

While a Precambrian topographic high probably is responsible for the presence of a portion of the structure (Weirich, 1929; Dille, 1956) and minor movements along the Wilzetta Fault in Devonian time (Pulling, 1979) could have generated anticlinal folds, the formation of the anticline most likely is related to strike-slip and dip-slip movements along the Wilzetta Fault in Morrowan and especially in Atokan and Desmoinesian time. The parent stresses causing these movements along the fault probably originated in the Ouachita Orogeny. This orogeny created northwest-southeast trending compressive principal stresses, stresses that could create or reactivate north-northeast-trending faults such as the Wilzetta Fault.

As discussed earlier, in the area of study the Wilzetta Fault shows dip-slip movement and thickening of the Oswego-Brown Limestone section along the eastern block of the fault. Dip-slip movement could cause anticlinal folding on both the upthrown and downthrown blocks, but the small amount of dip-slip movement alone during Pennsylvanian time (not much more than 100 feet) was not nearly enough to generate a fold with the magnitude of the Cushing anticline. Repeated strike-slip movement along the Wilzetta Fault suspected by Verish (1979), Stewart and Phipps (personal communication, 1982), and by the author, could generate anticlinal folds of the Cushing type (and magnitude), where the fold becomes increasingly sharp with depth and the amount of closure increases.

Dip-slip and probably strike-slip movement along the fault causing further growth of the fold, continued into early Missourian time.

Evidence for this is the episodic thickening of section on the downthrown block (Plates 2a and 2b) and thinning of section over the domes on the upthrown block (Plate 3a) as high in the stratographic section as the Hogshooter Limestone.

In summary, the growth of the anticline began in Precambrian time, was probably accentuated in Devonian time and became most pronounced in the Pennsylvanian time as a result of strike-slip and dip-slip movement along the Wilzetta Fault.

CHAPTER VI

STRATIGRAPHY

Precambrian

At least five wells have penetrated Precambrian rocks in the Cushing Field (Figure 20). As described by Merritt (1930), the Precambrian granite in the Gulf Oil Corporation's No. G26S North Glenn Sand Unit No. 2 was composed of "coarse-crystalline pink feldspar and fine crystalline anhedral quartz with minor amounts of magnetite and of hornblende altered to chlorite" (Jordan, 1959, p. 73). Granite penetrated in other wells has also been described as red, red-brown, or pink.

Ordovician

Ordovician strata unconformably overlie Precambrian granites in the Cushing Field. The different rock types composing the Ordovician System in this area are Arbuckle Dolomite, Simpson Sandstones, Fernvale-Viola Limestone, and the Sylvan Shale. Arbuckle dolomites are penetrated between 2,500 and 3,000 feet deep throughout most of the Cushing Field. They subcrop beneath the Pre-Pennsylvanian unconformity in Sections 18 and 19, T18N-R7E, and also in Section 3, T17N-R7E. The Arbuckle was deposited in Late Cambrian and Early Ordovician time. Oil and gas are produced from the Arbuckle in these structurally high locations beneath Pennsylvanian strata. Arbuckle dolomite has been

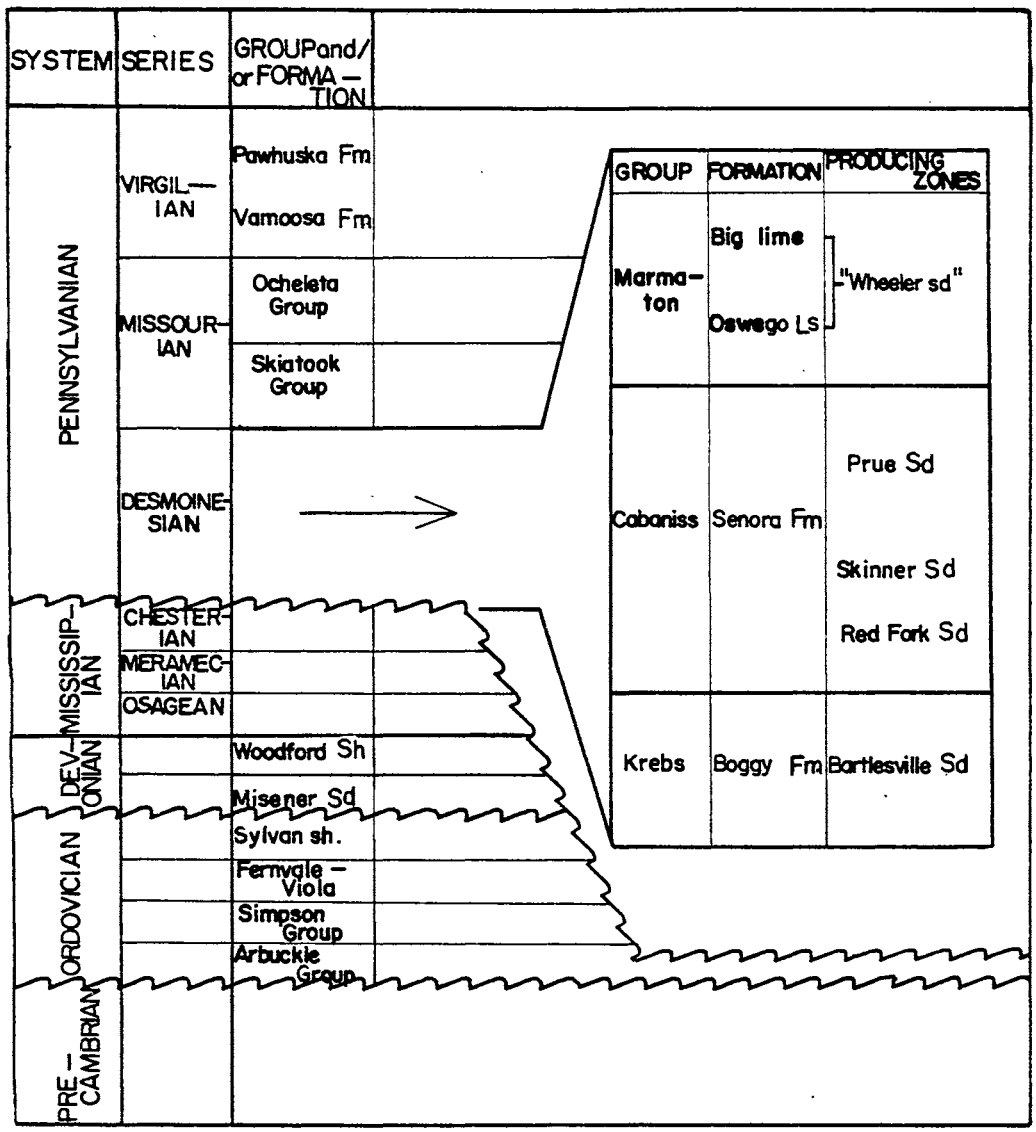

Figure 20. Stratigraphic Section, Cushing Field

described in nearby wells as "ranging from fine to coarse - crystalline texture, oolitic and cherty in part and containing occasional thin beds . . . of sandstone or arenaceous dolomite" (Jordan, 1959). The basal sandstone is named the Reagan Sandstone.

Simpson Group

In the Cushing Field, the Simpson Group includes the "Burgen" or "Hominy Sand," Tyner Sands and shales, and the "Wilcox" Sand. However, throughout most of the field, one or more of these members are absent.

The Simpson Group normally is present throughout the field directly beneath the Pre-Pennsylvanian unconformity. On the crests of domes it was eroded to absence. Simpson sands commonly are white or greenish gray, rounded, frosted, and contain interbeds of waxy shale (Riggs et al., 1958). Interbedded sandy dolomites and limestones locally are at the top of the group.

This group of sands has been one of the major oil and gas producing zones in the field though its production has been erratic and scattered throughout the field.

The Fernvale-Viola Limestones are considered here as a single rock unit, referred to as the Viola Limestone. The upper and lower boundaries, respectively, of the Viola Limestone are the first limestone beneath the Sylvan Shale and the top of the first underlying sandstone (frequently called the "First Wilcox"). Viola limestones are white to tan, coarse-crystalline and somewhat arenaceous at the base. The maximum thickness in the study area is 30 feet.

Recognized as a greenish gray fissile shale, the Sylvan Shale is thin and present only along the southern-most flanks of the anticline in

Sections 30-33, 35, 36 T17N-R7E and Sections 1, 2, 6, 7, 11, 12, 13-15, 18 T16N-R7E. Elsewhere in the field it is absent as a result of Pre-Pennsylvanian erosion and truncation.

Devonian

The Misener Sand is calcareous, supposedly of aolian origin (Riggs et al., 1958), and present in the Cushing Field only in isolated structurally low areas in the south and southwest. Small amounts of gas and oil have been produced from stratigraphic-structual type Misener traps.

Having been removed from the top of the anticline by Early Pennsylvanian erosion, the Woodford Shale (Chattanooga Shale) is present as a thin, 20 to 30-foot thick belt around the flanks of the Cushing anticline. Woodford Shale is thought to be the source of at least some of the oil in the Cushing oil field. According to Jordan (1959) and Puckett (personal communication, 1982), the Woodford Shale in Creek County commonly is a brownish-black, richly organic shale containing abundant pyrite and minor amounts of pyritic brown chert.

Mississippian

Mississippian strata are absent over the top of the Cushing anticline but exist around the flanks of the structure as a result of early Pennsylvanian erosion. No Mississippian production exists in the Cushing Field.

Mississippian rocks consist of Osagean - a black calcareous shale or argillaceous limestone that is glauconitic in part at the base; Meramecian - "cyclic thin-bedded strata of gray calcareous siltstone, silty to very fine sandy limestone and minor amounts of brownish gray silty,

calcareous shale" (Jordan, 1959); and Chesterian, light colored fossiliferous limestone with interbedded dark gray shales. A slight angular unconformity exists between Osage and Meramecian units (Jordan, 1959).

Pennsylvanian

The Pennsylvanian section consists largely of terrigenous clastic sediments. Early Desmoinesian sediments were the first to cover the Cushing anticline. Pennsylvanian (Desmoinesian) rocks unconformably overlie strata from Mississippian to Cambro-Ordovician along the axis of the Cushing structure (Figure 21). Clearly, parts of the Cushing structure were topographic highs throughout Desmoinesian and Missourian time as the Desmoinesian-Missourian stratigraphic section thins dramatically over the structure (Figure 22 and Plate 3a). This is also evident on the total format isopach map (Plate 4) thin area.

Desmonesian

Desmoinesian strata contain the most productive zones in the Cushing Field (the Bartlesville Sandstone and Oswego Limestone) as well as several minor producing sands (the Prue, Skinner, and Red Fork). Desmoinesian rocks are assigned to the Krebs, Cabaniss, and Marmaton Groups. Formerly the Krebs and Cabaniss Groups were referred to as the "Cherokee Group," a name which persists. Oakes (1953) proposed separation into the Krebs and Cabaniss Groups, which is the nomenclature now officially used by the Oklahoma Geological Survey.

Krebs Group. The Krebs Group is made up of the Hartshorne, McAlester, Savanna, and Boggy Formations. The Hartshorne and McAlester Formations are present only in the Arkoma Basin; they were not deposited

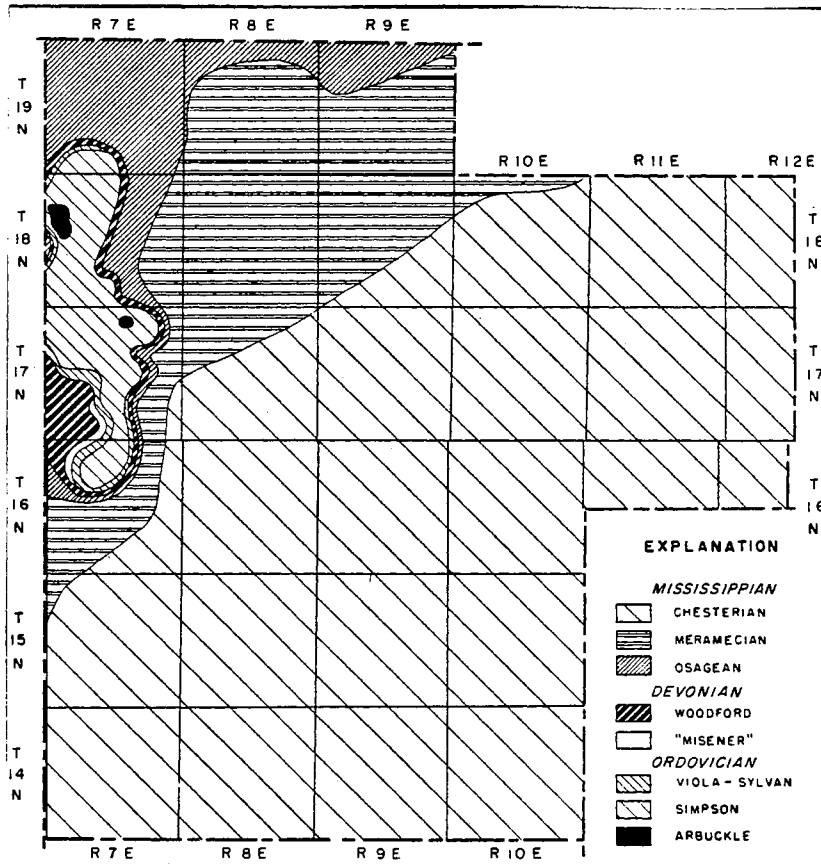

Figure 21. Pre-Pennsylvanian Subcrop Map Showing Truncation (from Jordan, 1959)

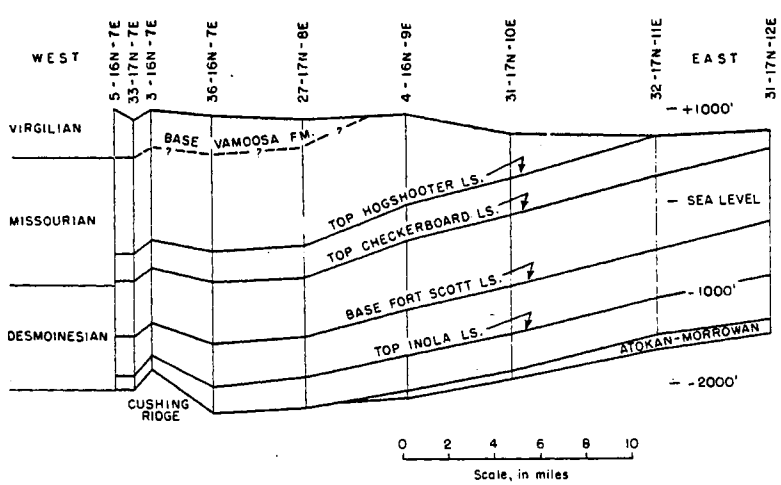

Figure 22. Structural Cross-section (West-East) Across Creek County Showing Thinning Over the Cushing Anticline (from Jordan, 1959)

the study area.

The Savanna Formation is composed of limestones (the Brown Limestone) and dark gray shales. The upper Brown Limestone represents a regional transgression and can be used as a time-stratigraphic marker. It has been designated as the lower boundary of the Bartlesville genetic increment (or Format unit) and was used in the construction of the isopach maps. The Brown limestones are eroded locally by channeling prior to deposition of the Bartlesville Sandstone.

The Boggy Formation consists of the Bartlesville sand zone which is underlain by the Brown Limestone and overlain by the Inola Limestone and the Red Fork sand zone.

Because the Bartlesville Sandstone will be described in detail in subsequent chapters, a brief description should be sufficient here.

The Bartlesville Sandstone is bracketed by the regionally transgressive, time-stratigraphic Inola and Brown Limestone marker beds. This was the format unit used in the construction of isopach maps. Existing mainly as lenticular sand bodies within a predominantly shale section, the character of the Bartlesville Sand changes greatly within distances of a few hundred yards. In the study area, thickness of the sand ranges from 0 to more than 100 feet (Plate 5). The overlying Inola limestone is rarely a clean limestone but more commonly is a 10 to 15-foot zone of thin interbeds of shale and limestone or shaly limestone. Due to the variable nature of the Inola, a persistent electric-log resistivity characteristic was chosen as the top of the Bartlesville sand zone and defined as being correspondent to the Inola Limestone (Figure 23).

In the Cushing Field, sand zone consists largely of shale and silt

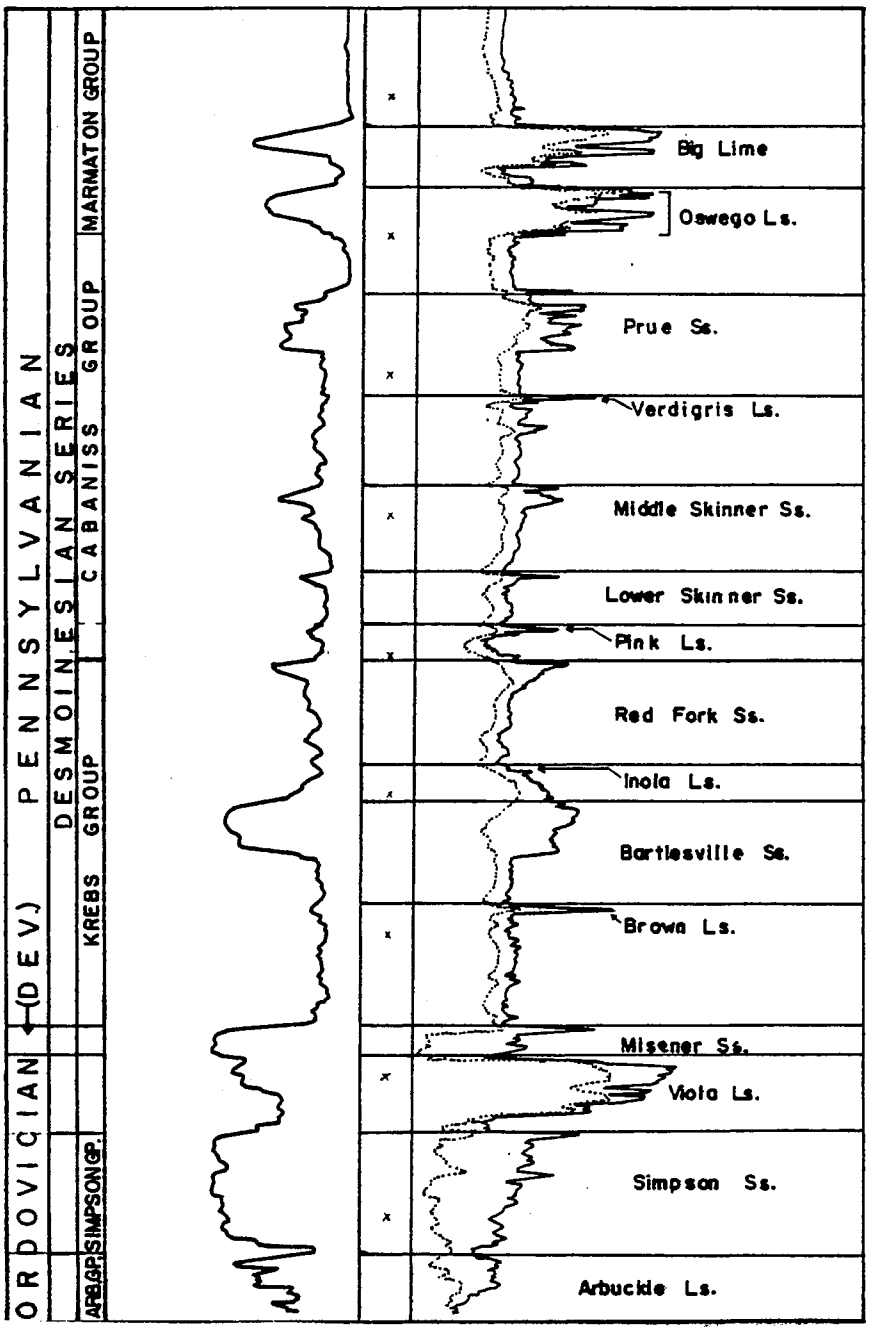

Figure 23. Type-log of the Cushing Oil Field Showing Boundaries of Major Stratigraphic Zones

stone of fairly uniform thickness. Ten to thirty-foot thick Red Fork sandstones have been penetrated, but they have produced only small amounts of oil.

Cabaniss Group. Separated into the Upper, Middle, and Lower Skinner sand zones and the Prue sand zone, the Cabaniss Group (or Senora Formation) is predominantly sand and shale. The regionally persistent limestone referred to as the "Pink" (Tiawah) Limestone at the base of the Skinner Zone and the Verdigris Limestone at the base of the Prue zone, record regional transgressions of the Desmoinesian sea and bound the Skinner genetic increment. The Prue genetic increment is bounded by the Verdigris Limestone below and the Oswego Limestone above.

Described by Riggs et al. (1958) as a medium-grained shaly sandstone, the Skinner sand ranges in thickness from 5 to 30 feet in the area where it produces in the Cushing Field. Cumulative production from Skinner sands is less than one million barrels of oil; comparatively, this sand is a minor producer (Riggs et al., 1958). Production from the Skinner exists mainly in small patches in the northern, eastern and southern ends of the field.

In the Cushing Field, the Prue Sand is described as fine- to coarse-grained, micaceous and relatively clean (Jordan, 1959). Ranging from 22 to 75 feet thick in the western portion of the field, the sand pinches out completely in the eastern part. Several million barrels of oil have been produced from the Prue sands.

Marmaton Group. The Marmaton Group is mainly carbonate rock; it is easily recognizable on electric logs throughout the northern portion of the Central Oklahoma Platform. The Marmaton comprises the Oswego Limestone, Labette Shale, and the Big Lime.

Oswego Limestone (called the "Wheeler sand" in the Cushing Field) is primarily a fine- to medium crystalline, fossiliferous limestone containing an oolitic facies. Average thickness in the Cushing Field is about 50 feet.

As discussed above, the Oswego Limestone is one of the major producing zones in the field. The Cushing Field discovery well was completed in the Oswego in March, 1912. Since then more than seven million barrels of oil have been produced from the Oswego as well as an unquantified amount of natural gas (Riggs et al., 1958). Initial production rates of some of the early Oswego wells were as much as 2,000 barrels of oil per day. Production from the Oswego had been limited to the northwestern and west central portions of the field (Riggs et al., 1958). The Oswego has produced in approximately 3,700 acres.

Overlying the Oswego Limestone and separating it from the "Big Lime" is the Labette Shale, 10 to 30 feet thick, and calcareous at some localities.

The Big Lime (Oolagah Limestone) is normally a fine crystalline, brown limestone with numerous interbeds of shale. To the west and south of the field, the limestone grades into shale and sandstone. No production from the Big Lime has been reported in the Cushing Field.

Missourian

Of the Missourian rocks, only the Layton Sand (Coffeyville Formation, Skiatook Group) has produced significantly large amounts of oil in the Cushing Field.

The Layton Sand is correlated with the upper part of the Coffeyville Formation; it lies beneath the Hogshooter Limestone and above the

Checkerboard Limestone. Thickness of the Layton in the field ranges from 0 to 100 feet. The sand is "coarse grained, porous, and comparatively soft and is fairly uniform in texture and porosity" (Beal, 1917). Oil and small amounts of gas were produced from the Layton Sand in the Cushing Field.

CHAPTER VII

DEPOSITIONAL ENVIRONMENT OF THE BARTLESVILLE

Numerous surface and subsurface investigations have been completed on the Bartlesville Sandstone. Most of these studies deal with the depositional environment or framework of the Bartlesville. Studies of regional scope have been completed by Bass (1934, 1937); Dane and Hendricks (1936); Howe (1951); Weirich (1953); Berg (1963, 1966); Hawisa (1965); Saitta (1968); Visher, Saitta and Phares (1971), and Hulse (1979). Detailed qualitative petrographic work on the Bartlesville has been done by Leathercock (1937) and minor amounts by Visher, Saitta and Phares (1971).

In addition to these specific studies of the Bartlesville, a wealth of surface and subsurface studies that discuss the Cherokee Group have been completed at various localities in eastern Oklahoma and southern Kansas. Nearly all of these studies include a written description of the Bartlesville Sandstone and/or a description of its depositional environment. Those which have been reviewed by the author are: McKeenry, (1953); Branson (1954); Howe (1956); Kirk (1957); Sartin (1958); Jordan (1959); Dalton (1960); McElroy (1961); Clayton (1965); Hanke (1967); Shulman (1967); Dogan (1969); Cole (1969); Harrison (1973); Shelton (1973); Verish (1975); Ebanks (1979); Bennison (1979); Pulling (1979).

Studies of the Bartlesville Sandstone completed within the confines

of the Cushing Field by Buttram (1914), Beal (1917), Bosworth (1920), Fath (1921), Weirich (1929), and Wardwell (1937) all describe the Bartlesville sand in a superficial way. Riggs' very thorough investigation (Riggs et al., 1958) of the production history and potential for secondary and tertiary production from the Bartlesville in the Cushing Field excluded a detailed analysis of the depositional environment and petrography of the Bartlesville Sandstone.

The goal of the present discussion is to describe the depositional environment of the Bartlesville Sandstone in the Cushing Field in light of (1) knowledge of the regional Cherokee and Bartlesville despositional framework, and (2) subsurface data collected from the Bartlesville in the Cushing Field.

Depostition of the Bartlesville

As defined earlier, the Bartlesville genetic increment of strata or format is defined as that interval between the Brown Limstone below and the Inola Limestone above. The limestones are thin, widespread, and are considered to be time-stratigraphic markers. The Bartlesville format follows the pattern of other formats within the Cherokee Group. This consists of a gradual thickening of the format over most of the platform from Kansas southward, and abrupt thickening down the slope into the Arkoma Basin (Figure 24). This thickening suggests active subsidence of the Arkoma Basin during deposition of the Bartlesville (Saitta, 1968); Shelton, 1973). Depths of water probably never were greater than 300 feet in the basin (Bennison, 1979) and were much shallower on the platform.

The general depositional pattern of the Bartlesville has been

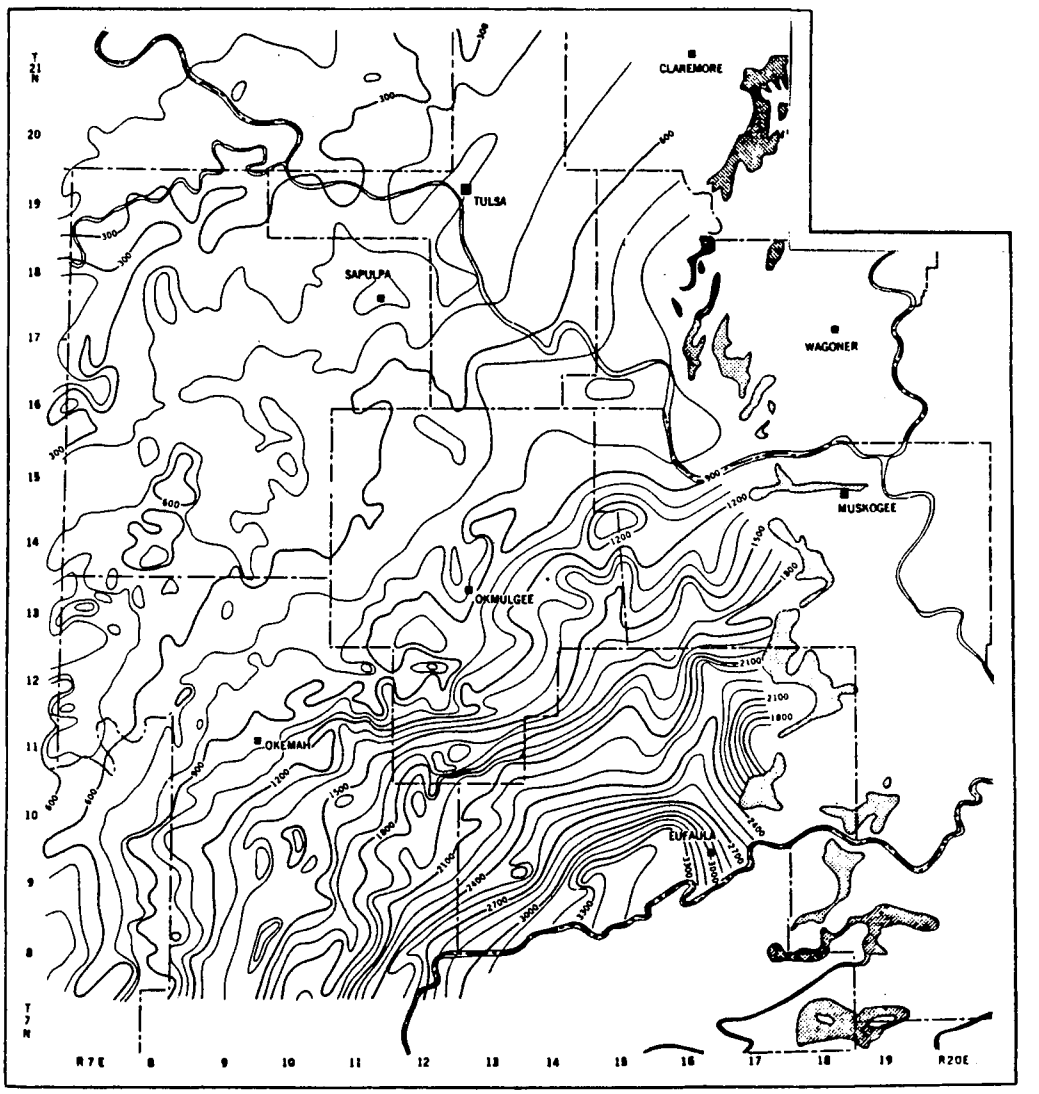

Figure 24. Isopachous Map of the Interval Between the Inola Limestone and the Mississippi Chat (from Saitta, 1968)

documented well by Weirich (1953), Saitta (1968), Visher (1968), Phares (1969), Visher, Saitta and Phares (1971), Shelton (1973), and Hulse (1979).

Cherokee Deposition

The Cherokee Group, and especially the Bartlesville sand, forms a "belt which is arcuate around the Ozark uplift and convex to the west-southwest" reflecting the influence of the Nemaha Ridge (Shelton, 1973, p. 64). Visher, Saitta and Phares (1971) stated that not only were the sands transported from the north but that the Cherokee Group represents a single major drainage system (Figure 25). The sequence of delta progradation, over-extension, avulsion and delta abandonment, compaction, submergence and finally limestone or shale deposition was repeated throughout early and middle Desmoinesian time. Avulsion that initiated each stage of delta abandonment occurred farther and farther northward, reflecting the general transgression northward of the Cherokee Sea.

> Sedimentation was continuous, but the regressive period of sand deposition was discontinuous . . . Generally successive sand units do not overlie each other but are present in areas where shale deposited during a previous regressive period would have undergone sufficient compaction to provide an embayment in the shoreline (Visher, Saitta and Phares, 1971, p. 1213).

These authors cite evidence that the younger sandstones developed farther to the north. This suggests deeper water in the south and northward transgression of the sea.

Two basic working hypotheses commonly are advanced as explanations of the general transgression of the Cherokee Seas; both were summarized by Bennison (1979, p. 283).

1. A long, northward-moving crustal wave evolved from

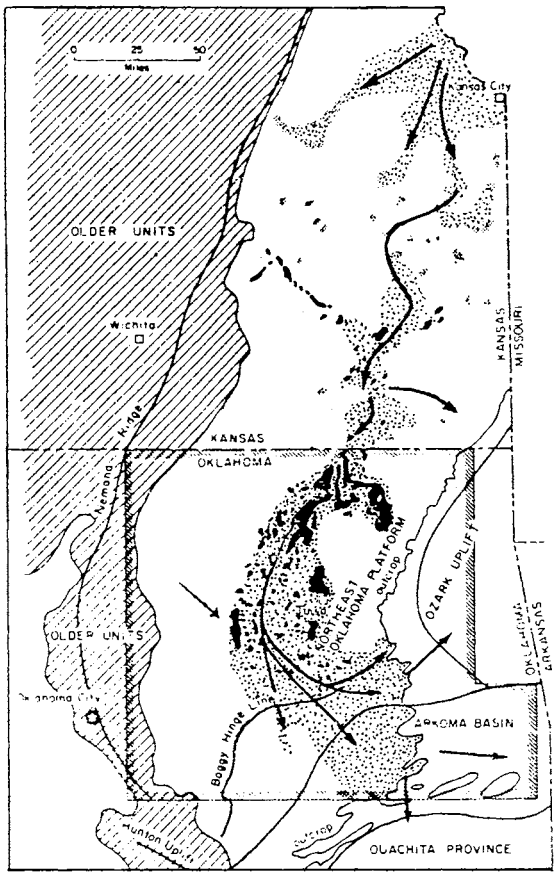

Figure 25. Index Map Showing Oil Fields That Produce From the Bartlesville Sandstone and the Dispersal Pattern of Sandstone (from Shelton, 1973, and modified from Cisher, 1968)

> convergence of the North American and North African plates or from activity along the now buried Llanoria complex in the northern Gulf of Mexico. The crustal wave resulted in northward shift of the basin axis and hingeline, and therefore of the Cherokee Sea.
>
> 2. Eustatic fluctation of sea level was caused by waxing and waning of glaciers in Gondwanaland. If waning of glaciation were predominant, this could have led to overall transgression of the Cherokee Sea.

Regional Deposition of the Bartlesville

According to Visher, Saitta and Phares (1971, p. 1228), deposition of the Bartlesville sand resulted from progradation of a delta that "probably is an intermediate type between highly elongate and lobate delta types." Shelton (1973) described the size of the depositing stream as being slightly larger than the Brazos River near Old Town, Texas. He also identified vertically stacked sand bodies and related this to slow subsidence of the Arkoma Basin and eustatic rise of sea level.

Apparently, the stream moved first in a southwestward direction, building a delta lobe over the area now encompassed by eastern Pawnee, eastern Osage, and western Creek Counties (which includes the area under study, Figure 26). The stream then avulsed to the southeast at a point south and slightly west of Bartlesville, Oklahoma (Figure 26) (Shelton, 1973). The final event in the deposition of the Bartlesville Sandstone was

> . . . abandonment of the delta by the stream supplying the clastics necessary for continued delta development. The sediments underwent normal compaction and a marine transgression covered the entire area . . . With the source of the clastics diminished and the continued transgression of the sea, the Inola Limestone was deposited (Phares, 1969, p. 55).

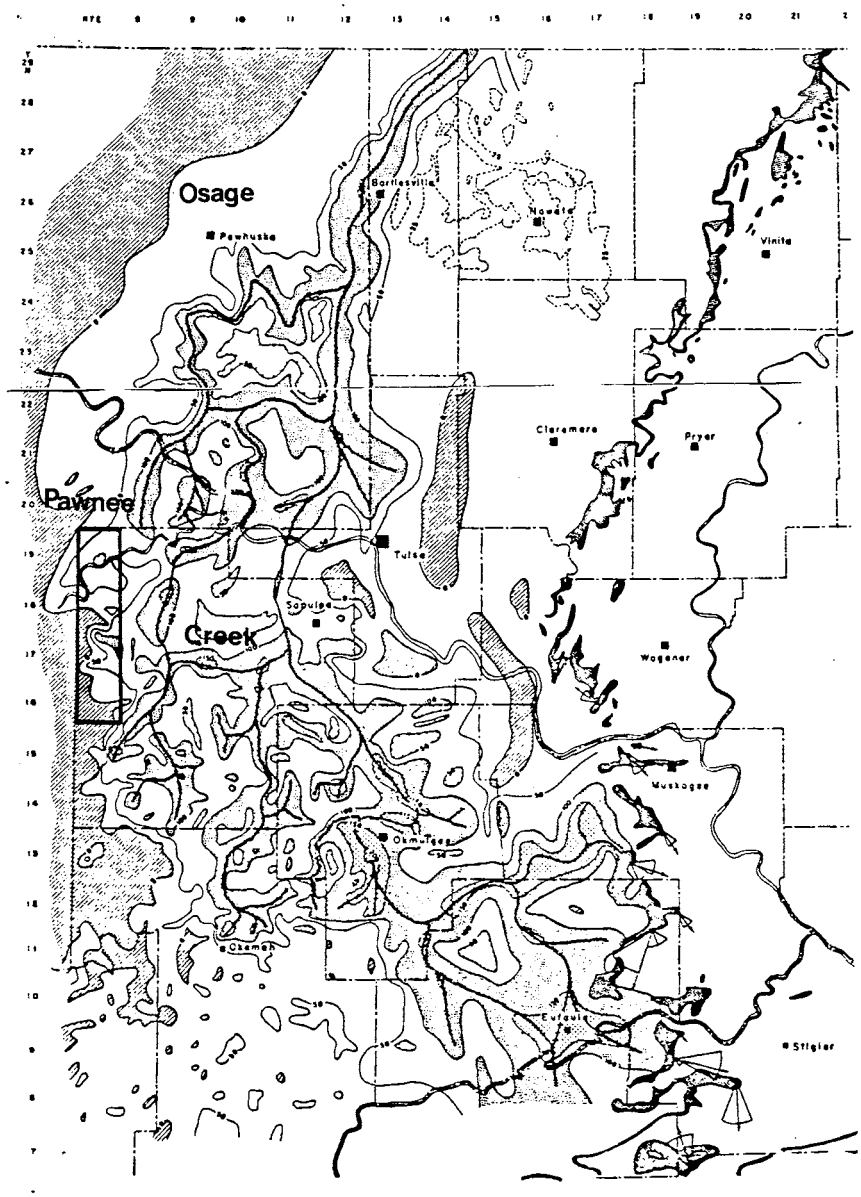

Figure 26. Bartlesville Sandstone Isolith Map (from Visher et al., 1971)

Local Deposition of the Bartlesville

In the area of study, Bartlesville Sandstones exhibit both delta plain and fluvial characteristics. The sand consists of two major bodies, a third minor body and a fourth, thin silty sand at the very top of the section directly beneath the Inola Limestone. These first-mentioned three sands are stacked upon each other at numerous places. In ascending order they seem to be: (1) delta-distributary channel deposit; (2) and (3) fluvial channel sand and point bar deposit; (4) transgressive marine sand. Methods used to estimate the depositional environments were (1) examination of nine cores, (2) construction and analyze net-sandstone-isopach, total-format-isopach and electric log signature maps, and (3) construction and examination of twelve stratigraphic cross-sections and two structural cross-sections of the Bartlesville format. More than 400 electric logs were used in the construction of the subsurface maps and cross-sections.

Additionally, deposition of the Bartlesville seems to have been influenced by the local structure fabric, namely the Wilzetta Fault and domes of the Cushing anticline.

Discussion of Maps

Net Sandstone Isopach Map (Plate 5)

The net sandstone isopach map is a contour map consisting of values of the total amount of sandstone contained in the Bartlesville format unit. Determination of net sandstone was made with the use of the SP curve, sandstone being defined as any point on the SP curve 20 mv or more to the left of the shale base line.

Inspection of the net-sandstone isolith map reveals three thick sandstone trends of sandstone that is thicker than 90 feet. These trends extend from Section 32 T19N-R7E to Section 15-T18N-R7E, Section 24-T18N-R7E to Section 17-T17N-R7E and from Section 25-T18N-R7E to Section 35-T17N-R7E. Each of these trends is composed of two or more sand bodies. The geometry of the thickest sand trends, especially toward the west-southwest portion of the map, suggest that these sands were deposited by distributary channels within a lobate to elongate deltas The streams entered the area from the north and east. Whereas the sand trends are quite wide, the streams that deposited the sands were probably much more narrow. Individual streams probably deposited sand bodies less than 60 feet thick (Shelton, personal communication, 1982).

Total-format Isopach Map (Plate 4)

The Bartlesville total-format isopach reveals trends that are much similar to those of the net sandstone isolith map. This is due to two reasons: (1) Sections primarily of shale tended to compact more than sections of sandstone. Thus, intervals containing sand would tend to be thicker. (2) Rates and amounts of sedimentation in channels where sandstones probably deposited may have been much greater than in interdistributary areas of flood plains where the shales probably were deposited.

One of the most noteworthy aspects of Plate 4 is the thinning of the format over structurally high locations. Examples of this exist in Sections 7, 17, 18-T18N-R7E (Dropright Dome), Sections 27, 28, 33, 34, T18N-R7E (Drumright Dome), Section 3-T17N-R7E (Mt. Pleasant Dome), and Sections 15, 16, 21, 22-T17N-R7E (Shamrock Dome). This can also be clearly seen on the north-south structural cross-section (Plate 3a

Mark 1 well). As has been documented in numerous other investigations, domes of the Cushing anticline were exposed paleotopographic highs during Early Pennsylvanian. Also, as has been discussed in this paper, evidence indicates that the Cushing anticline continued to grow throughout Desmoinesian and even into Missourian time, growth of the structure probably being related to movement along the Wilzetta Fault. Continued growth of the major fold definitely would inhibit deposition of sediments over the areas of maximal growth and maximal topographic relief.

Electric-log Signature Map (Plate 6)

The electric-log signature map was of great use in delineating continuous sand bodies and defining geometries of individual channels. Four sand bodies were identified from log signatures. Each had an abrupt basal contact and either an abrupt or transitional upper contact. Based on log signatures, geometries of the general sand-thickness trends, sequences of sedimentary structures in cores (refer to the Appendix) and lack of marine fauna, the conclusion drawn was that the sand bodies were deposited by streams (either delta distributaries or meandering fluvial streams) without marine influence.

Two major channels were identified. The first and lowermost one deposited a sand body (as thick as 60 feet) that lies just above the Brown Limestone. Based on SP characteristics, the sand body is well developed; basal and upper contacts are abrupt, suggesting a delta-distributary channel. At places, the channel eroded into or through the Brown Limestone. The area over which the lower sand body was deposited is colored in red (Plate 6).

The second major channel deposited sand less than 50 feet thick;

it occupies the middle portion of the format. This second channel obviously came after the first sand body had compacted and subsided. Examination of the areas containing the second sand body (colored yellow) reveal a pattern more meandering than that of the first channel. Also, the SP signature of the second sand body, particularly in the west-southwestern portion of the map, is characteristic of a point bar deposit of a meandering fluvial stream (Plate 6).

The lowermost and middle channels appear to have had largely similar patterns except in the northern part of T18N-R7E and the northern part of T16N-R7E. Overlapping of channels resulted in stacked sand bodies observable throughout the central portion of the map (where red and yellow patterns overlap) and on stratigraphic cross-sections, particularly FF', GG', and HH'. At some locations the sand bodies are continously vertical, indicating that the middle channel eroded into the lowermost sand body. Good examples of this are seen in Sections 4, 9, 10, 15, 16-T17N-R7E (Plate 6).

The third sand body is more difficult to discern; it appears to have been deposited over a much smaller area. This sandstone lies between the second sand body and the position of the Inola Limestone. It may have resulted from lateral shifting of the stream within the second (middle) channel. Trend of the channel that deposited this sand body meanders within the path of the other two channels. The channel appears to have been a small, meandering fluvial channel which left behind point-bar deposits. The upper parts of point bar sequences are absent in many of the sand bodies (i.e., an abrupt upper contact is more common than the transitional upper contact characteristic of point-bar deposits). This absence could have resulted from reworking

of the upper silts and shales by the transgressive sea that deposited the Inola Limestone.

The fourth and uppermost sand body in the interval is most easily detected in the areas where shale is the predominant lithology throughout the Bartlesville interval, and where the other three sand bodies are absent. Presumably, the region shown in Figure 26 is on the fringe of a delta lobe, there being no significant Bartlesville sand deposition to the west of the area. Directly underlying the Inola Limestone, this sand is very silty and clayey; it barely can be classified as a sandstone. It being positioned where it is, being silty sandstone and being on the edge of a delta lobe suggests that this sand body is a strandline deposit composed of delta sands reworked by the Cherokee Sea as it transgressed northward.

Stratigraphic Cross-sections

Twelve east-west stratigraphic cross-sections were constructed to help determine lateral continuity of the sand bodies within the Bartlesville format (Plates 2a, 2b). Labeled AA' through LL', the cross-sections extend across the Cushing Field from the northern area of T18N-R7E to the northern part of T16N-R7E. The four sand bodies discussed above are shown as follows: sand body 1 - red; sand body 2 - yellow; sand body 3 - blue; sand body 4 - green. Sand body 1 is present on all cross-sections except MM' and NN' in the southern part of the field; sand body 2 is on all cross-sections; sand body 3 is on cross-sections DD' through JJ'; and sand body 4 is on cross-sections FF', GG' and KK' only.

One significant feature illustrated by the cross-sections is the thickening of section from the base of the Oswego to the top of the

Inola Limestone on the downthrown eastern block of the Wilzetta Fault. Thickening of section ranges from 65 to 125 feet (cross-sections JJ' and LL, respectively). Cross-section HH' does not cut the fault, and cross-section GG' cuts only the minor cross fault in the south-central part of T18N-R7E. In several cases (cross-sections CC', FF', KK', and LL') sandstones are developed better on the downthrown block, suggesting that the stream followed a fault scarp. Evidently this is common along recent strike-slip faults in California (Billings, 1972). This thickening of section clearly indicates that the Wilzetta Fault was active during deposition of middle and late Desmoinesian sediments and that there were dip-slip movements along the fault, the eastern block being downthrown.

A second important feature brought out by the cross-sections is the lack of lateral continuity of the sand bodies. In several instances the character of the sand body changed completely within 1/2 mile. Major variation between wells separated by one or more miles is commonplace.

A third feature revealed by these cross-sections (as well as by the electric-log signature map) is the vertical stacking of sand bodies. Cross-sections CC', DD', and FF' point out this feature most distinctly. As can be seen on some of the electric logs, determination of individual sand bodies is impossible because of the close stacking of the bodies.

Core Description

Nine cores were available for examination and sampling. Core locations are plotted on Figure 27, and core descriptions can be found in the Appendix. Cores were examined for gross lithology, constituents,

grain size, and sedimentary structures. Analysis of the cores, especially of the nature and vertical sequence of sedimentary structures, aided in the determination of depositional environments. Each of the cores is briefly described and interpreted in the following paragraphs.

Getty Oil Co. Cobb 6, Section 3-T17N-R7E

Core from the Getty Oil Co. Cobb 6 was described by Shelton (1973) and by the author. The core contains two stacked sand bodies probably deposited by separate channels. Sand body 1 occurs from 2446 to 2428 feet; sand body 2 from 2425 to 2382 feet. The two bodies are separated by a four-foot zone of intraformational conglomerate composed of clay rip-up clasts and fine to medium grained sand. The SP curve indicates that the zone is shaly, but the SP deflection was affected by the clay rip-up clasts. The clasts represent a high energy flow regime commonly found in the thalweg of a channel. The abrupt lower contact suggests channel scouring. The cored interval consists primarily of quartz sand with traces of feldspar, mica, calcite, carbonized fragments, occasional small siderite clasts and pyrite. Grain size in sand body 1 remains essentially constant at fine to medium grained. In sand body 2, grain size tends to fine upward from fine to medium grained at the base of the interval to very fine to fine grained at the top of the interval. Sedimentary structures are massive bedding, small to medium scale trough cross-bedding, initial depositional dip, parallel laminations and small amounts of bioturbation and soft sediment deformation. The sequence of structures is ambiguous, but their nature suggests stream channel deposition. Specific channel type cannot be determined from the core analysis alone.

Sinclair Oil Co. B. B. Jones 21, Section 4-T17N-R7E

The interval cored (2590 to 2656 feet) contains part of sand body 2 (from 2600 to 2656 feet) and all of sand body 3 (2590 to 2599 feet). Separation of the two bodies is based on scour marks and the presence of an intraformational conglomerate composed of clay rip-up clasts. Sharp basal and upper contacts characterizes both sand bodies. The Bartlesville format extends from 2590 to 2656 feet. Constitutents in these sands are the same as in the Getty Cobb 5 . Additionally, a trace of glauconite is present. The sand is fine to medium grained. Sedimentary structures are mainly small to medium scale cross-bedding and parallel laminations. Traces of massive bedding, concretions of calcite, soft sediment deformation carbonaceous laiminae are also present. Stream channel deposition is suggested by the nature of the sedimentary structures; however, the sequence of structures is not diagnostic.

Sinclair Oil Co. L. Yarhola 24, Section 9-T17N-R7E

The cored interval (2646-2700 feet) contains sand body 2. This core is located approximately 1/2 mile away from the Sinclair Oil Co. B. B. Jones 21, and has the same characteristics as the B. B. Jones 21. SP characteristics of the two wells are similar.

Gulf Oil Co. P. Brown 9, Section 33-T17N-R7E

The Bartlesville format extends from 2720 to 2780 feet; the top of the sand is 2736 feet and the interval cord is from 2736 to 2776 feet. Both the upper and lower contacts of the sand are abrupt. The cored

interval consists of sand body 1. The sand contains quartz with small amounts of feldspar, siderite, carbonaceous matter, and traces of galena, mica, calcite, and pyrite. Calcite, pyrite, and galena are authigenic constituents. Sedimentary structures are parallel laminations, massive bedding, small to medium-scale trough cross-bedding, soft sediment deformation and carbonate laminae. The fine to medium sand size decreases to very fine in the upper ten feet of the interval. The sand is believed to have been deposited by a distributary stream channel. This conclusion is based on SP curve shape, lack of grain size change over most of the interval, and location with respect to sand trends observed on the electric log signature map and the net sandstone isolith map.

Sinclair Oil Co. S. Boone 6, Section 34-T17N-R7E

Twenty-four of a possible thirty-nine feet of sand were cored in this well. The interval cored extends from 2766 to 2790 feet. The elctric log indicates that the Bartlesville format extends from 2767 to 2806 feet. The sand body, most likely sand body 1, has a sharp lower contact and less abrupt upper contact. Constituents are the same as in the other cores. The sand is predominantly fine to medium grained. Bedding is largely massive though small to medium-scale trough and planar cross-bedding and parallel laminations are frequently seen. Small amounts of bioturbation, soft sediment deformation and coaly laminae also are present. A stream channel origin, probably a deltic distributary, is suspected for this sand body based on the above data as well as evidence gathered from the maps.

Sinclair Oil Co. P. Brown 8, Section 34-T17N-R7E

Thirty-two feet of sand body 1 were cored. The P. Brown 8 and the S. Boone 6 are closely situated, and this is reflected in the similar thickness, constituents, sedimentary structures, SP signature, and the inferred delta distributary depositional environment.

Sinclair Oil Co. Lesta Keys 46, Section 28-T17N-R7E

Most of the cored interval consists of interbedded shales and sands. The interval cored, 2784 to 2837 feet, contains the lower portion of sand body 3, all of sand body 2, and probably the upper portion of sand body 1 (2830-2837 feet). Sand body 3 (2784-2795 feet) is very shaly and shows little SP development. The sand in all three bodies is fine to medium grained. Dominant sedimentary structures are parallel laminations, small-scale trough cross-bedding and some massive bedding. Soft sediment formation, common in sand body 2, is absent in sand body 1. Intraformational conglomerate composed of clay clasts is present at 2830 feet.

Sinclair Oil Co. Cushing CO-OP Water Flood Supply S-1, Section 3-T17N-R7E

The cored interval extends from 2610 to 2645 feet, while the Bartlesville zone, predominantly sandstone, lies between 2593 and 2725 feet. Part of sand body 2 (2640 to 2645 feet) and probably all of sand body 3 are contained in the cored interval. While located only a very short distance from the Lesta Keys 46, both sands in the Cushing Co-op have a much better developed SP and were also more coarsely grained (medium vs fine to medium). Predominant sedimentary structures are small to

medium-scale trough cross-bedding, massive bedding and parallel laminations. Some soft sediment deformation is present. This sand body appears to have been deposited in an alluvial channel. Evidence to support this statement is the same as for the Lesta Keys 46.

ARCO Hettie Dunson 42, Section 33-T17N-R7E

Electric logs for this core were not available. Also, the condition of the core is very poor. Consequently, very little could be determined about sedimentary structures and depositional environment. Constituents are the same as in the other cores. Medium grain size predominates. The interval is characterized by sand and a large amount of intraformational conglomerate composed of clay clasts. Very little shale can be seen. The sand appears to have been deposited in a high energy environment and could well have been located in the thalweg of a stream.

Depositional Environment Conclusions

Based on a thorough review of the literature, examination of eight cores, construction and analyis of electric log signature, net sandstone isolith, and total format isopach maps, two structural cross-sections and twelve stratigraphic cross-sections through the Cushing Field and a literature survey, the following conclusions can be made:

1. Deposition of the Cherokee Group probably resulted from a single major drainage pattern (Visher, Saitta and Phares, 1971).

2. The Bartlesville Sandstone represents a regressive progradational phase of the general Cherokee transgression during Desmoinesian time. Thickening of the unit into the Arkoma Basin suggests active subsidence of the basin during Bartlesville deposition.

3. In the study area, the Bartlesville format represents progradation of a delta lobe. This lobe was later abandoned as the depositing stream avulsed to the southeast.

4. Four different sand bodies are present in the Bartlesville format in the study area. Sand bodies 1, 2, and 3 are frequently stacked upon each other. Sand body 1 was most likely deposited in a delta distributary channel; sand bodies 2 and 3 were probably deposited in the same fluvial channel (but a different channel from the one which deposited sand body 1). Deposition of two separate sand bodies resulted from lateral shifting of the fluvial stream; sand body 4 is clayey and silty. It is most likely a strandline deposit left by the Cherokee Sea as it transgressed northward.

5. Deposition of the Bartlesville in the study area was influenced by structural geology. Stream channels have generally avoided structural highs.

6. Thickening of the Oswego to Brown Limestone section, and generally better sand development on the downthrown eastern block of the Wilzetta Fault, indicate the fault was active during Cherokee deposition and that a paleo-fault scarp existed and influenced Bartlesville Sandstone deposition.

7. Abandonment of the delta was the final event in the depositional history of the Bartlesville Sandstone. Deposition of the Inola Limestone ensued.

CHAPTER VIII

PETROLOGY

While a large number of subsurface stratigraphic studies of the Cherokee Group have been completed in and around the thesis area, none gives a detailed description of the petrology, diagenetic features or porosity types present in the Bartlesville Sand. The purpose of this chapter is to review the literature on petrology of the Bartlesville Sand, list the detrital and authigenic minerals that were identified in this study, and describe the methods used to identify them. Descriptions of morphology of the authegenic minerals will be left for Chapter IX.

Investigations by Bass (1934), Hanke (1967), Hawisa (1965), McElroy (1961), Phares (1969), Saitta (1968), Pulling (1979), and Verish (1978) all generally describe the Bartlesville as being largely composed of white to light gray-buff, very fine to medium grained, angular to subangular quartz with traces of chert, feldspars, mica, hornblende, rutile, zircon, and other minor minerals. Cements identified were siderite (Bass et al., 1937) quartz and calcite (McElroy, 1961), or dolomite (Leatherock and Bass, 1937).

The most detailed petrologic studies of the sand were done by Leatherock and Bass (1937) and Visher et al. (1971). Leathercock and Bass noted a large percentage (10 to 20 percent) of rock fragments and a regionally uniform composition and texture. Visher et al. (1971)

described the Bartlesville in northeast Oklahoma as a subgraywacke, having recognized large amounts of feldspar, mica, rock fragments, and matrix. Clay minerals identified as kaolinite, iron chlorite and illite. Illite and chlorite were suspected of being diagenetic alteration products of kaolinite, the supposed original clay minerals. Apparently both of these studies were qualitative in nature. No quantitative petrologic data were presented.

Methododology

Methods used to determine qualitative and quantitative mineralogy were: x-ray diffraction of powdered and "clay-extracted" (Kittrick, Patrick and Hope, 1963) samples, routine thin-section examination and scanning electron microscopy (SEM). The SEM was fitted with an energy dispersive x-ray analyzer (EDAX). X-ray diffraction of powdered samples and SEM/EDAX provided means of identifying gross mineralogy, while thin-section examination was used for quantitative mineralogic determination.

More than 300 points were counted from each thin section. The amount of each mineral was then averaged.

X-ray diffraction of clay-extracted samples gave semi-quantitative values of the amounts of each clay mineral present. Areas under 100 percent intensity peaks were calculated and then used in Equation 1 or 2 to determine the approximate percentages of each clay type.

1. Three clay minerals present:

$$I_i(.29) + I_{ch}(.55) + I_k(.15) = cI_{Total}$$

2. Two clay minerals present (i.e., kaolinite and illite)

$$I_i(.29) + I_k(.15) = cI_{Total}$$

I_i = area under illite curve

I_{ch} = are under chlorite curve

I_k = area under kaolinte curve

$^cI_{Total}$ = total area

(.29), (.55), and (1.15) = absorbtion coefficients for the respective clays

(Personal communication, Al-Shaieb, 1982)

Percentages of mixed layer clays were not calculated, as the absorbtion coefficients were unavailable.

Detrital Constituents

Thin sections from four cores were examined for quantitative mineralogy (Figure 27). The data were then plotted on a quartz/feldspar/rock fragment ternary diagram (Figures 28 and 29; the raw data are presented in Table I). The sandstone, which classifies primarily as a subarkose, was originally probably askosic in composition, since a significant percentage of the feldspars have been leached from the sample or altered to clay as a result of hydrolysis reactions.

Quartz, the major detrital constituent, ranges from 38.9 to 74 percent and averaged 59.4 percent of the sample. Feldspars (plagioclase and potassic feldspar--mainly microcline) (Figures 30 and 31) are also abundant, varying from 2.9 to 17.3 percent averaging 9.4 percent of the sample, while rock fragments (chert, micaceous and quartz metamorphic rock fragments, shale clasts and carbonate clasts, Figure 32) are in least abundance, ranging from .4 to 14.3 percent and averaging 4.5 per cent of the sample. Detrital matrix (Figure 33) averages 2.4 percent. Other detrital constituents are present, but each accounts for less

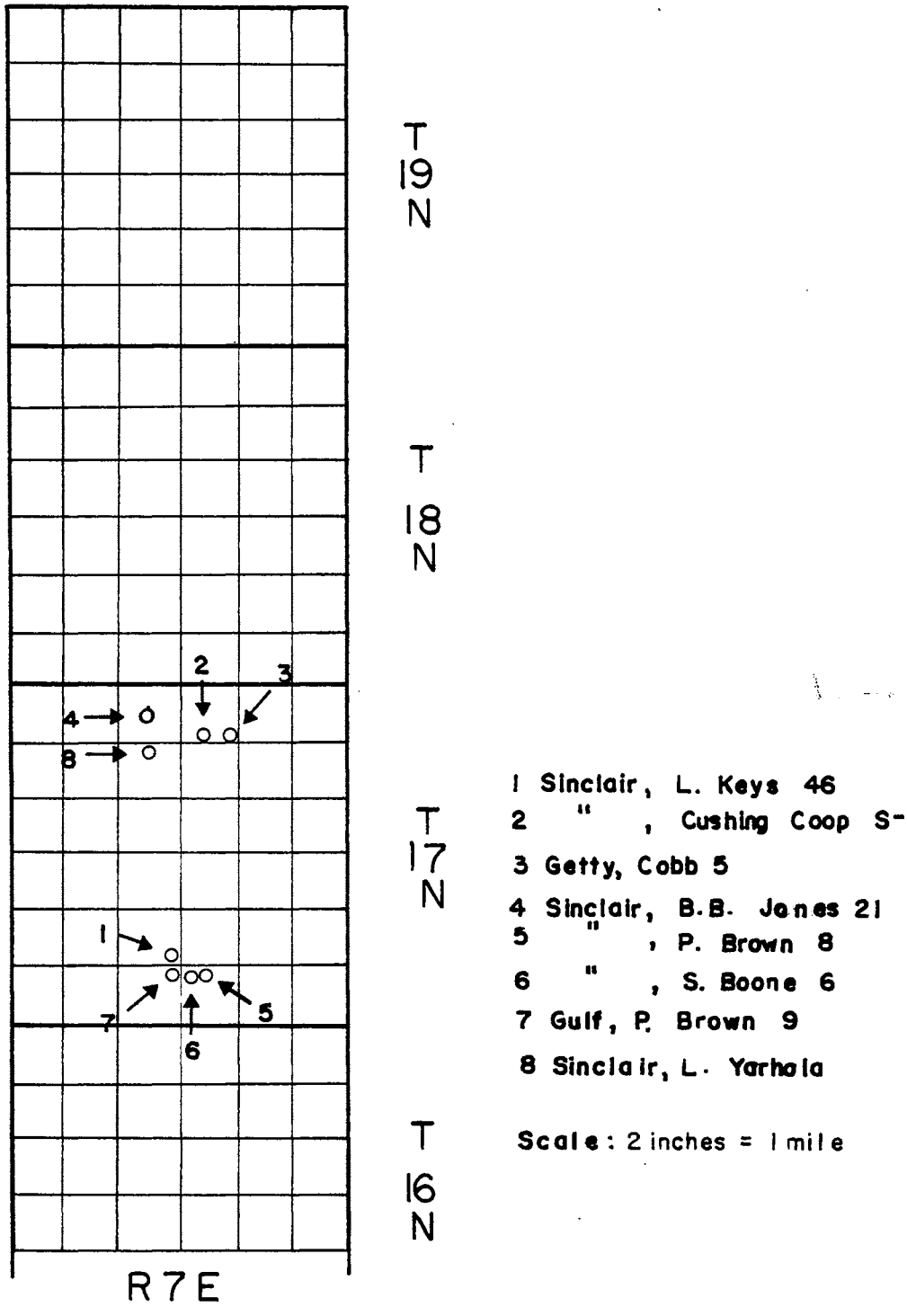

Figure 27. Map Showing Locations of the Cores Used in the Study

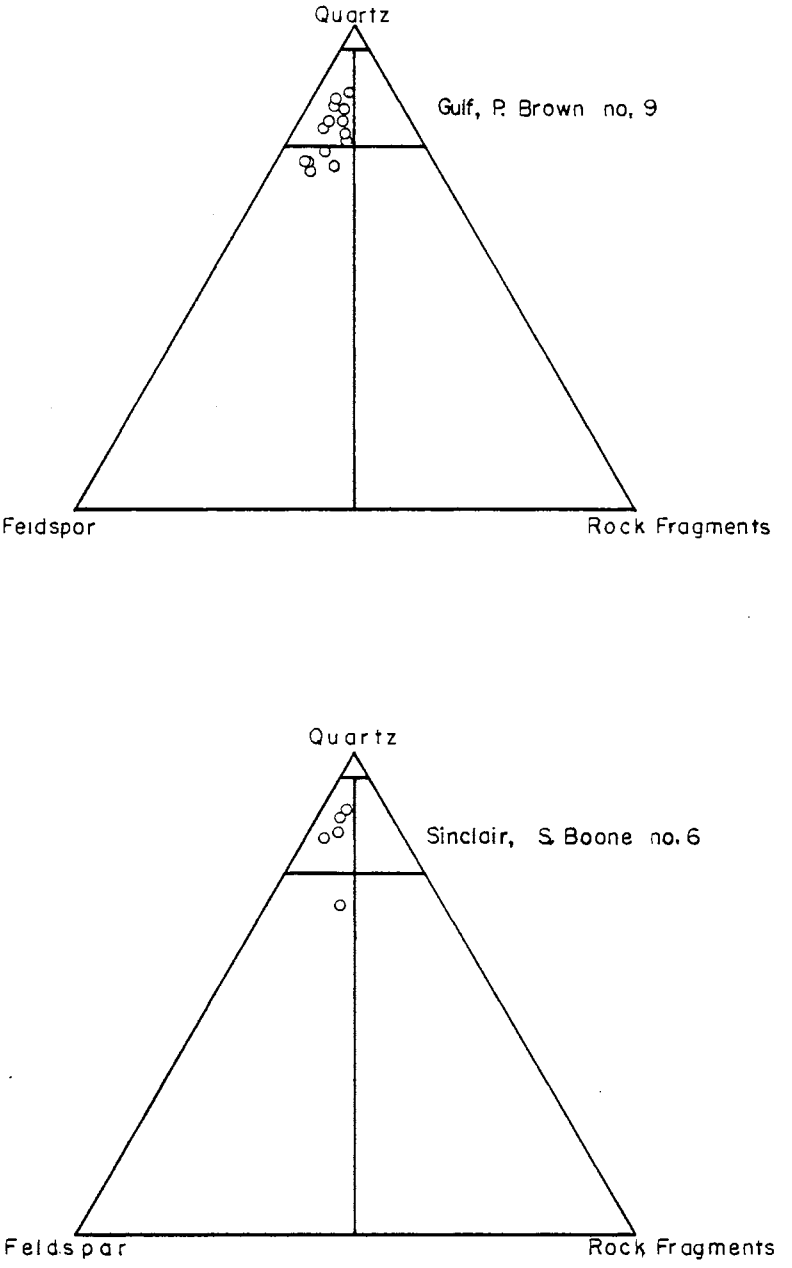

Figure 28. Ternary Diagram Depicting the Mineralogic Composition of the Gulf P. Brown 9 Core and the Sinclair S. Boone 6 Core. (Percentages are corrected to 100 percent; original data based upon thin section examination.)

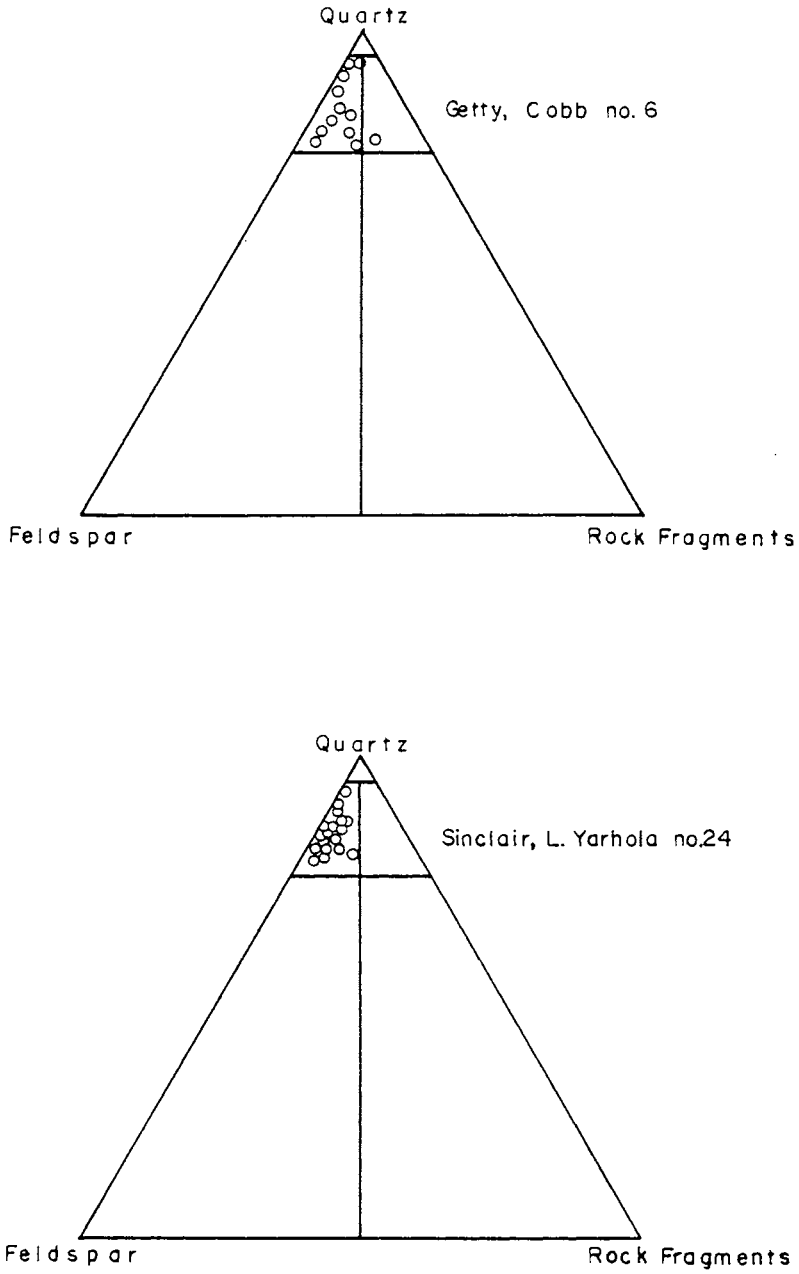

Figure 29. Ternary Diagram Depicting the Mineralogic Composition of the Getty, Cobb 6 and Sinclair, L. Yarhola 24 Cores. (Percentages are corrected to 100 percent; original data based upon thin section examination.)

TABLE I

CORRECTED VALUES OF MINERALOGIC COMPOSITIONS BASED ON THIN SECTION EXAMINATION

Getty Oil Co. Cobb #6				Gulf Oil Co. P. Brown #9				Sinclair Oil Co. L. Yarhola #24				Sinclair Oil Co. S. Boone #6			
Depth	Qtz	Fspar	RF	Depth	Qtz	Fspar	RF	Depth	Qtz	Fspar	RF	Depth	Fspar	Qtz	RF
2391	94.4	5.6	0.0	2737	71.8	23.4	4.8	2651	83.7	13.1	3.2	2772	81.9	14.8	3.3
2396	92.0	7.2	0.8	2740	74.2	19.3	6.5	2653	81.8	13.7	4.5	2775	83.3	11.4	5.3
2402	94.3	3.7	2.0	2743	70.0	24.0	6.0	2655	85.0	14.4	0.6	2780	87.5	8.3	4.2
2406	79.2	17.2	3.6	2744	72.2	22.6	5.2	2659	86.6	12.4	1.0	2782	67.0	18.0	15.0
2410	88.3	10.2	1.5	2745	87.1	6.8	6.1	2662	87.5	8.3	4.2	2790	86.0	9.8	4.2
2414	80.4	16.3	3.3	2746	78.9	15.6	5.5	2670	87.1	11.0	1.9				
2416	83.2	11.4	5.4	2747	85.2	10.7	4.1	2673	86.7	10.8	2.5				
2419	84.1	12.3	3.6	2748	77.2	13.4	9.4	2676	87.5	8.8	3.7				
2426	76.7	17.6	5.7	2752	82.6	13.2	4.2	2681	88.2	9.4	2.4				
2431	78.7	12.8	8.5	2755	79.4	15.1	5.5	2684	79.7	12.2	8.1				
2435	78.0	10.4	11.6	2759	82.5	11.3	6.2	2687	88.9	9.8	1.3				
2441	82.1	14.7	3.2	2772	73.0	20.4	6.6	2690	82.0	15.6	2.4				
2444	74.8	16.2	9.0	2773	76.0	13.8	10.2	2692	92.7	7.5	0.8				
2447	76.3	12.9	10.8	2775	80.6	11.9	7.5	2694	83.3	14.9	1.9				
				2776	71.4	18.3	10.3	2697	80.5	18.0	1.5				
								2699	81.3	16.0	2.7				
								2700	82.0	16.7	1.3				

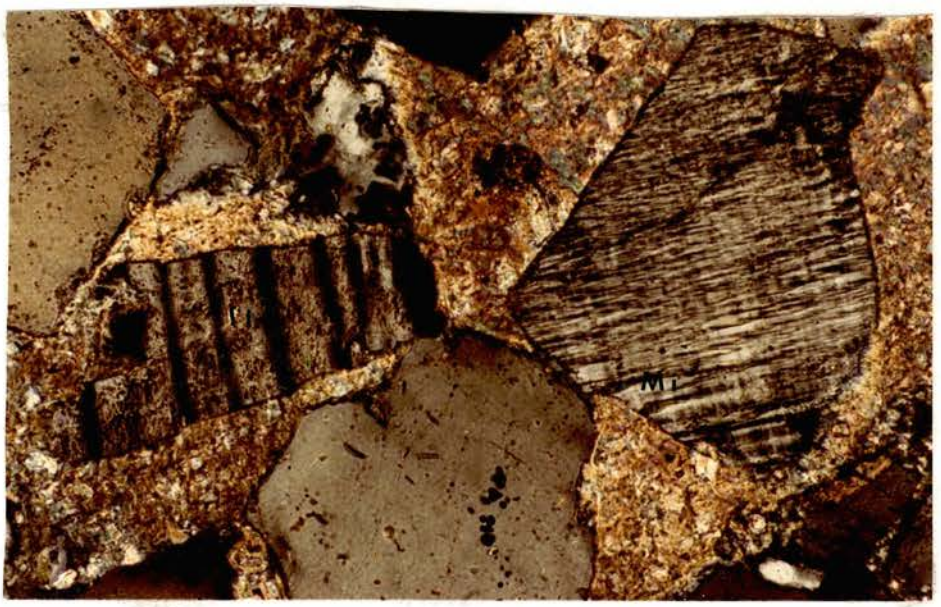

Figure 30. Photo-micrograph Under Crossed Nicols of Calcite, Plagioclase and Microcline

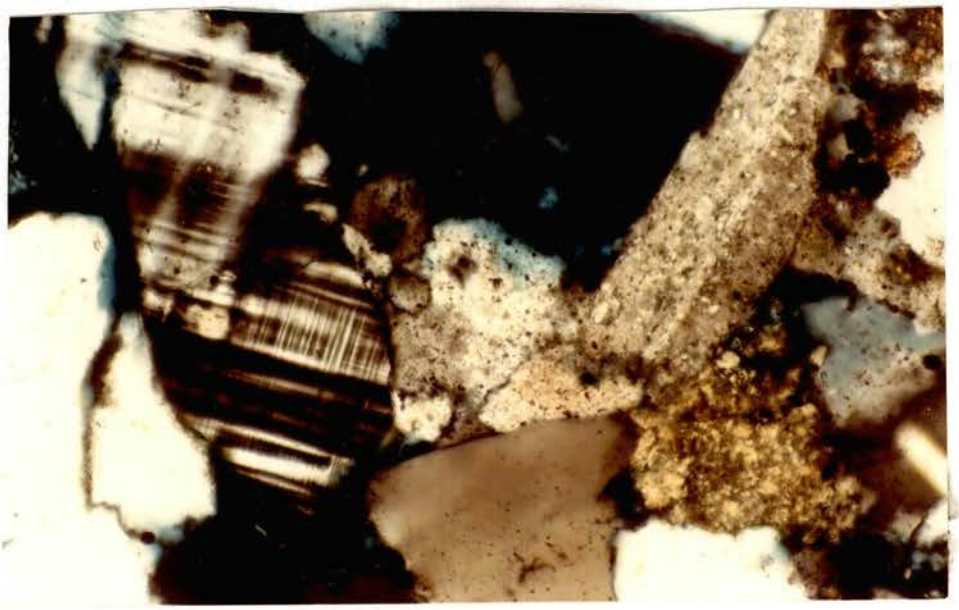

Figure 31. Photo-micrograph Under Crossed Nicols of Microcline

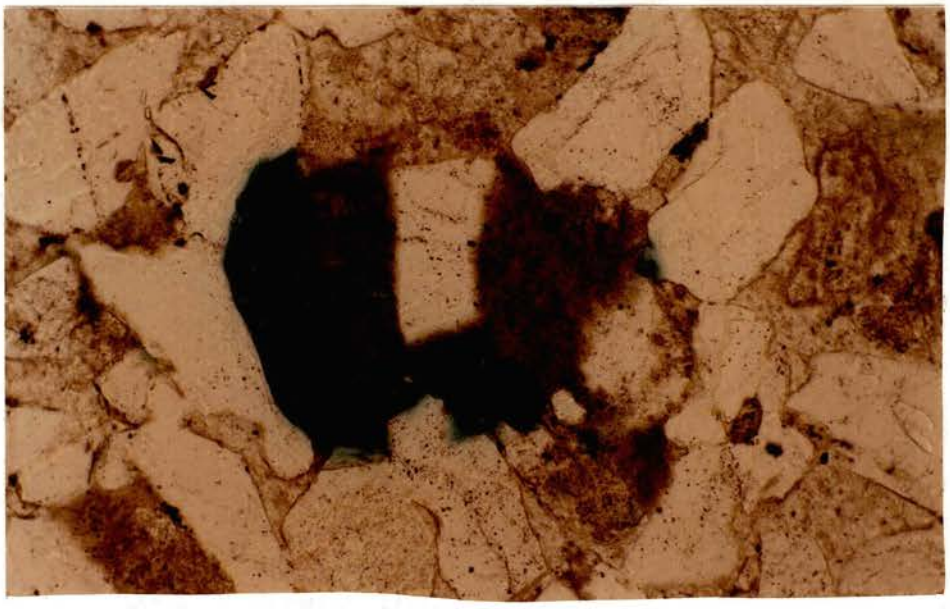

Figure 32. Photo-micrograph of Secondary Porosity Created From the Dissolution of Detrital Matrix (plane polarized light)

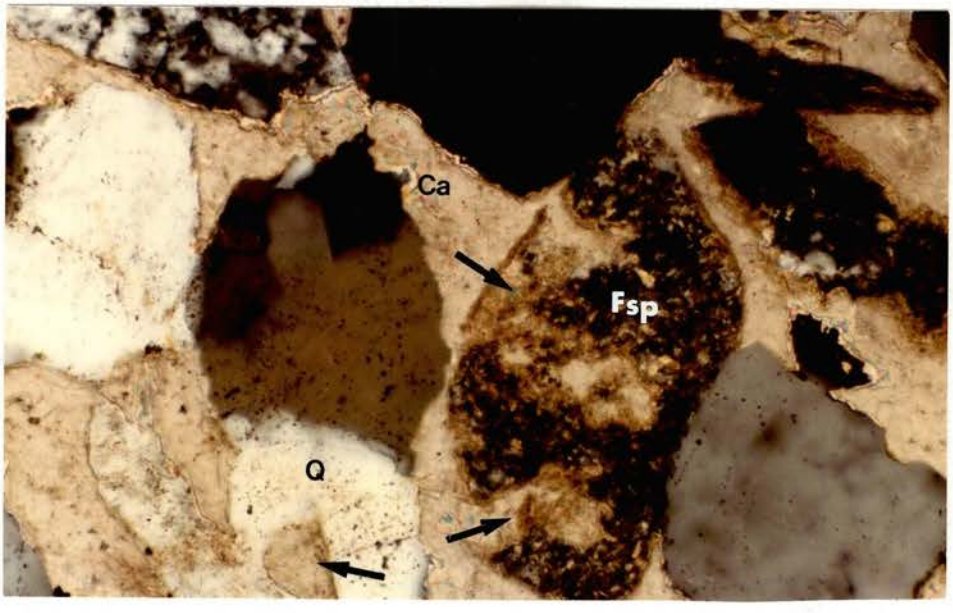

Figure 33. Photo-micrograph of Calcite Replacement of Quartz and Feldspar (crossed nicols)

than one percent of the sample: glauconite, hematite (Figures 36 and 37), zircon (Figures 34 and 35), muscovite (Figures 36 and 37), hornblende, magnetite, rutile, and carbonaceous matter.

The only exceptions to the uniform subarkose-arkose composition (Figures 38 and 39) are several sand samples from the Getty - Cobb No. 6 core. These samples approach a quartz arenite in mineralogy, and are from a distinctly separate 20-foot sand body near the top of the interval. The difference in mineralogy was most likely caused by a difference in depositional environments, the nearly quartz arenite samples being part of a transgressive sand sequence. Mineralogic partitioning probably was the sorting mechanism resposible for the deficiency of feldspar and rock fragments.

Texturally, all samples are predominantly fine to medium grained. Siltstone and very fine grained sandstone are present usually when detrital clays are abundant. Because of the important roles played by diagenetic processes in modifying the reservoir, present grain shapes and textures (subangular to angular) are probably much different than the original shapes and textures. The original grain shape was probably more rounded.

Authigenic Constituents

Authigenic minerals, excluding syntaxial quartz overgrowth, average approximately 9.7 percent of all of the samples. The average amount of syntaxial quartz overgrowth was difficult to measure accurately, but accounted for approximately five percent of each sample. Authigenic minerals are: quartz (syntaxial overgrowth, Figure 41); microquartz (Figures 53 and 54); opal and chalcedony(Figures 42 and 43); traces of

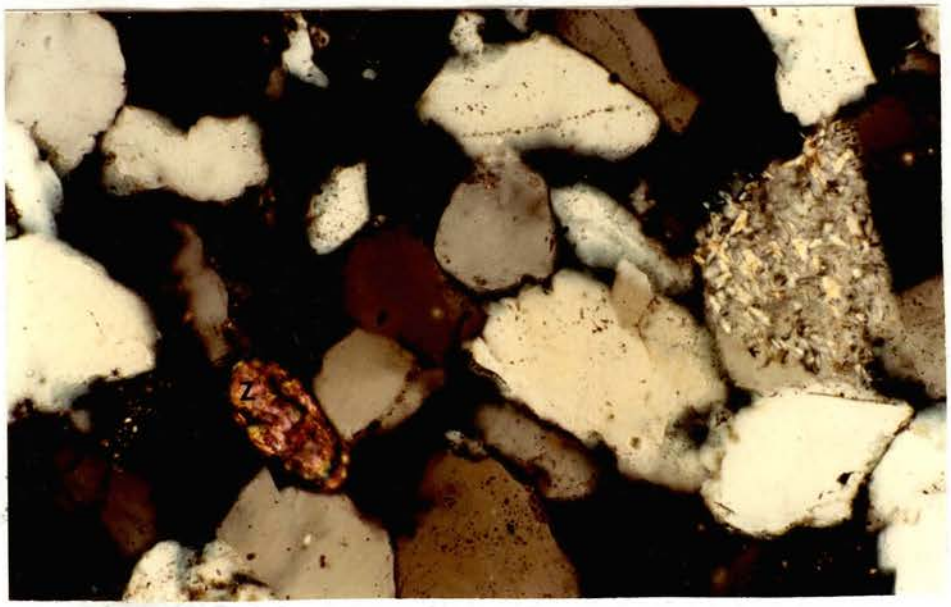

Figure 34. Photo-micrograph of Zircon and Feldspar Altering to Clay (crossed nicols)

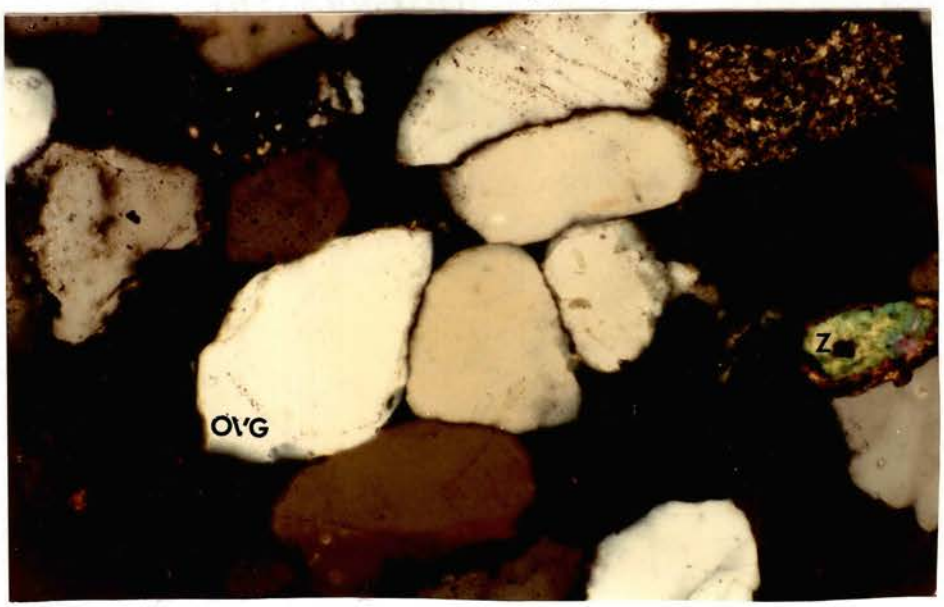

Figure 35. Photo-micrograph of Zircon and Quartz Overgrowth (crossed nicols)

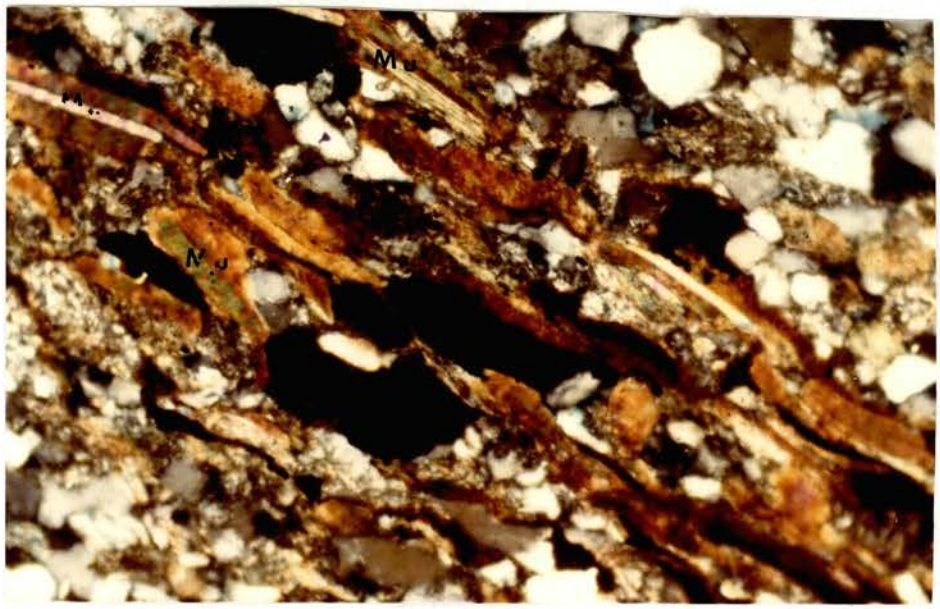

Figure 36. Photo-micrograph of Hematite and Muscovite (crossed nicols)

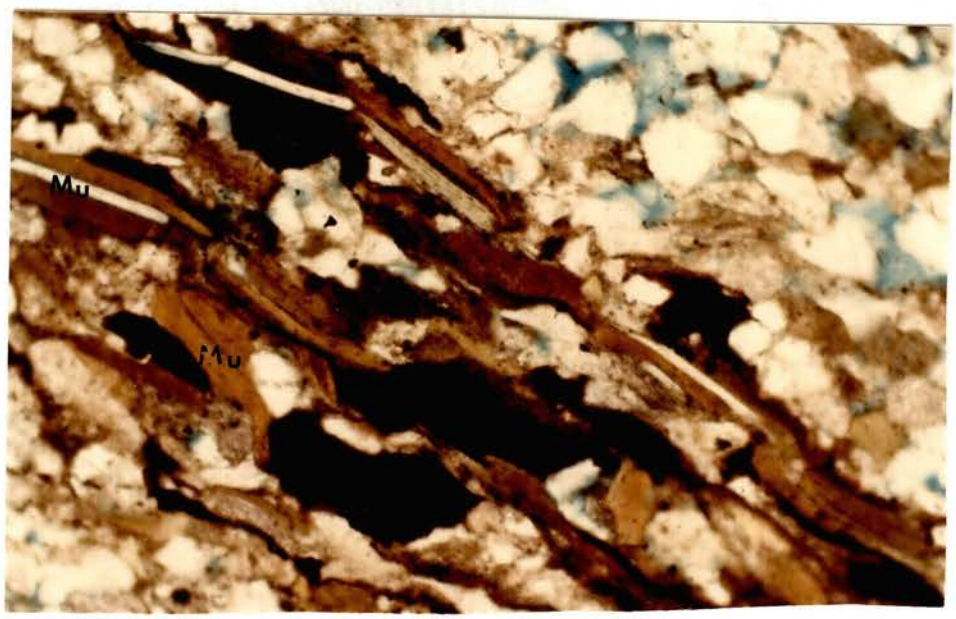

Figure 37. Photo-micrograph of Hematite and Muscovite (plane polarized light)

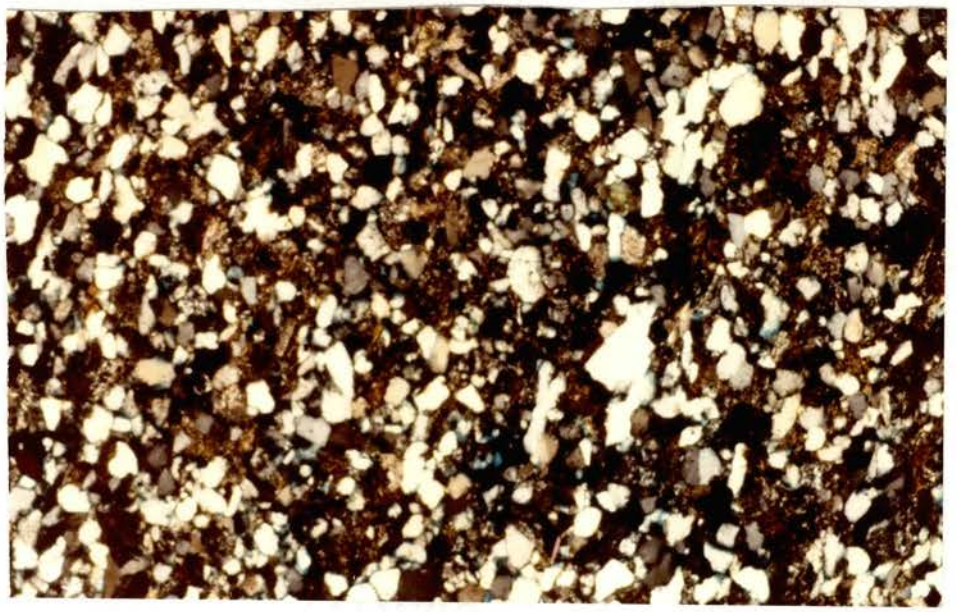

Figure 38. Photomicrograph of an Arkosic Facies (crossed nicols)

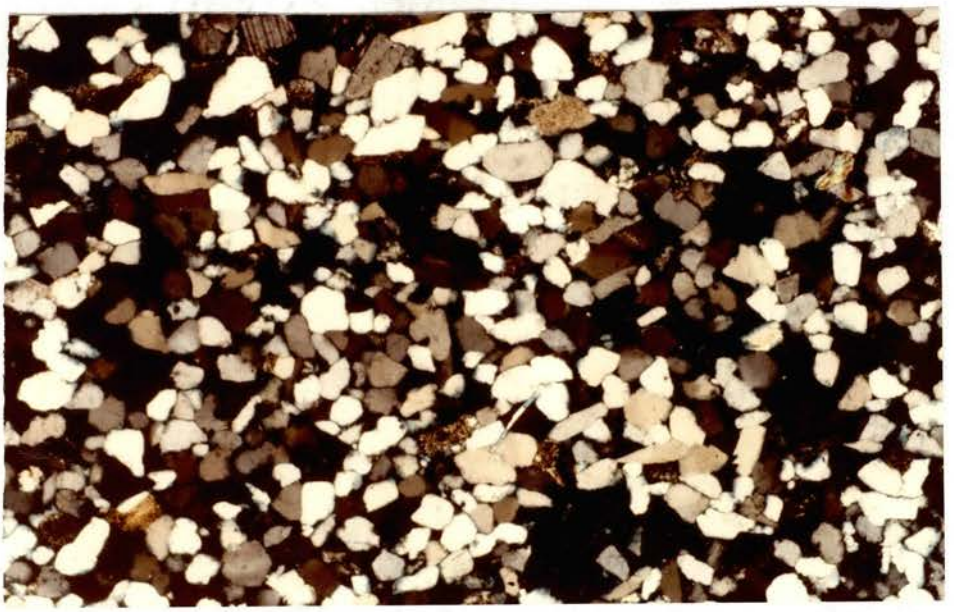

Figure 39. Photomicrograph of a Quartz Arenite Facies

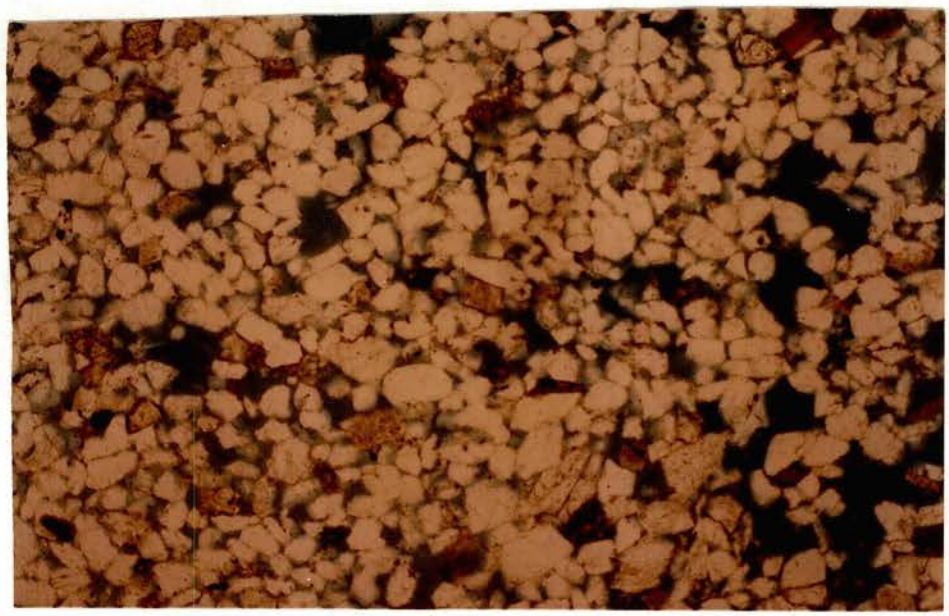

Figure 40. Photo-micrograph of Quartz Arenite Facies (plane polarized light)

Figure 41. Photo-micrograph of a Quartz Overgrowth With a Chlorite Dust-Rim (crossed nicols)

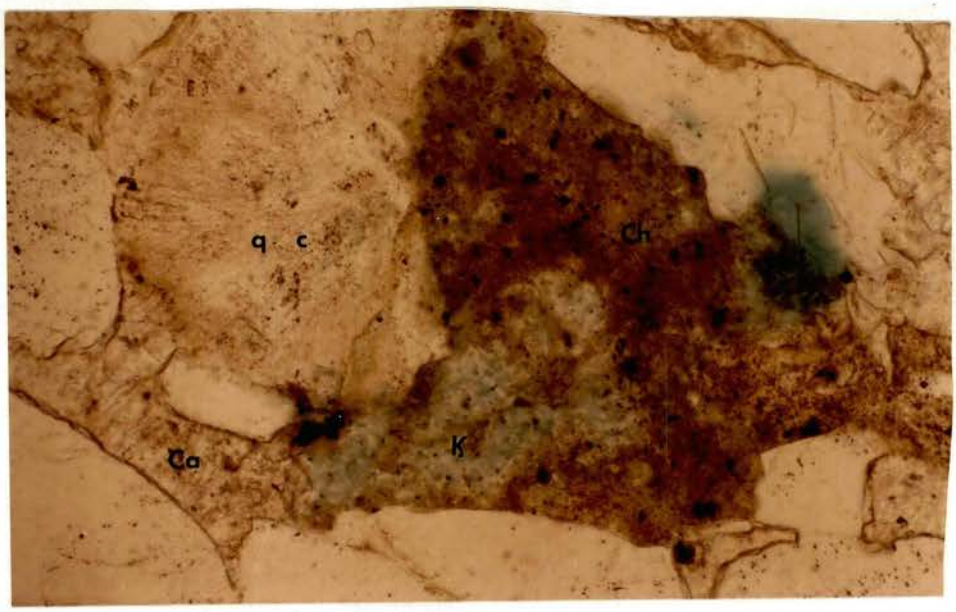

Figure 42. Photo-micrograph of Chaledony, Calcite and Kaolinite Altering to Chlorite (plane polarized light)

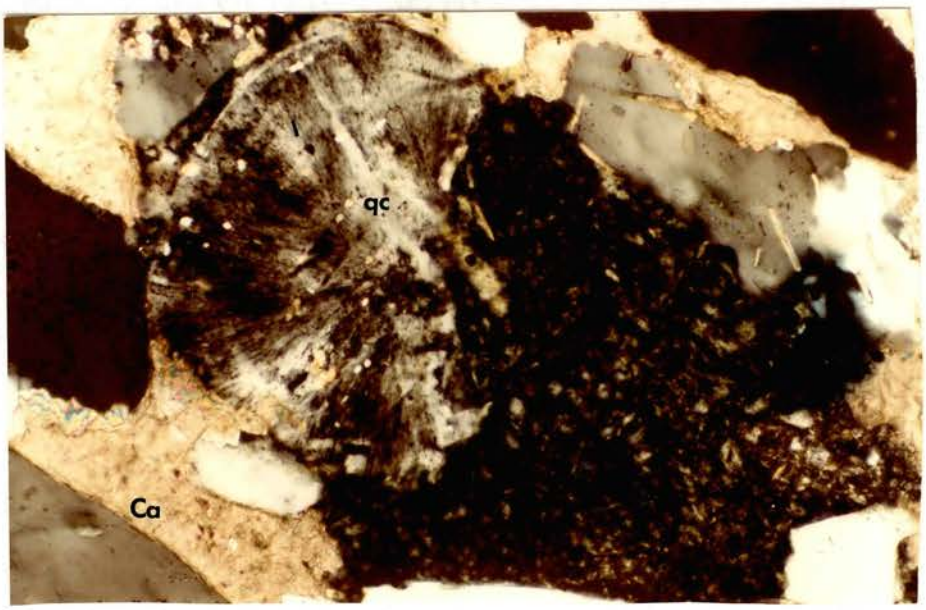

Figure 43. Photo-micrograph of Figure 42 (crossed nicols)

feldspar overgrowths, calcite (Figures 30, 32, 43, and 44); siderite (Figure 45); hematite (Figures 36 and 37); pyrite (Figures 69 and 70); leucoxene, galena, collophane and authigenic clays: kaolinite (Figures 46 and 47); illite (Figure 34); chlorite (Figures 38 and 39), and traces of mixed layer illite-smectite). Syntaxial quartz overgrowths and the authigenic clays are by far the most abundant and will be described in detail. The other minerals each make up less than one percent of the mineralogic composition and will be described in Chapter IX on diagenetic features.

Quartz Cements

Syntaxial quartz overgrowths account for approximately five per cent of each sample. Micro-quartz, opal and clalcedony are more rare as cements. Only scattered occurrences of chalcedony and opal exist in the samples.

Clays

Authigenic clays are also relatively abundant, averaging 3.9 per cent of the samples. With the use of the x-ray diffractometer and formulae I and II, the approximate percentages of the different clays were calculated. The percentage of each clay type is: kaolinite, 57.5 per cent; illite, 27.2 per cent; chlorite, 15.3 per cent. These values include both detrital and authigenic clays. Figure 48 depicts the sharp x-ray diffraction peaks characteristic of the well crystalline authigenic clays after clay extraction. X-ray diffraction peaks of the generally less crystalline detrital clays are more broad.

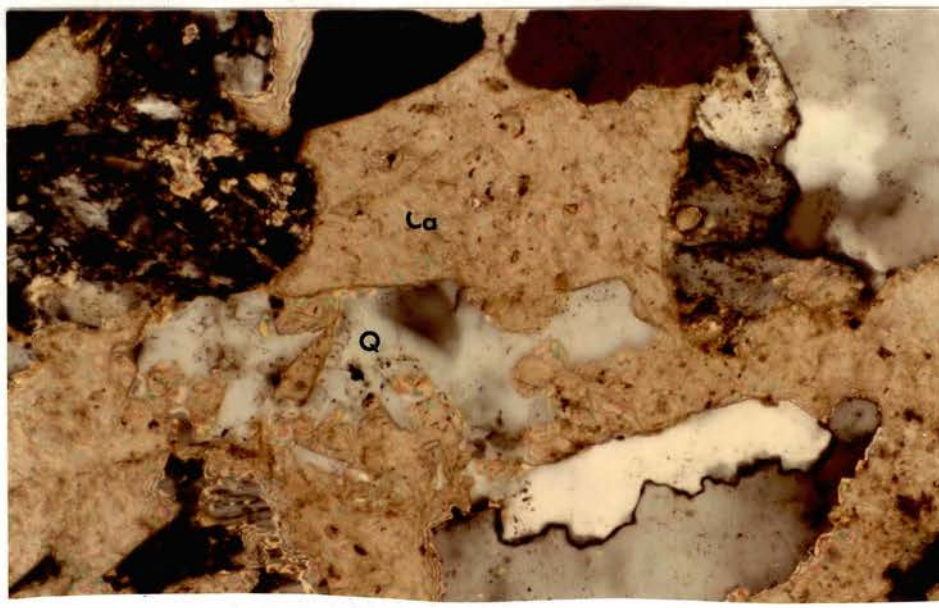

Figure 44. Photomicrograph Showing Calcite Replacement of Quartz

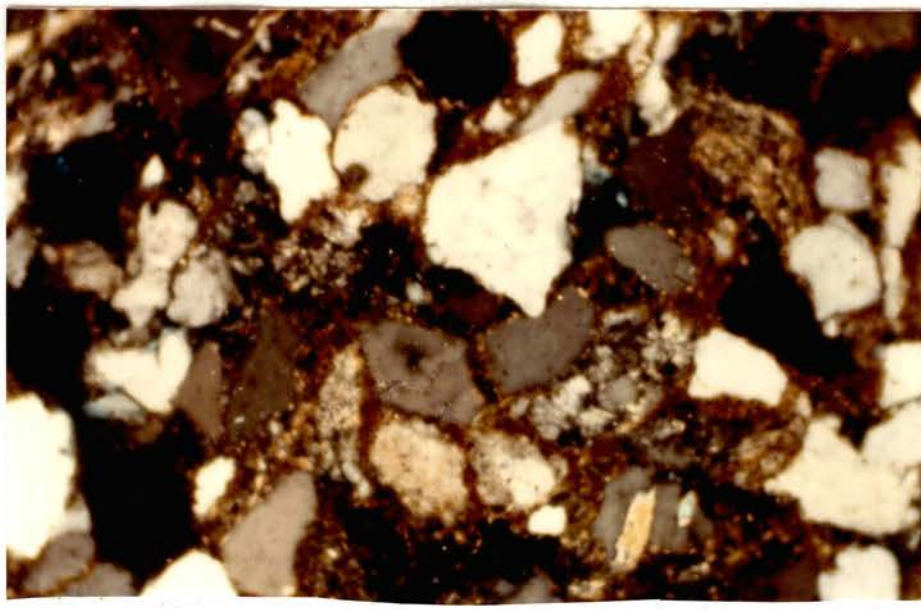

Figure 45. Photomicrograph Shwing Grain Rimming Chlorite and Siderite

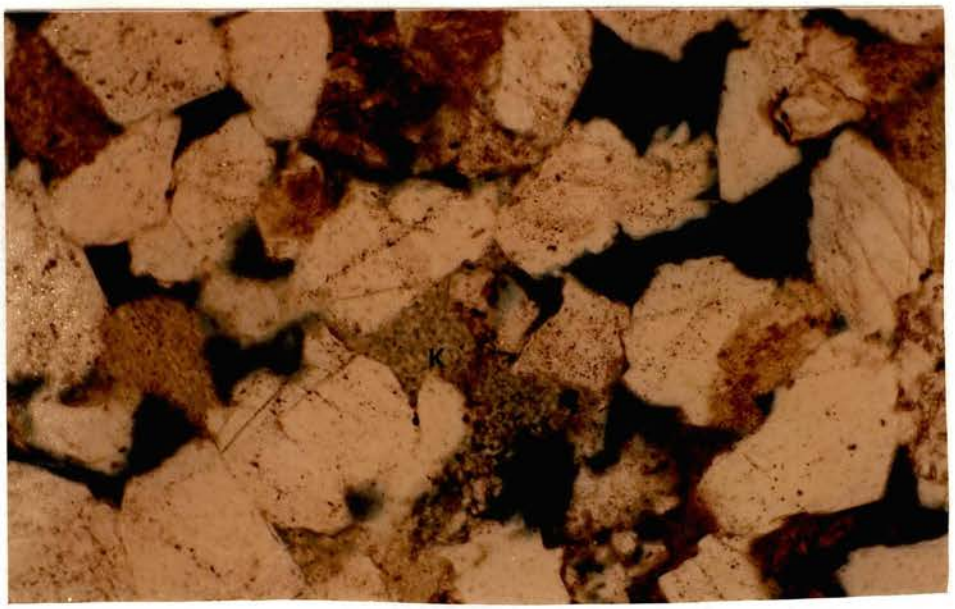

Figure 46. Photo-micrograph of Pore-Filling Kaolinite and Siderite (plane polarized light)

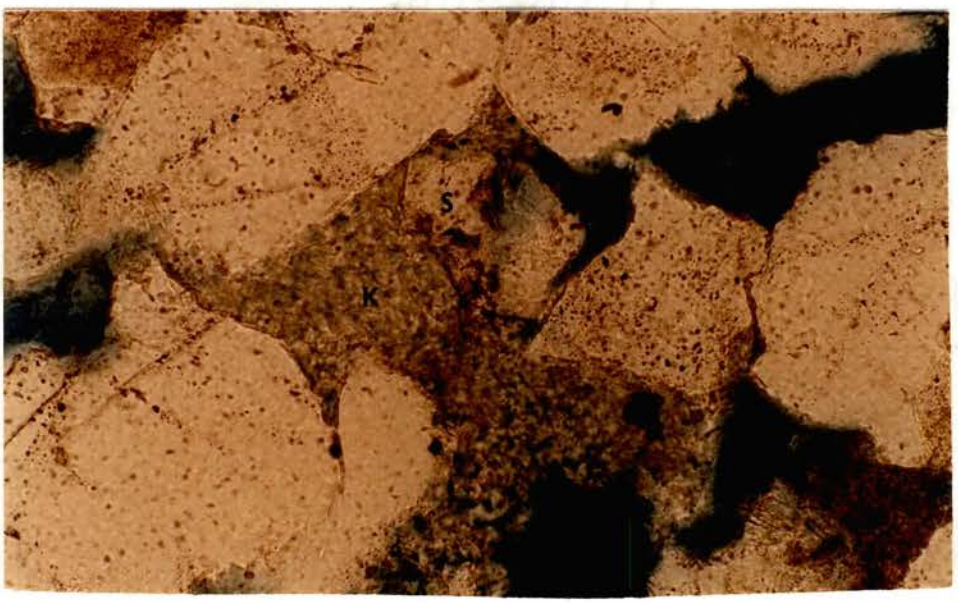

Figure 47. Higher Magnification of Figure 46

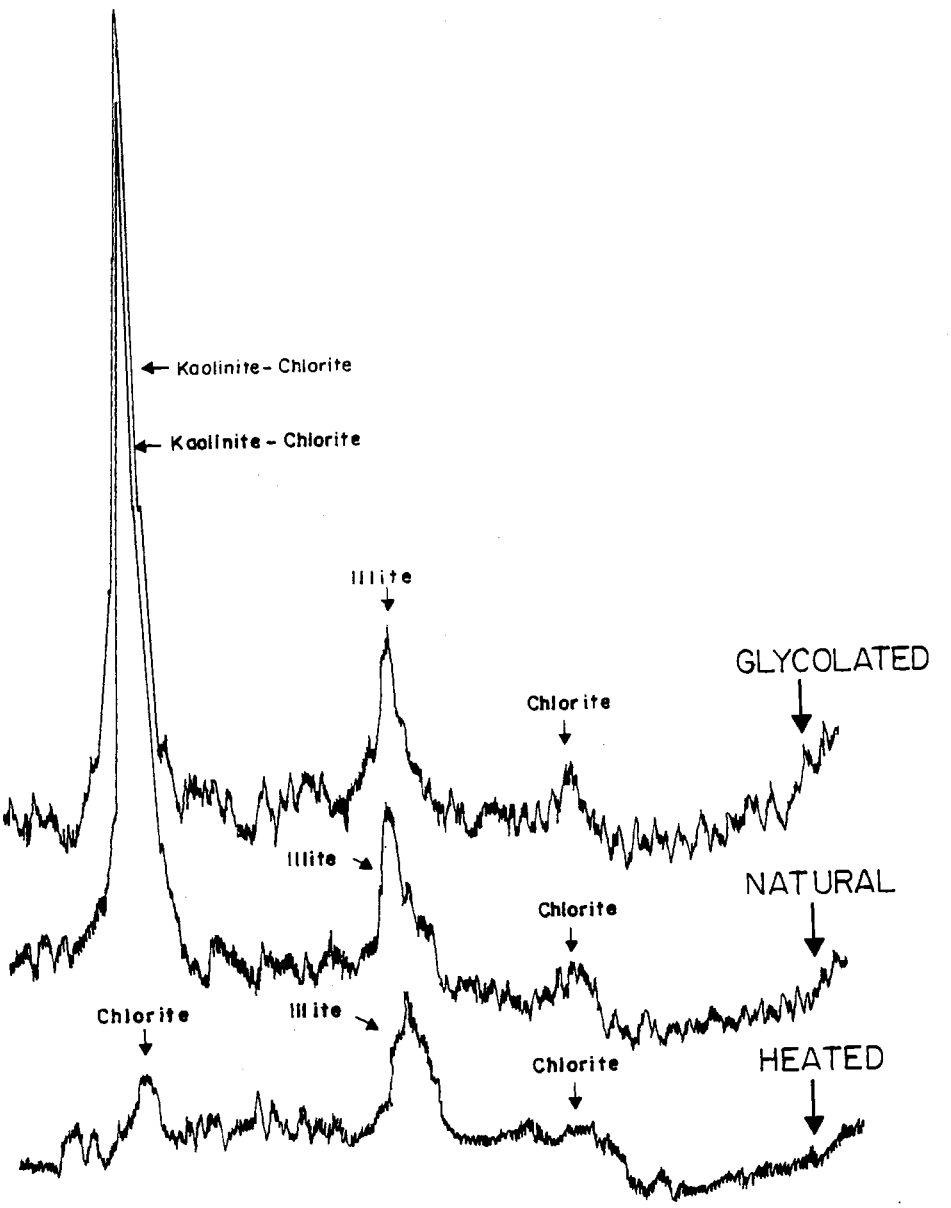

Figure 48. X-ray Diffraction Peaks of Authigenic Clays Found in the Bartlesville Sand

CHAPTER IX

DIAGENETIC FEATURES

To a large degree, the present morphology and mineralogic compositions of the Bartlesville Sandstone have been shaped by diagenetic processes. Four general groups of diagenetic features have been recognized and documented in thin-section and scanning electron photomicrographs. These groups consist of dissolution features, precipitates, alteration products, and replacement features. This chapter contains the description and documentation of these diagenetic features, while Chapters XII and XIII discuss the diagenetic processes in detail.

Dissolution Features

Partial to complete dissolution of detrital grains is a common occurrence in all of the Bartlesville samples examined. The dissolution of quartz is a common event. It consists of either partially corroded syntaxial quartz overgrowths (Figures 49, 50, 55, 56, 65, and 66) or, in the absence of overgrowths, partially dissolved original grain surfaces (Figures 50 and 77). Occasionally, the points of dissolution of quartz grains occur at the contacts of quartz and partially dissolved (hydrolyzed) feldspar grains (Figure 67).

Feldspars are the most frequently dissolved grains. In fact, a large percentage of the secondary porosity in this reservoir results from feldspar dissolution. Initially, dissolution often began along

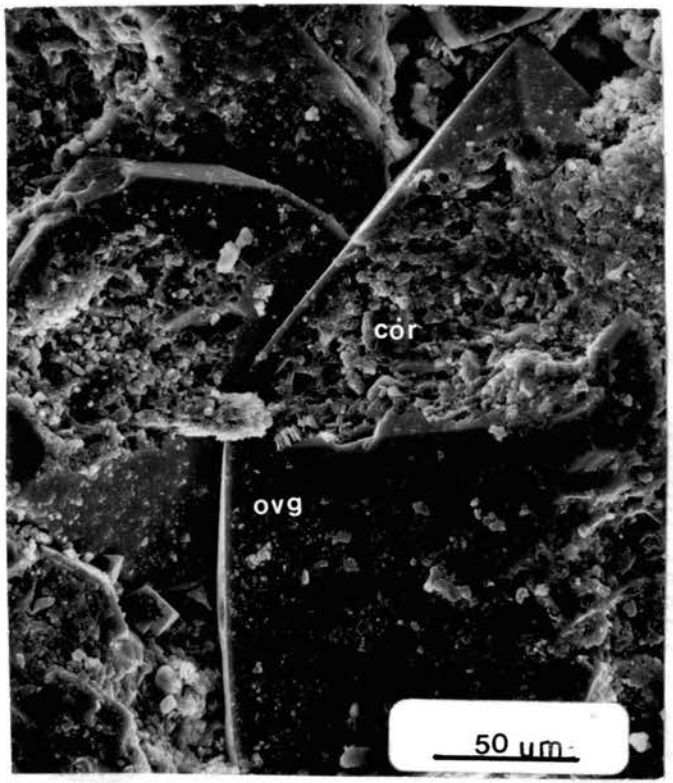

Figure 49. SEM Micrograph of Partially corroded Quartz Overgrowth

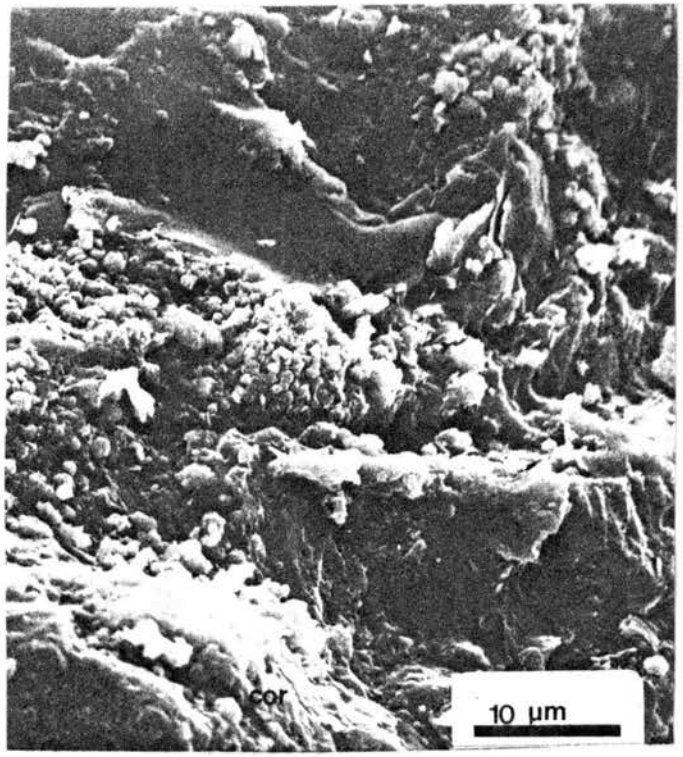

Figure 50. SEM Micrograph of a Corroded Quartz Grain

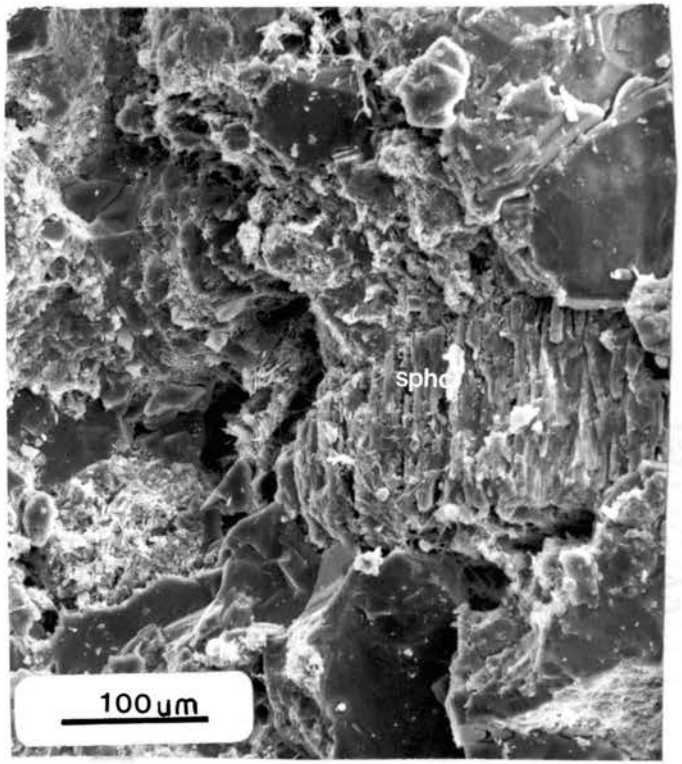

Figure 51. SEM Micrograph of Feldspar Dissolution Along Cleavage Planes Creating "Honeycombed" Porosity

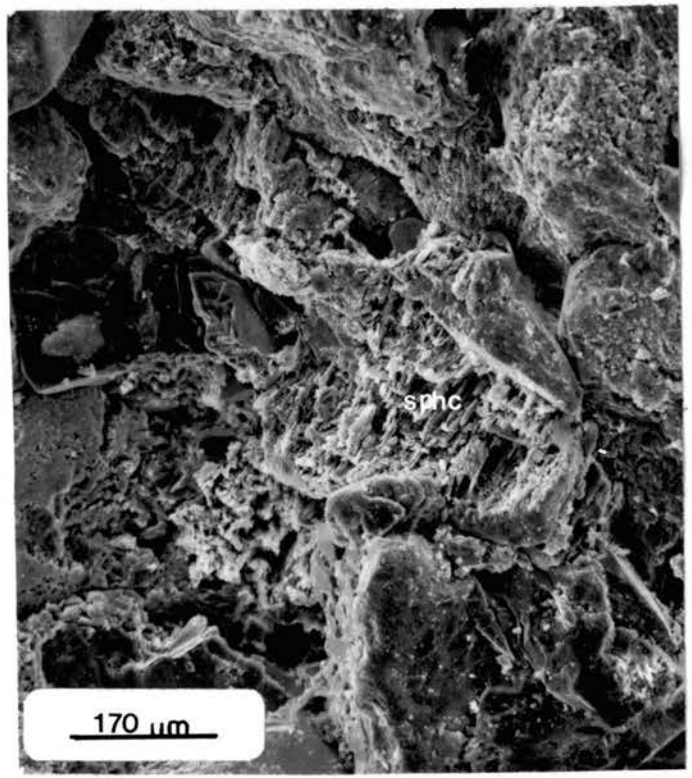

Figure 52. SEM Micrograph of Feldspar Dissolution Along Cleavage Planes Creating "Honeycombed" Porosity

cleavage planes (Figures 51, 52, and 78). These zones contain the weakest bonds and thus are most susceptible to ionic substitution. Advanced stages of feldspar grain dissolution left small amounts, if any, of the original detrital grain. These phenomena also have been documented by Morgan and Jordan (1970), Heald and Laresse (1973), and by Pittman (1978). Pittman (1978) states:

> In my opinion, porosity created by the dissolution of feldspar (or dissolution of carbonate that has replaced feldspar) is common worldwide in sandstones of all ages. Dissolution may affect portions of feldspar grains or essentially the entire grain. If feldspar is abundant in the sandstone, considerable porosity can originate in this manner (p. 160).

Another example of the very first stages of feldspar dissolution can be seen in the distinct hydration rim found occasionally enclosing plagioclase grains (Figures 69 and 70). This rim is 6 μm thick and forms a sharp boundary with the unaffected portion of the feldspar grain. The examples in Figures 69 and 70 resemble closely the "hydrated" feldspar rim described by Surdam and Boles (1978).

A final dissolution feature recognized in one thin section (Figure 33) was the dissolution of detrital matrix. This phenomenon was rare.

Precipitates

Nine different precipitates have been identified in the Bartlesville Sandstone in the Cushing Field. Four of these are different forms of quartz cement, while the others are authigenic clays (kaolinite, chlorite, and illite), carbonate, pyrite and galena.

Syntaxial quartz overgrowths are present in all samples. The overgrowths when not corroded and pitted form smooth planar surfaces. If free to grow into pore spaces, the overgrowths often develop sharp

terminations (Figures 53 and 54). Evidence indicates that thick overgrowths occurred by way of the stacking of thin layers of quartz upon each other, creating a layered appearance (Figures 55 and 56). Each layer represents a stage of precipitation. Alternating periods of precipitation and non-precipitation/dissolution occurred. Minor fluctuations in the pH of the pore fluids could cause this varve-like accumulation. Short periods of dissolution and precipitation are also indicated in Figure 62. The quartz overgrowth in the upper right hand corner of the photo is free of any corrosion, yet the overgrowth in the lower right hand corner contains dissolution pits. The fact that these two overgrowths are close enough together to have developed in the same micro-environment suggests multiple periods of quartz precipitation, the overgrowth in the right hand corner being a later event.

Interestingly, several thin sections from different cores contained quartz overgrowths which were not in optical continuity with the quartz substrate. Both the substrate and overgrowths usually showed undulose extinction. A possible explanation is that stress applied to the grains caused rotation of the overgrowths as well as undulosity.

It appears that pore-lining clays had a minimal effect on quartz overgrowth development, as can clearly be seen in Figures 63, 64, and 41. The photo-micrographs show that the dust rim, consisting of chlorite, did not inhibit precipitation of a quartz growth.

Microquartz is also a relatively common precipitate found in the Bartlesville Sandstone in the Cushing Field. It commonly grew into pores that were already lined or partially filled with clays (Figures 61 and 62). Microquartz crystals, nearly always euhedral (Figure 62), used detrital quartz grains as substrate. While difficult to distinguish

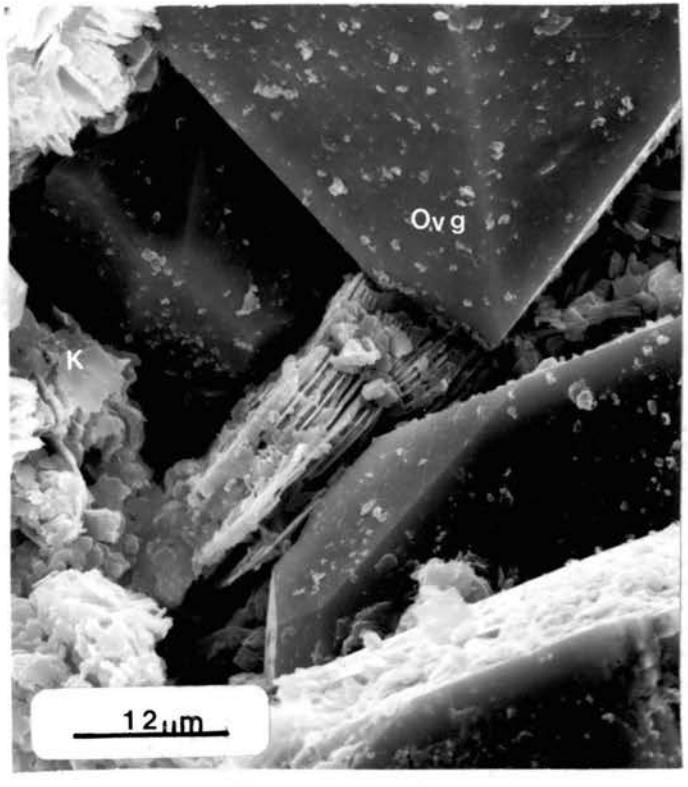

Figure 53. SEM Micrograph Showing Euhedral Syntaxial Quartz Overgrowths and Pore-Filling Kaolinite

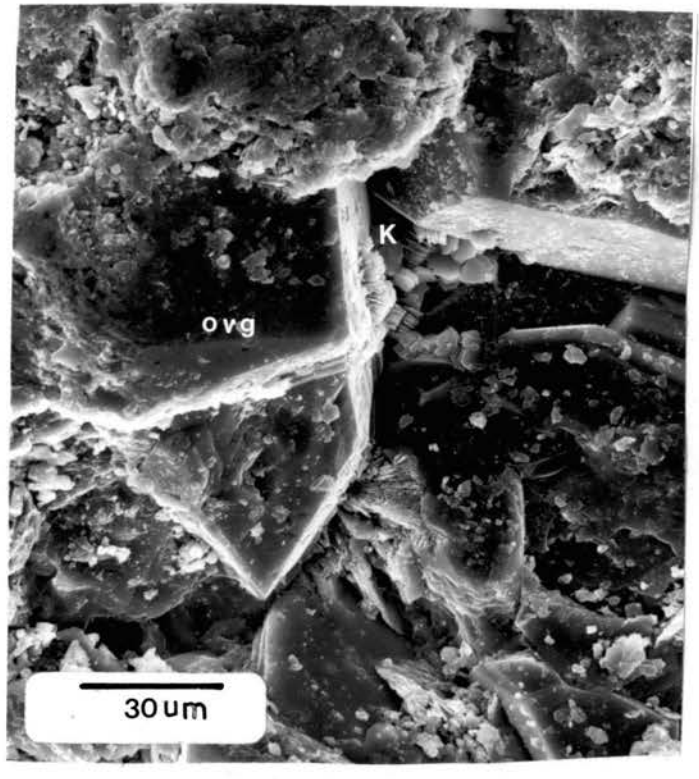

Figure 54. SEM Micrograph Showing Euhedral Syntaxial Quartz Overgrowths and Pore-Filling Kaolinite

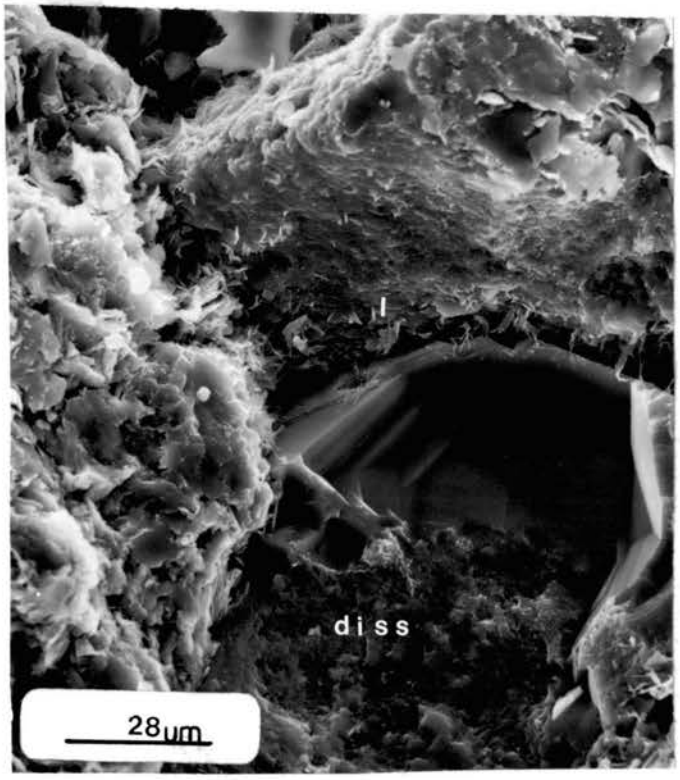

Figure 55. SEM Micrograph of Syntaxial Quartz Overgrowths, Quartz Dissolution, and Pore-Lining Illite

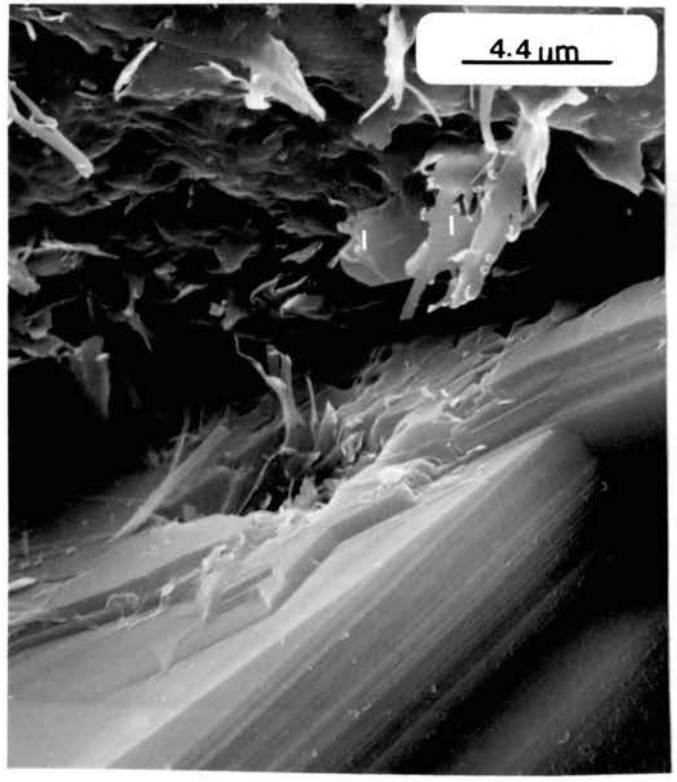

Figure 56. Higher Magnification of Figure 55

clearly in thin-section, microquartz was readily identifiable with the SEM.

Authigenic chert, while uncommon, is another form of quartz precipitate present in this reservoir. It is most often associated with what appears to be authigenic carbonate. It is somewhat difficult to distinguish from detrital chert, however.

Chalcedony is the final quartz precipitate to be discussed. It is very rare and could be identified only in thin section (Figures 42 and 43).

Authigenic clays are present in all SEM samples and nearly all thin sections. Kaolinite and chlorite are predominant, while illite is less common.

Morphologically, chlorite occurs mainly as a pore-lining clay (Figures 58, 59, 60, 61, 62, 63 and 64). It commonly coats quartz grains with a layer of bladed crystals, the edges randomly oriented with respect to each other. Chlorite appears to be variously situated with respect to quartz overgrowths, chlorite apparently growing out of dissolution pits (Figure 74, chlorite precipitation a later event) and at other times clearly being covered by syntaxial quartz overgrowths (chlorite precipitation an earlier event). Odom, Willand and Lassin (1978) documented a similar feature in the St. Peter Sandstone. This again suggests either multiple phases of quartz or chlorite precipitation. Chlorite also occurs, but more rarely, as a pore-filling clay (Figures 42 and 43). The origin of chlorite in this morphology is ambiguous, however, as its presence could well be the result of the complete alteration of illite or an unstable detrital grain.

Kaolinite, the other clay in abundance, is present filling pores (Figures 46, 47, 57, 58, 59, 60, 53, 54, and 73) and also as an alteration

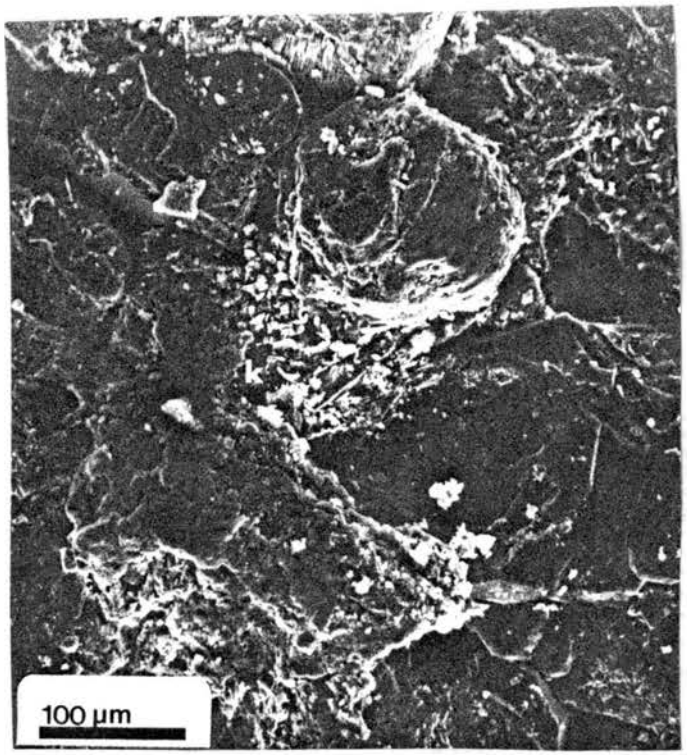

Figure 57. SEM Micrograph of Pore-Filling Kaolinite

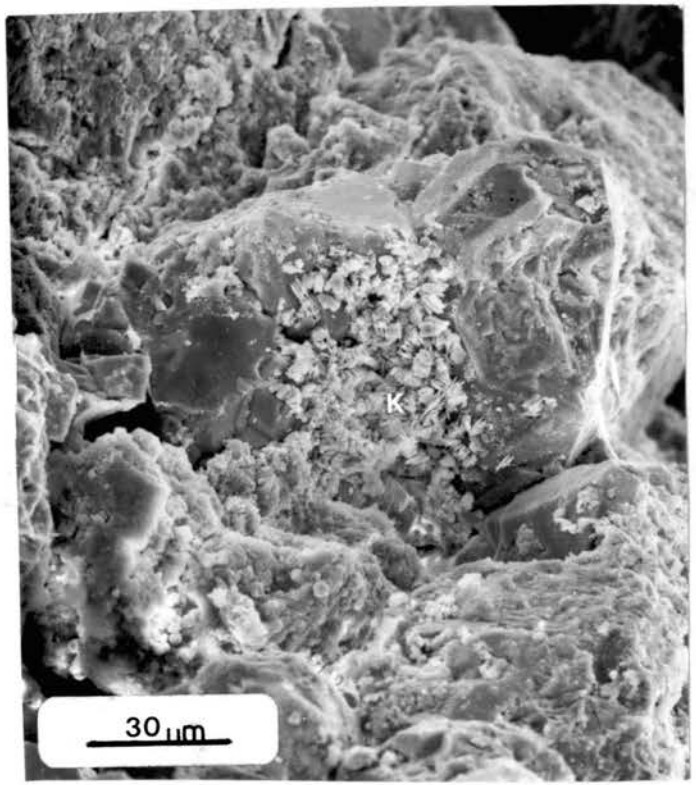

Figure 58. Higher Magnification of Figure 57

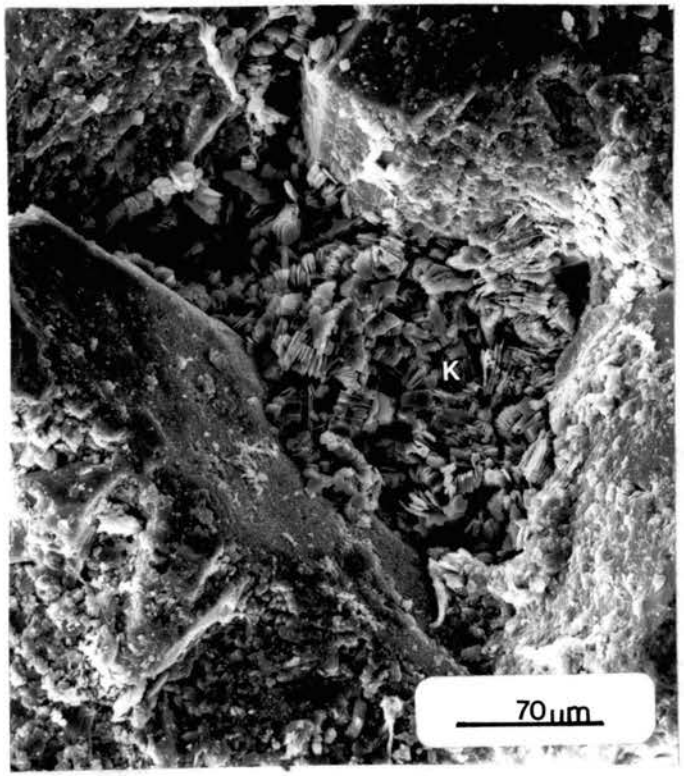

Figure 59. SEM Micrograph of Pore-Filling Kaolinite and Pore-Lining Chlorite

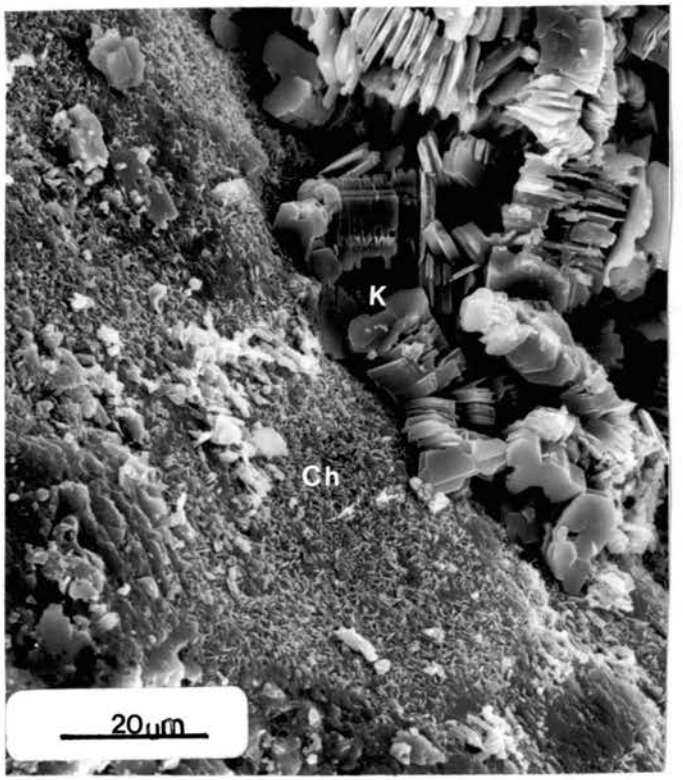

Figure 60. Higher Magnification of Figure 59

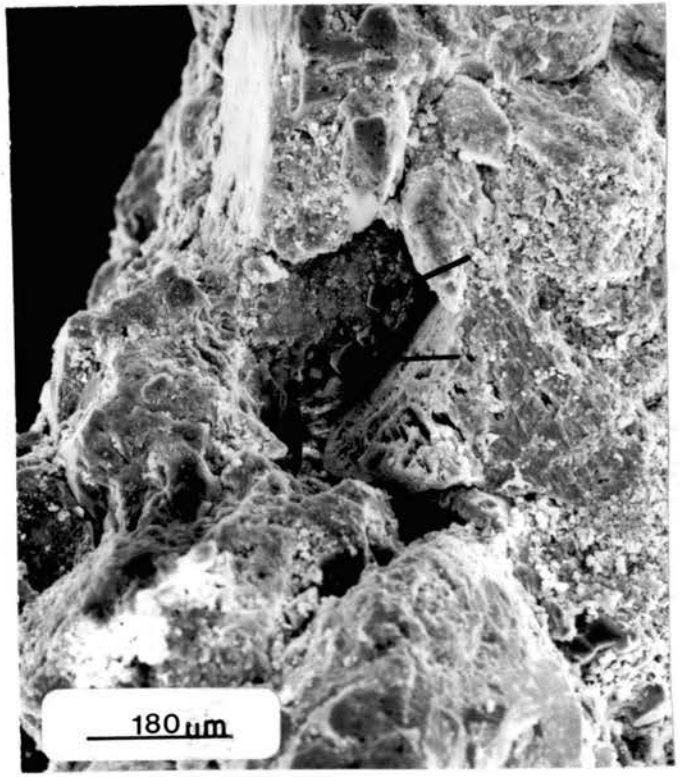

Figure 61. SEM Micrograph of Pore-Lining Chlorite and Pore-Filling Microquartz

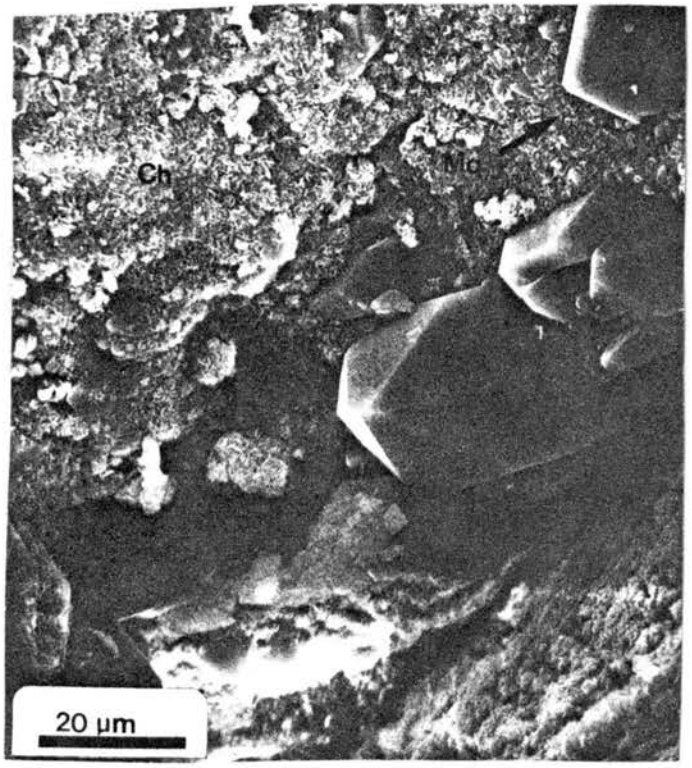

Figure 62. Higher Magnification of Figure 61

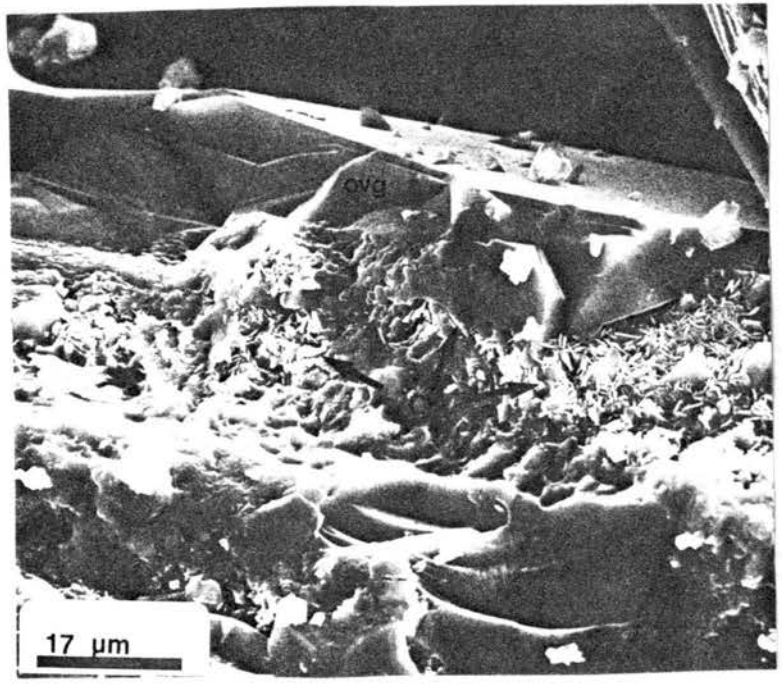

Figure 63. SEM Micrographs Showing a Sequence of Events: 1) Dissolution of Quartz; 2) Precipitation of Pore-Lining Chlorite (Ch); 3) Quartz Overgrowth (ovg); 4) Dissolution of Quartz (Cor)

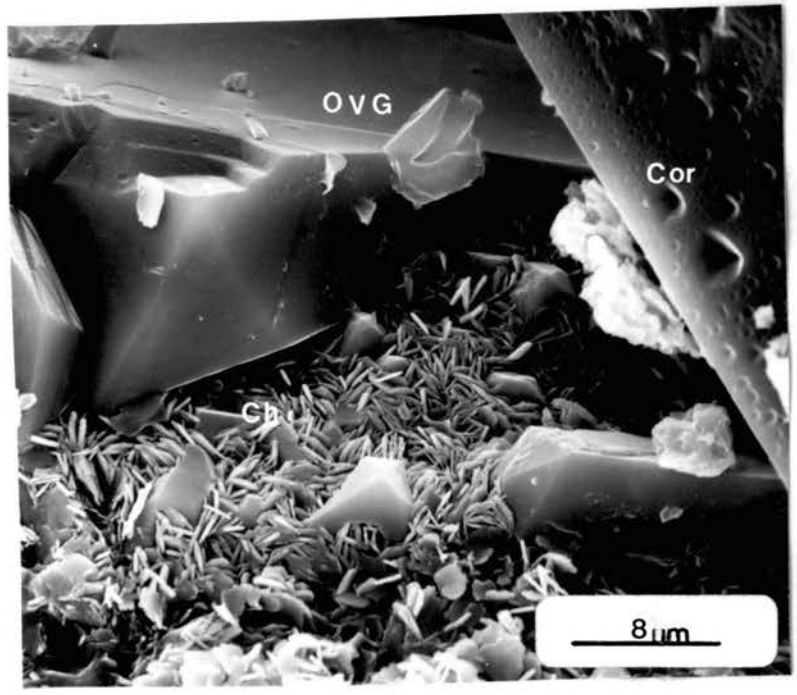

Figure 64. Higher Magnification of Figure 63

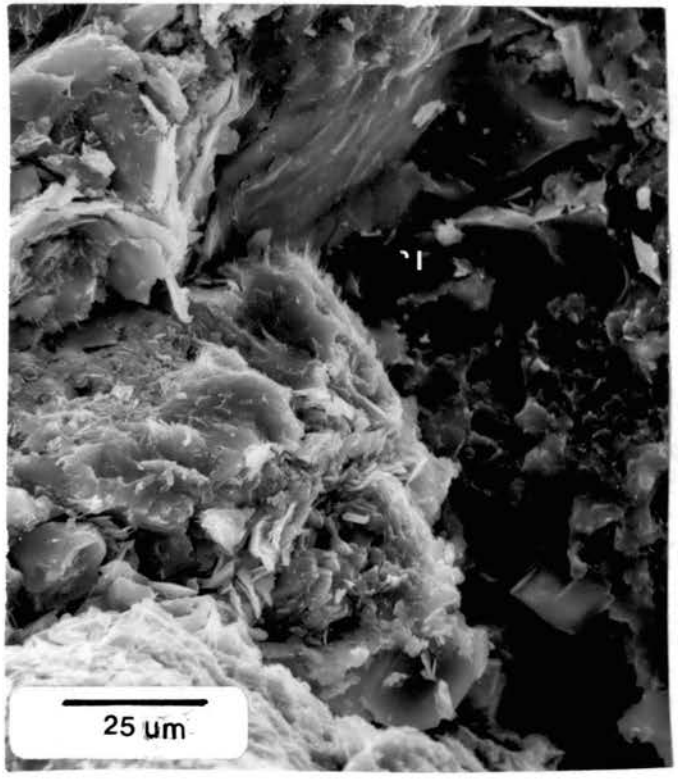

Figure 65. SEM Micrograph of Pore-Lining Illite

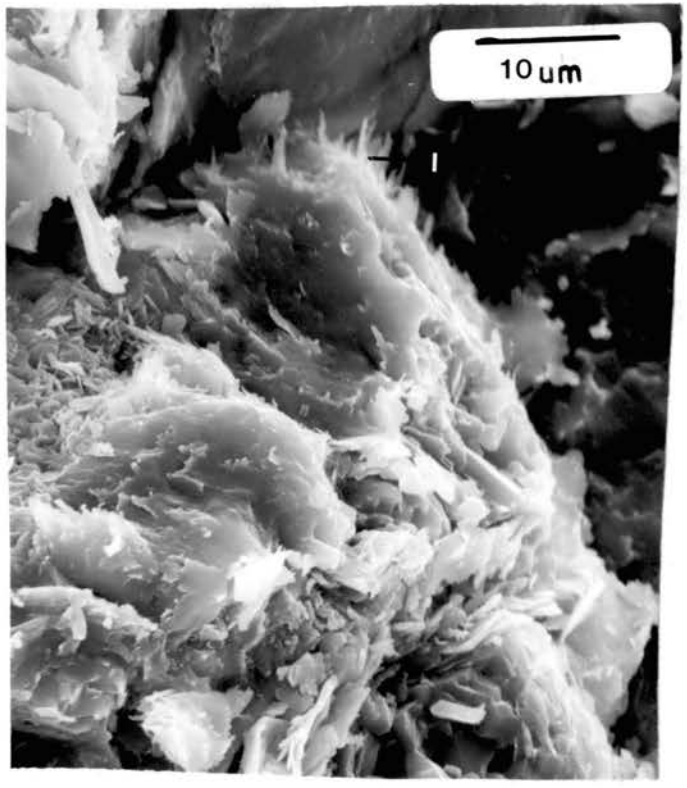

Figure 66. Higher Magnification of Figure 65

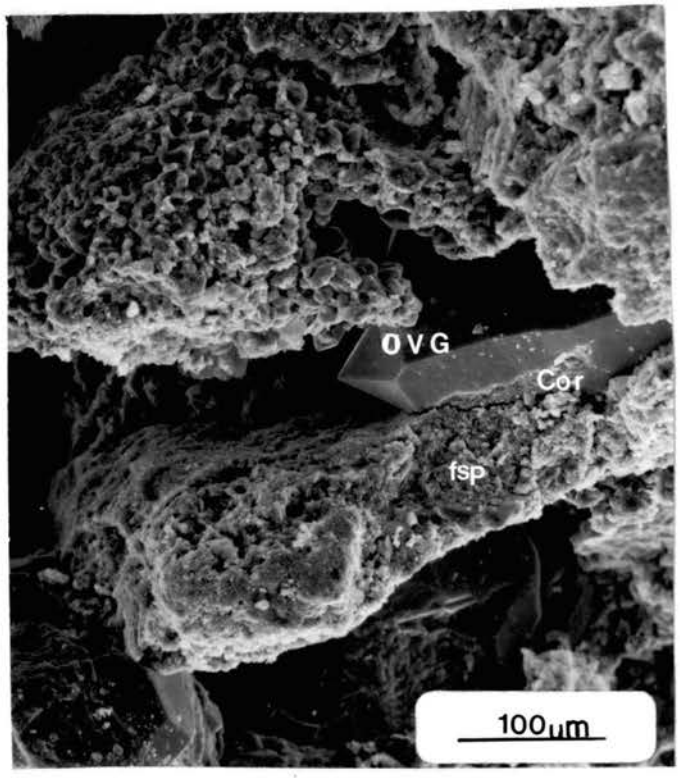

Figure 67. SEM Micrograph Showing Corroded (cor) Quartz Overgrowth (ovg) Lying Next to a Partially-dissolved Feldspar Grain (fsp)

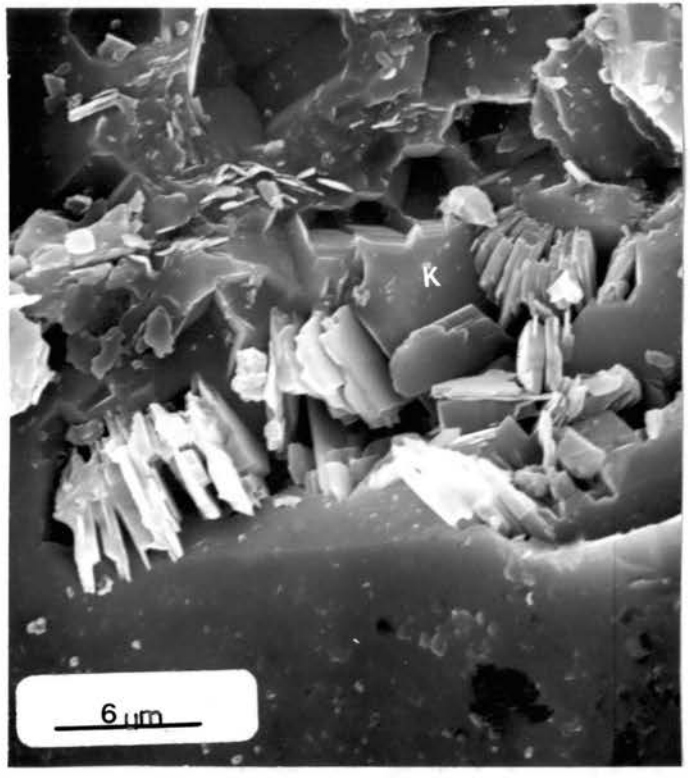

Figure 68. SEM Micrograph Showing Kaolinite (K) Filling Dissolution Pits in Quartz Grain

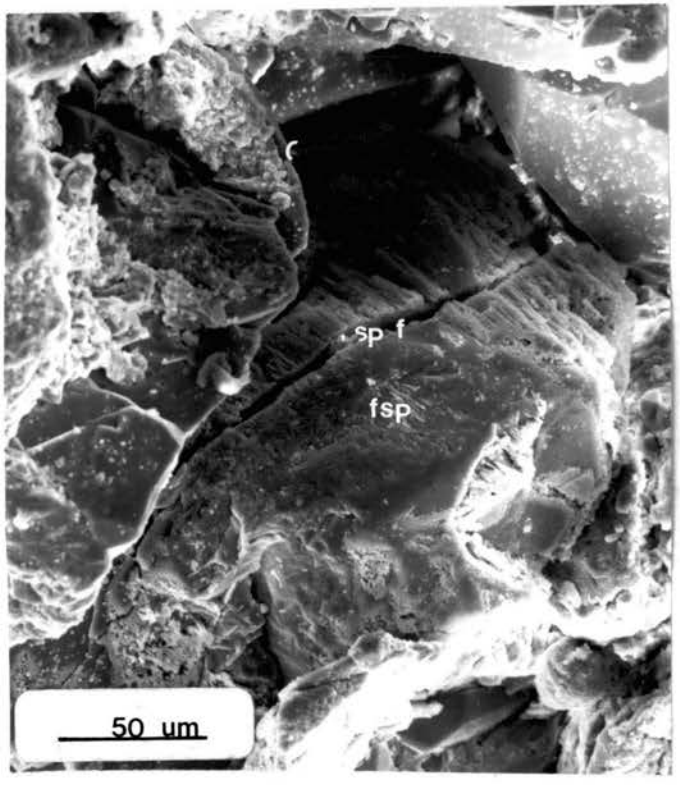

Figure 69. SEM Micrograph Showing a Fractured Feldspar Grain (fsp) Creating Secondary Porosity (sp-f)

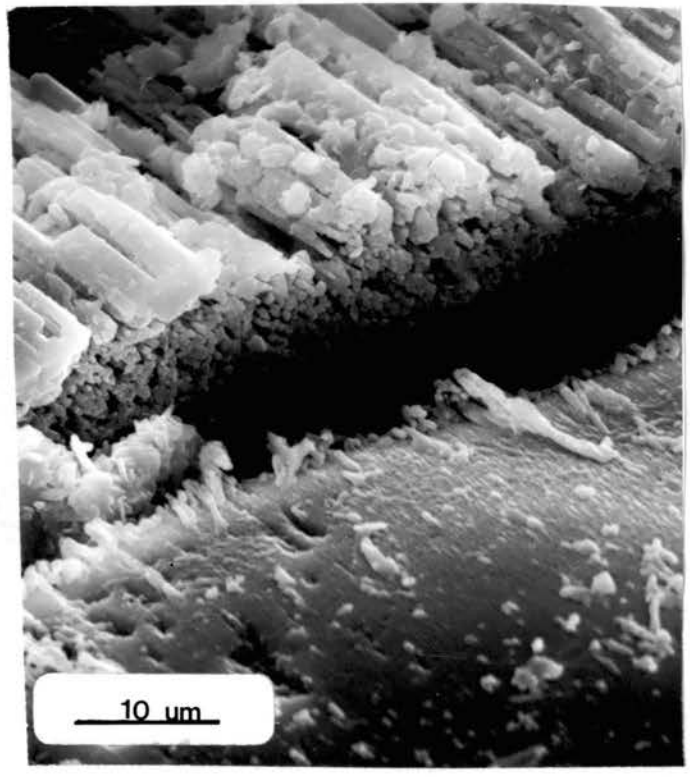

Figure 70. Higher Magnification of Figure 69

product of feldspar. Generally well crystallized, the kaolinite is vermicular in form and seemed randomly distributed in the pore spaces. Kaolinite appeared more abundant in SEM samples than in the corresponding thin sections.

Calcite cement is much less abundant in the Bartlesville than quartz or either of the clays and usually occurs in small zones or as sporadically distributed nodules. Where well developed, the crystals are normally large, filling all of the pores and completely surrounding the detrital grains (Figures 30, 32, 43, and 44). Small crystals are also sometimes scattered about in pores (Figure 73).

Only one occurrence of galena was noted and this was in a hand specimen. The galena is present as a fracture filling and is associated with a calcite nodule situated just above the basal shale zone in the Gulf Oil Company's P. Brown No. 9 core. Depth of occurrence was 2,776 feet. The lead and sulphur necessary for the precipitation of the galena most likely came from pore waters expelled from the underlying clays during compaction of the sediments.

Pyrite is the last precipitate to be discussed. Figures 71 and 72 clearly indicate the framboidal nature of the pyrite. This, along with the abundance of light sulphur isotopes determined from isotopic analysis of the included sulfur, suggest the pyrite originated as a result of bacterial action. Pyrite is often found in association with carbonaceous matter, hematite and also with the finer sediments.

Alteration Products

Four major alteration processes represented in the Bartlesville samples are: kaolinization and illitization of feldspar; chloritization

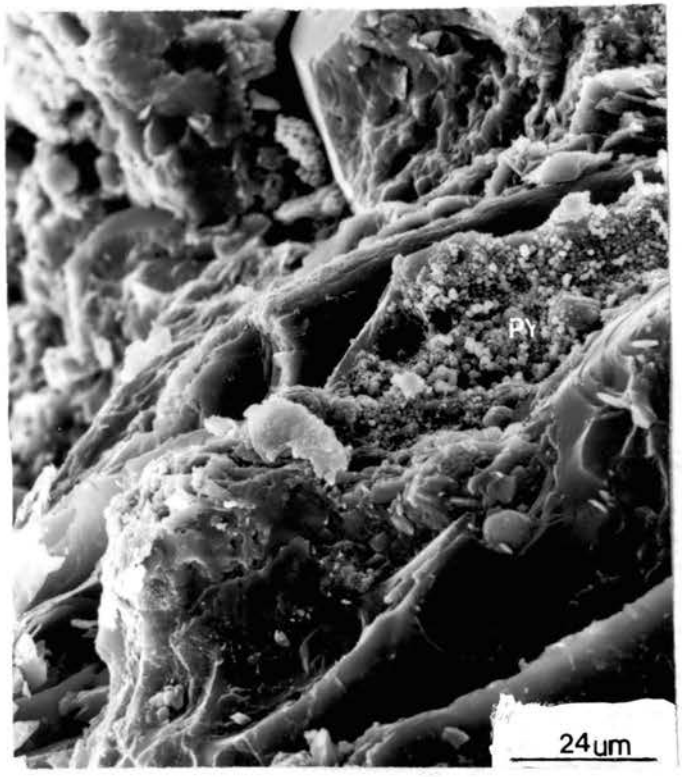

Figure 71. SEM Micrograph of Framboidal Pyrite

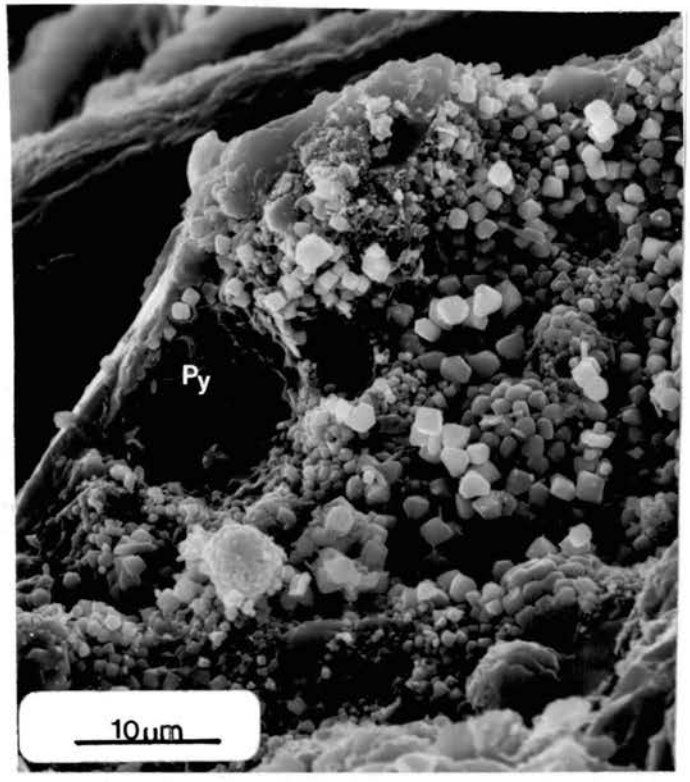

Figer 72. Higher Magnification of Figure 71

of illite and kaolinite; pyrite and other iron-rich minerals altering to hematite; siderite as an alteration product of calcite.

Kaolinization of feldspar is a very common feature readily identifiable with the SEM. A direct relationship between the altered feldspar and nearby kaolinte is often difficult to establish (Figures 57 and 58). However, in some cases the feldspar grain was clearly being kaolinized (Figures 75 and 76).

Illitization of feldspars, easily identifiable in thin section, is also a common feature. Feldspar grains (both plagioclase and microcline) range from completely fresh to entirely altered to clays, often to illite. The degree of illitization (and kaolinization) was in response to the micro-environment surrounding the grains.

Chloritization of illite has probably been common in the Bartlesville Sandstone. While the actual chloritization process is difficult to document precisely, the relative lack of authigenic illite (most illite appears to be detrital) together with the abundance of authigenic chlorite, strongly suggests that the alteration of illite to chlorite is very common.

Chloritization of kaolinite was more rare and can be observed in Figure 76.

Hematite (Fe_2O_3) exists usually in association with pyrite, fine sediments and clays, carbonaceous matter and oil (Figures 36 and 37). It is assumed to be an oxidized alteration product of iron minerals such as biotite, hornblende, magnetite and pyrite. Upon dissolution, these minerals released significant quantities of iron into solution. The iron was later to be fixed as hematite, among other minerals.

Another mineral in which iron is fixed is siderite, an iron

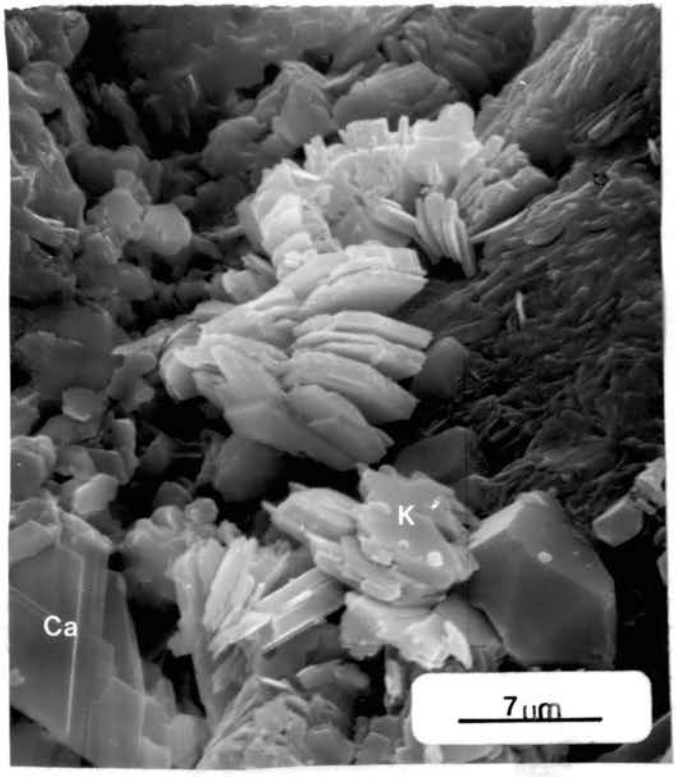

Figure 73. SEM Micrograph of Calcite, Pore-Filling Kaolinite (K) and Microquartz (mq)

Figure 74. SEM Micrograph of an Ambiguous Relationship Between a Quartz Overgrowth (ovg) and Chlorite (ch)

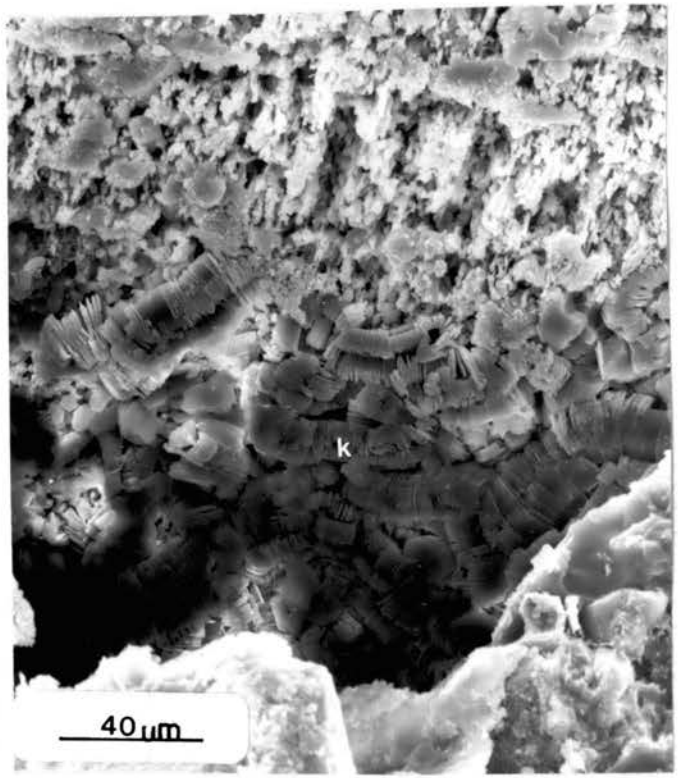

Figure 75. Micrograph of Feldspar (fsp) Altering to Kaolinite (K) and Kaolinite Altering to Chlorite

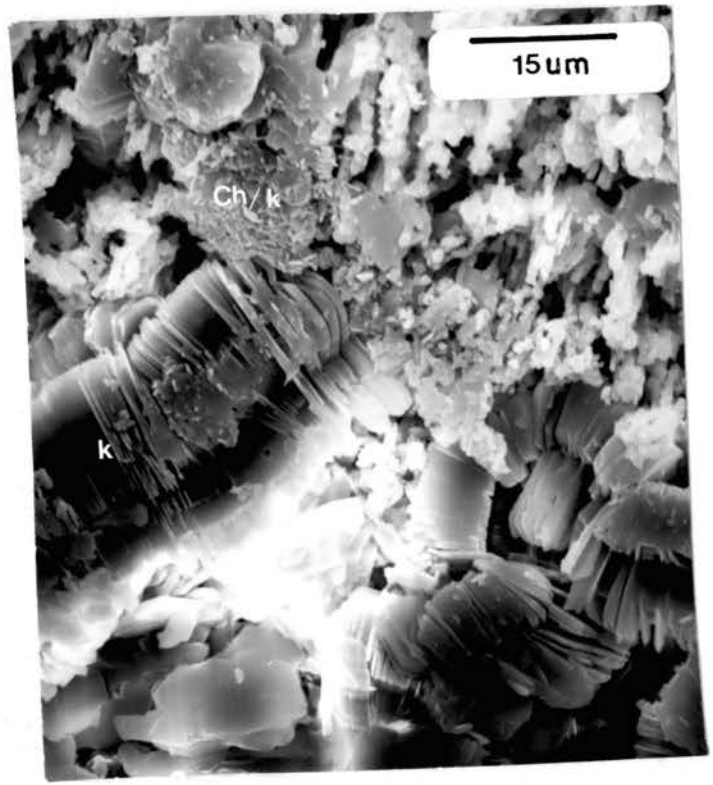

Figure 76. Higher Magnification of Figure 75

carbonate ($FeCO_3$). Siderite exists as either large, detrital rip-up clasts or as an iron-rich alteration product of calcite (Figure 45). Siderite, as an alteration product, is present in small amounts. When observed, it either partially fills pores or rims detrital grains (Figure 45).

Replacement Features

Calcite replacement of detrital grains is the only replacement feature noted in the samples. Calcite replacement is conspicuous only in the small zones and nodules containing large amounts of calcite cement. Feldspars are the most common grains replaced (Figures 30 and 32), but monocrystalline quartz also shows some signs of at least partial replacement by calcite (Figure 44).

CHAPTER X

POROSITY

Identification of porosity types was based upon thin section examination. Identification was enhanced by the impregnation of samples with blue epoxy prior to thin sectioning. Two general types of porosity are found in the Bartlesville Sandstone in the Cushing Field. These are: primary or intergranular porosity resulting from primary depositional processes; secondary porosity resulting from fracturing, shrinkage, dissolution, or a combination of these methods. The purpose of this chapter is to describe and document the various types of porosity present in the Bartlesville Sandstone in the Cushing Field.

Primary Porosity

Primary intergranular porosity is of relatively minor importance in the Bartlesville Sandstone in the study area. Of the 14.7 per cent total porosity, only 3.6 per cent is primary in origin (the remaining 11.1 per cent is of secondary origin). Of that 3.6 per cent, a significant portion is probably secondary porosity resulting from the dissolution of pore-filling cement. This type of secondary porosity is difficult, if not impossible, to detect. The best examples of intergranular primary porosity can be seen in Figure 79.

Secondary Porosity

Secondary porosity, predominant in this reservoir, consists of

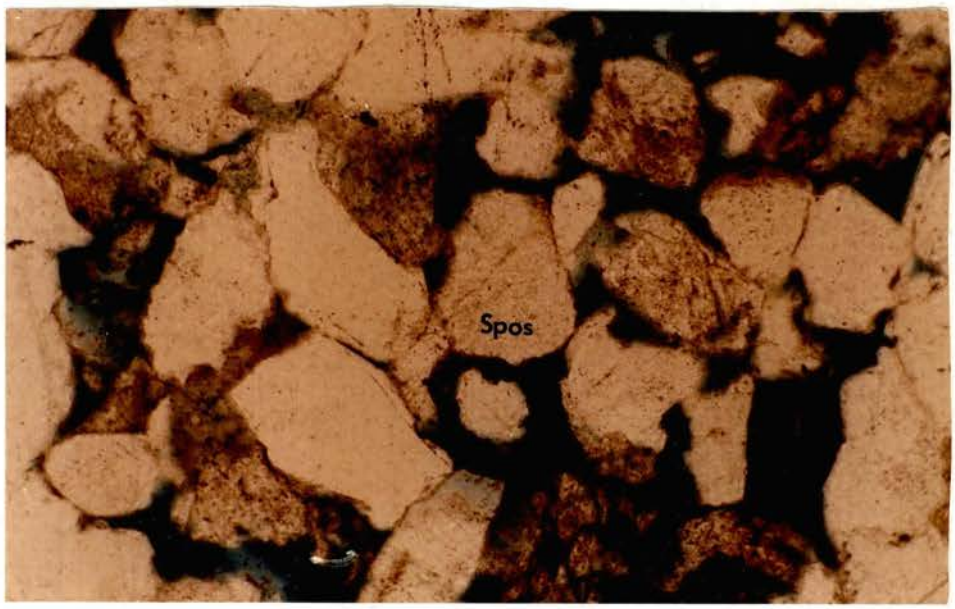

Figure 77. Photo-micrograph of an Oversized Secondary Pore (sp-os)

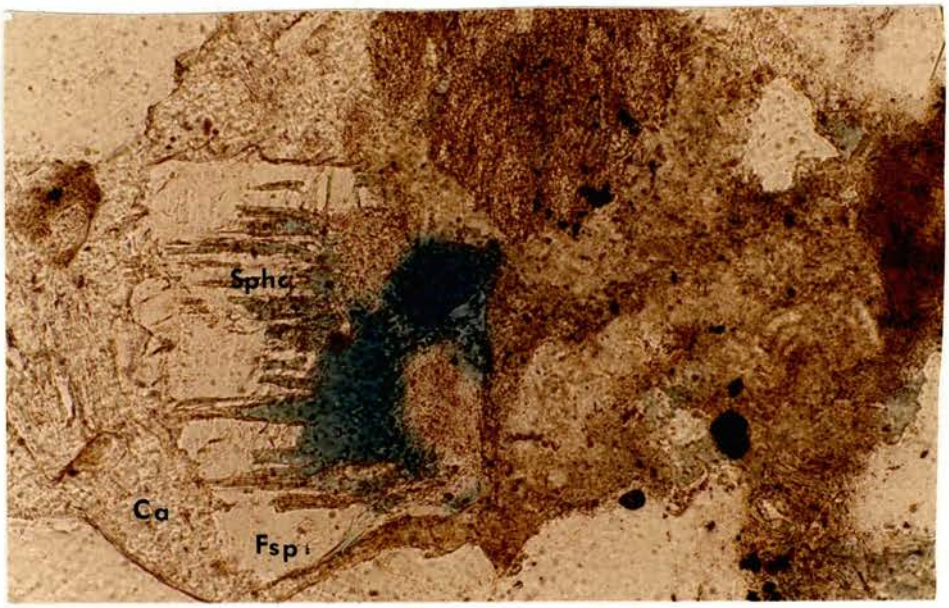

Figure 78. Photo-micrograph of Partial Feldspar Dissolution Along the Cleavage Planes Resulting in "Honeycombed" Secondary Porosity

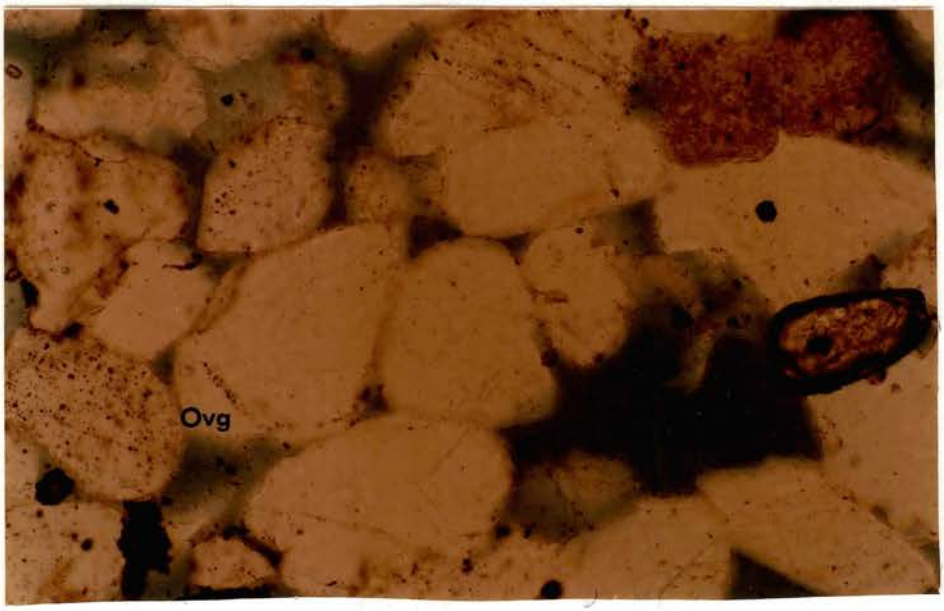

Figure 79. Photo-micrograph of Zircon and a Syntaxial Quartz Overgrowth

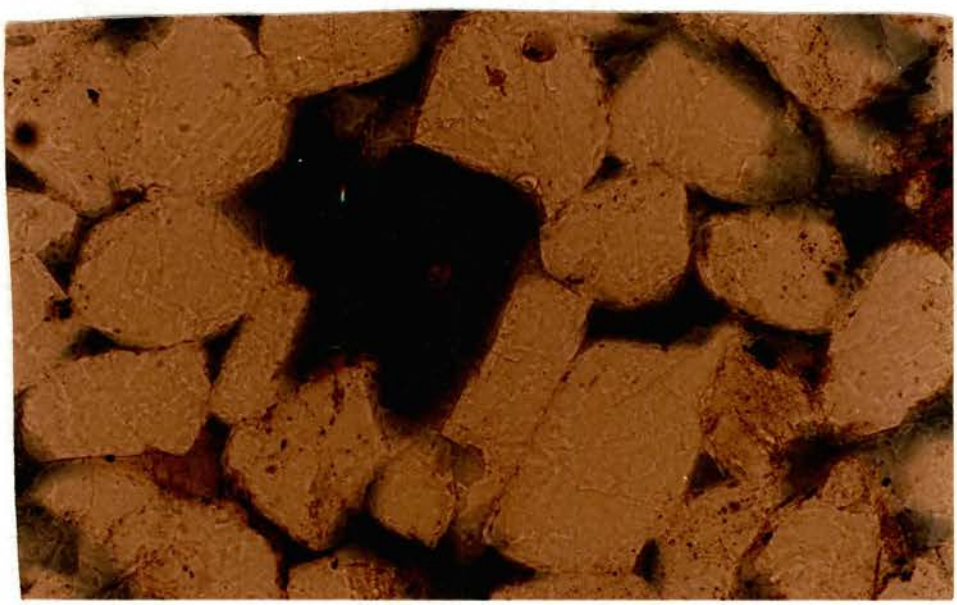

Figure 80. Photo-micrograph of a Grain Mold

grain molds, oversized pores, "honeycombed" pores, micro-pores, fracture pores, and various combinations of these. The causes of partial and/or complete grain and matrix dissolution are authigenic cement dissolution; authigenic replacement mineral dissolution; dissolution of feldspar along crystallographic lines of weakness; filling of pores with authigenic clays--especially kaolinte--and fracturing of grains, respectively. These types of secondary porosity are most prevalent in medium grained zones free of detrital matrix.

Complete dissolution of feldspar grains which produced grain molds has significantly enhanced both total and effective porosity in the Bartlesville. The fact that most of these molds are impregnated with blue epoxy indicates that the pores are interconnected. Pores consisting of grain moldsare commonly larger than the surrounding grains and take on various shapes depending upon the shape of the original detrital grain (Figures 79 and 80). Grain molds are more often found in medium grained rather than very fine and fine grained facies.

Oversized pores resulting from corrosion of detrital grain rims is another feature often observed in this reservoir (Figure 77). All detrital grains experienced corrosion at some time, including monocrystalline quartz. The corrosion of grains varied in intensity and occurred at different times depending upon the location within the reservoir. Locally, quartz overgrowths are very pronounced and free of dissolution. At other places, corrosion destroyed the overgrowths and the resulting grain surface is rough and pitted (Figure 49). While the increase in porosity is not as great as is that for complete feldspar dissolution, corrosion of grain surfaces resulting in oversized pores is important as it has undoubtedly increased permeabilities

significantly as a result of the enlargement of pore throats.

Partial feldspar dissolution yielding "honeycombed" porosity (Schmidt and McDonald, 1978) is a feature common in the Bartlesville in the study area. As mentioned before, dissolution of feldspar normally begins along cleavage or twin planes, areas of weakest bonding (Figures 51, 52, and 78). This partial dissolution along preferred crystallographic lines forms distinct patterns which reflects the crystal structure of the feldspar, and this dissolution results in the honeycombed porosity described by Schmidt and McDonald (1978) and by Scholle (1979).

Micro-porosity, commonly well developed between clay plates, is most often found in association with kaolinite booklets (Figures 42, 46, and 47. The small size of these pores necessarily inhibits fluid flow. Consequently, effective porosity is not enhanced by micro-porosity.

The final type of secondary porosity developed in the Bartlesville in the Cushing Field is fracture porosity. This was seen in only a few grains (Figure 70) and did not contribute significantly to total and effective porosity.

CHAPTER XI

PARAGENETIC SEQUENCE

Figure 81 is a graphical presentation of the sequence of diagenetic events that led to the present state of the Bartlesville Sandstone in the Cushing Field. Stage and paragenetic sequence are represented by the vertical and horizontal axes, respectively. Each event is depicted by a solid line (process continuously active) or a dashed line (process sporatically active) indicating the length of time during which each diagenetic process was working.

It should be emphasized that the rock-water system is dynamic, quite complex and when examined over geologic time, cannot be considered to be in equilibrium. The presence and duration of each of the diagenetic processes was a direct response to the changing composition of the pore fluid, the detrital constituents, the temperature and the pressure. Small variations in the pH of the pore fluids caused pore water compositional changes which upset short-term equilibrim and resulted in the reversal of processes for a "short" period of time. This is most clearly depicted in Figures 55 and 56, showing the varve-like quartz overgrowth and variegated layers. This indicates that quartz precipitated and dissolved under conditions which were changing. It is for this reason that seemingly conflicting processes could occur at the same time (indicated by overlapping dashed lines), i.e., chalcedony precipitation (under acidic conditions) going on at the same time as calcite

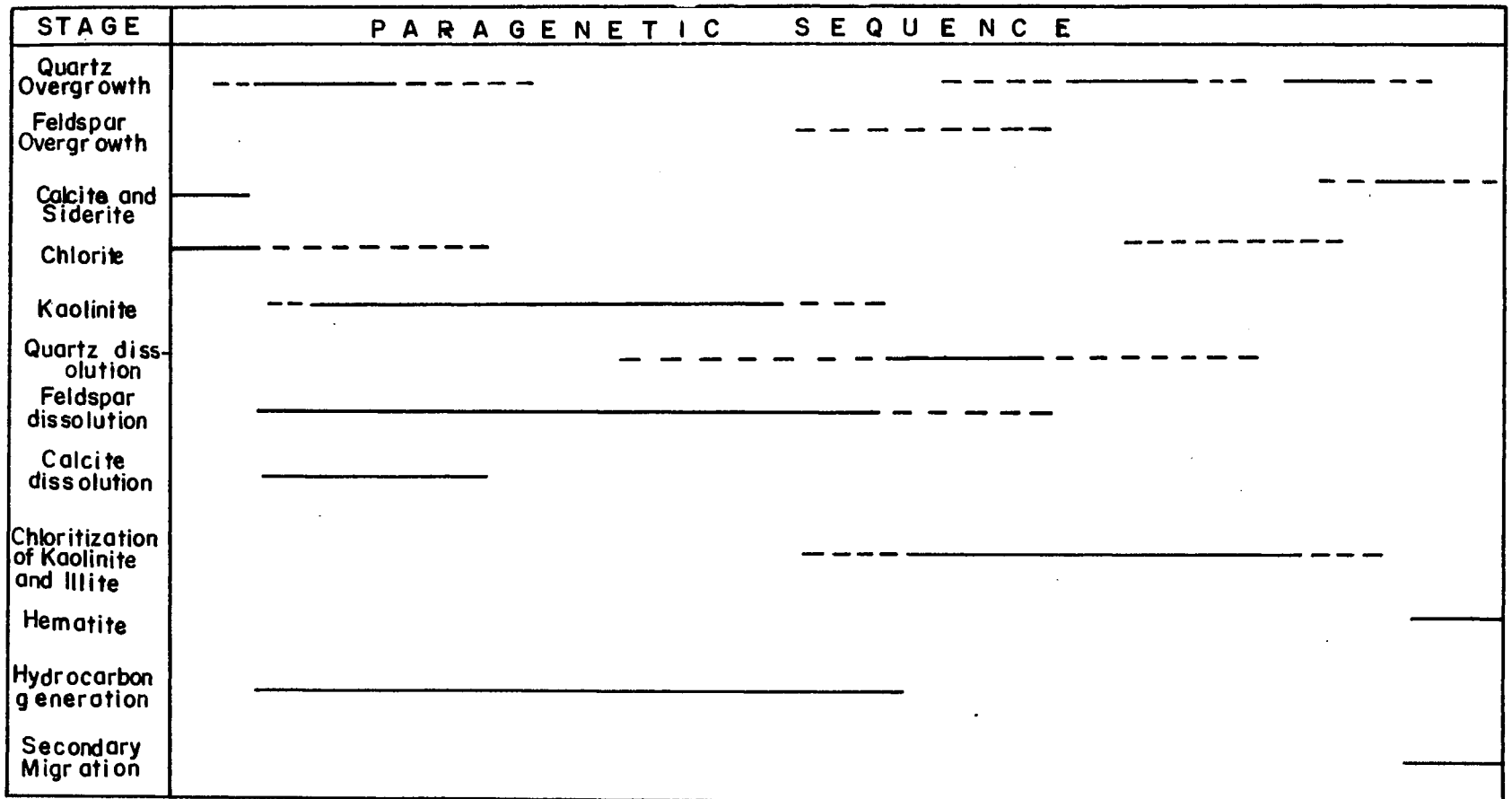

Figure 81. Paragenetic History of the Bartlesville Sandstone in the Cushing Oil Field. (Solid lines indicate that the process was continuous without interruption; dashed lines indicate sporadic activity.)

precipitation (which requires basic conditions).

The system was also strongly influenced by major and even minor tectonic changes (aside from general basin subsidence). Minor fracturing, faulting and folding, all present in this area, could have greatly changed the path and speed of migrating pore fluids, introduced new pore fluids and created different solutions which, in turn, would have affected the diagenetic sequence of events. Additionally, the nature of the depositional environment had a large impact over how the fluids migrated and which ions were in solution. In this case, the Bartlesville was deposited as part of a large delta complex. Rapid variations in lithology are characteristic of the sand bodies deposited in this delta, a factor which strongly influenced the routes, speed and even composition of migrating pore fluids. Given the same detrital constituents, original pore water and tectonic history (geothermal gradient, depth of burial, faulting folding, etc.) but instead a barrier beach deposit, the diagenetic imprint would probably be much different.

A general order of diagenetic events based on empirical observations is

1. formation of chlorite rims,
2. precipitation of quartz overgrowths,

   initial dissolution of feldspars and their alteration to clays,

   beginning of generation of hydrocarbons in the Cherokee Group, (hypothesized)
3. chloritization of kaolinite and illite,
4. precipitation of microquartz,
5. precipitation of chalcedony,
6. precipitation of Fe-calcite and siderite.

CHAPTER XII

DIAGENETIC PROCESSES

Diagnetic reactions responsible for the present mineralogic composition of the Bartlesville Sandstone are the focus of this chapter. These reactions took place between the migrating pore fluids and the detrital and authigenic constituents. The reactions can be separated into three groups:

1. reactions involving quartz and calcite,
2. feldspar hydrolysis reactions,
3. reactions involving Fe^{2+} and Fe^{3+}.

Reactions Involving Quartz and Calcite

pH is a major factor in controlling the dissolution and precipitation of quartz and calcite. Figure 82 demonstrates the inverse relationship that exists between quartz and calcite, with respect to pH. At pH greater than 9, all forms of quartz are highly soluble while calcite is insoluble. Conversely, at pH less than 8, calcite is very soluble and quartz, insoluble. Thus, acidic to slightly basic solutions saturated with respect to silica should result in the precipitation of quartz in some form while basic solutions saturated with respect to calcite should precipitate calcite. A discussion of causes of the variable pH will be left for the final chapter.

The equilibrium reactions involved are:

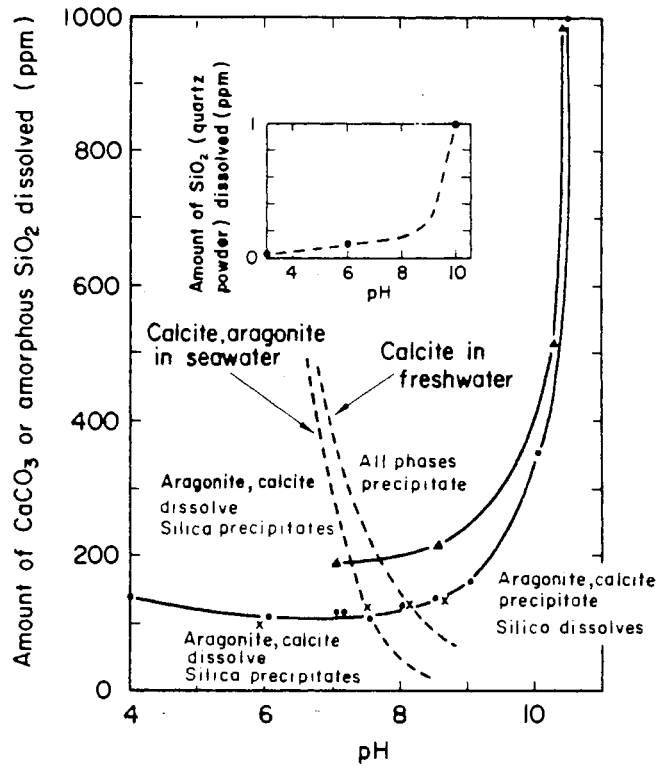

Figure 82. Effect of pH at Approximately 25°C on the Solubility of Calcium Carbonate, Quartz and Amorphous Silica. (Blatt, H. 1966, Diagenesis of Sandstone: Processes and Problems, Wyoming Geol. Assoc., 12, Ann. Conf.: 65A-0)

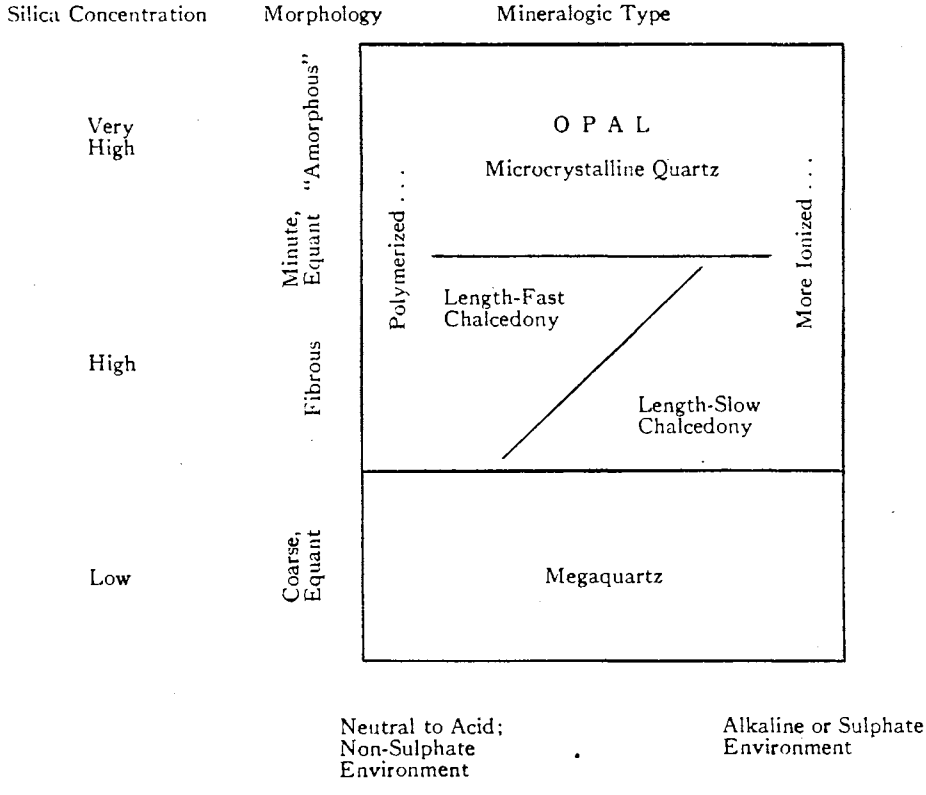

Figure 83. Relation of Silica Concentration, Morphology, Quartz Mineral Type and pH (from Folk and Pottman, 1979)

Silica -

$$SiO_2 + 2H_2O_{(aq)} \rightleftarrows H_4SiO_{4(aq)}^{*} \qquad \text{*indicates major species}$$

$$H_4SiO_{4(aq)} \rightleftarrows H_3SiO_{4(aq)}^{-} + H_{(aq)}^{+}$$

$$H_3SiO_{4(aq)}^{-} \rightleftarrows H_2SiO_{4(aq)}^{2} + H_{(aq)}^{+}$$

Calcite -

$$\begin{array}{l} H_2O_{(aq)} + CO_{2(g)} \\ \quad\downarrow\uparrow \\ CaCO_{3(s)} + H_2CO_{3(aq)} \rightleftarrows Ca_{(aq)}^{2+} + 2HCO_{3(aq)}^{-} \end{array}$$

The morphology of quartz depends upon a number of factors of which pH, silica activity, and the presence of "seeds" on which quartz can precipitate are most important (Figure 83). Mega-quartz (syntaxial overgrowths), chalcedony and micro- (or minute-equant) quartz are all present in the Bartlesville Sandstone. The presence of micro-quartz and chalcedony suggest that at one time silica activity was very high.

Feldspar Hydrolysis Reactions

The dissolution of feldspar results from hydrolysis reactions which are pH sensitive. As pH decreases, the reverse should occur; namely, feldspar dissolve (or alter to clay) and silica precipitate. The major dissolution reaction taking place is:

$$(\tfrac{1}{2}Ca,Na,K)\ Al_3SiO_{8(s)} + 6H_2O_{(aq)} + 2H_{(aq)}^{+} \rightleftarrows 3H_4SiO_{4(aq)} + 2(OH)_{(aq)}^{-}$$
$$+ \left(\tfrac{1}{2}Ca^{2+},\ Na^{+},K^{+}\right)_{(aq)} + 3Al_{(aq)}^{3+}$$

Additionally, if a feldspar is hyrolyzed, a very basic micro-environment surrounding the grain should result and quartz grains in close proximity should show some sign of corrosion or dissolution. Figure 67 demonstrates this relationship nicely, the quartz overgrowth exhibiting signs of corrosion only in the area situated next to the partly dissolved feldspar grain.

As already discussed and documented in detail in previous chapters, the alteration of feldspar to clay (illite and kaolinite) is commonplace. These clay alteration products also result from hydrolysis reactions. Two major reactions are involved, both of which need acidic solutions to go in the forward direction:

(Potassic Feldspar) (Illite)

$$3KAlSi_3O_{8(s)} + 2H_2CO_{3(aq)} + 12H_2O_{(aq)} \rightleftarrows KAl_3Si_3O_{10}(OH)_2 + 2K^+_{(aq)} + 6H_4SiO_{4(aq)} + 2HCO^-_{3(aq)}$$

(Al-Shaieb and Shelton, 1981)

(Potassic Feldspar)

$$2KAlSi_3O_{8(s)} + 2H_2CO_{3(aq)} + 9H_2O_{(aq)} \rightleftarrows Al_2Si_2O_5(OH)_{4(s)} + 2K^+_{(aq)} + 4H_4SiO_{4(aq)} + 2HCO^-_{3(aq)}$$

(Al-Shaieb and Shelton, 1981)

Reactions Involving Fe^{2+} and Fe^{3+}

The third group of diagenetic reactions thought to have been active in this reservoir are those involving the fixation of ferrous iron (Fe^{2+}) and the oxidation of ferrous iron minerals to hematite. A discussion of mechanisms whereby ferrous iron activity was raised to the saturation point in the pore fluids will take place in the final chapter.

Ferrous iron has been fixed mainly in pyrite, siderite and chlorite.

Morphologically, pyrite (FeS_2) exists in small framboidal clusters (Figures 71 and 72). The sulphur with which the iron has bonded appears to be rich in the S^{32} isotope based on isotopic analysis. This indicates that the sulphide ion formed from the reduction of a sulphate ion by anaerobic bacteria. This dismisses the possibility of the pyrite being part of a hydrocarbon induced diagenetic aureal (HIDA) (Al-Shaieb, 1981). If the sulphur in the pyrite had originated from sulphur in the oil, the sulphur would be enriched in S^{34}.

The stability fields of pyrite and siderite on an Eh-pH phase diagram are similar with the exception that pyrite can exist in slightly more acidic conditions than can siderite (Figure 84).

As indicated by the stability diagram, the oxidation of iron in pyrite or siderite can occur at low Eh and at variable pH. Oxidation of Fe^{2+} in pyrite and siderite would proceed as follows:

(Pyrite) (Hematite)

$$2FeS_{2(s)} + 15/2O_{2(s)} + 4H_2O_{(aq)} \rightleftarrows Fe_2O_{3(s)} + 4SO_{4(aq)}^{2-} + 8H_{(aq)}^{+}$$

(Krauskopff, p. 225, 1979)

(Siderite) (Hematite)

$$2FeCO_{3(s)} + O_2 + H_2O_{(aq)} \rightleftarrows Fe_2O_{3(s)} + 2HCO_{3(aq)}^{-} + 2H_{(aq)}^{+}$$

Chlorite is formed as an alteration product of both kaolinite (Figure 76) and illite according to the reactions:

(Kaolinite) (Chlorite)

$$3.5Fe^{2+} + 3.5\ mg^{2+} + 9H_2O + 3Al_2Si_2O_5 \rightleftarrows Fe_{3.5}Mg_{3.5}Al_{6.0}O_{20}(OH)_{16} + 14H^{+}$$

(Boles and Franks, 1979)

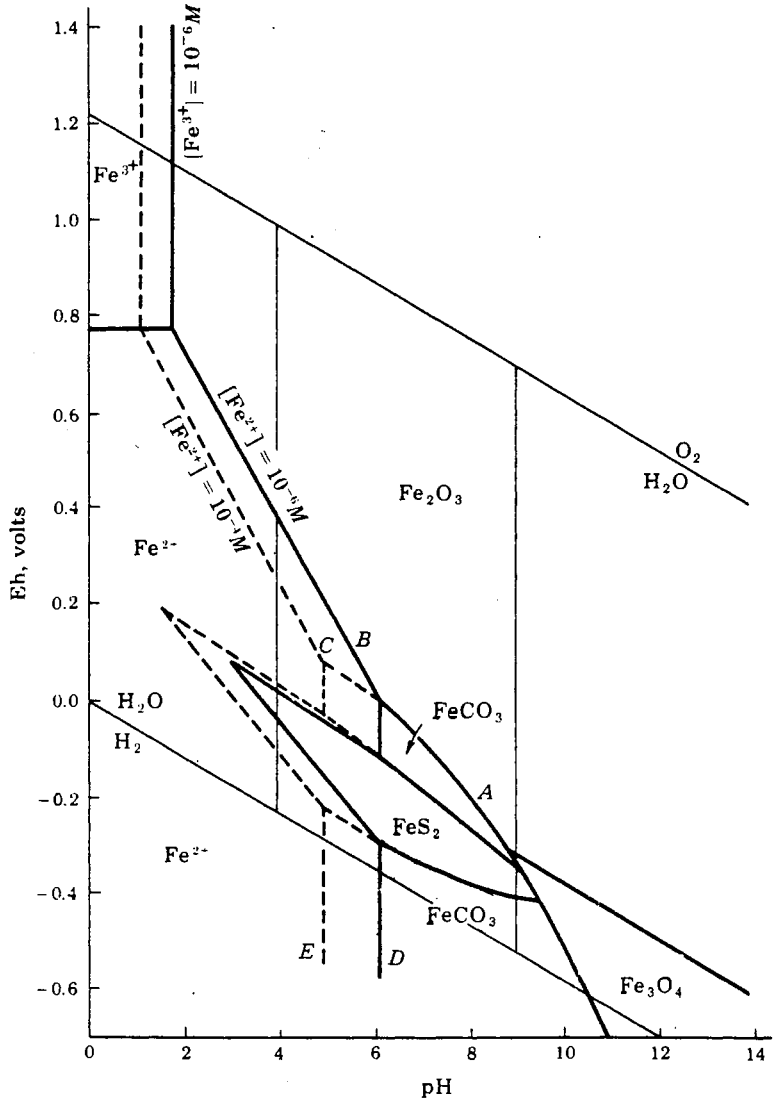

Figure 84. Eh-pH Diagram Showing Stability Fields of Common Iron Minerals With ($CaCO_1$ = 1 M Seq = 10^6 (from Krauskopff, 1979 - after Garrels and Christ, 1965)

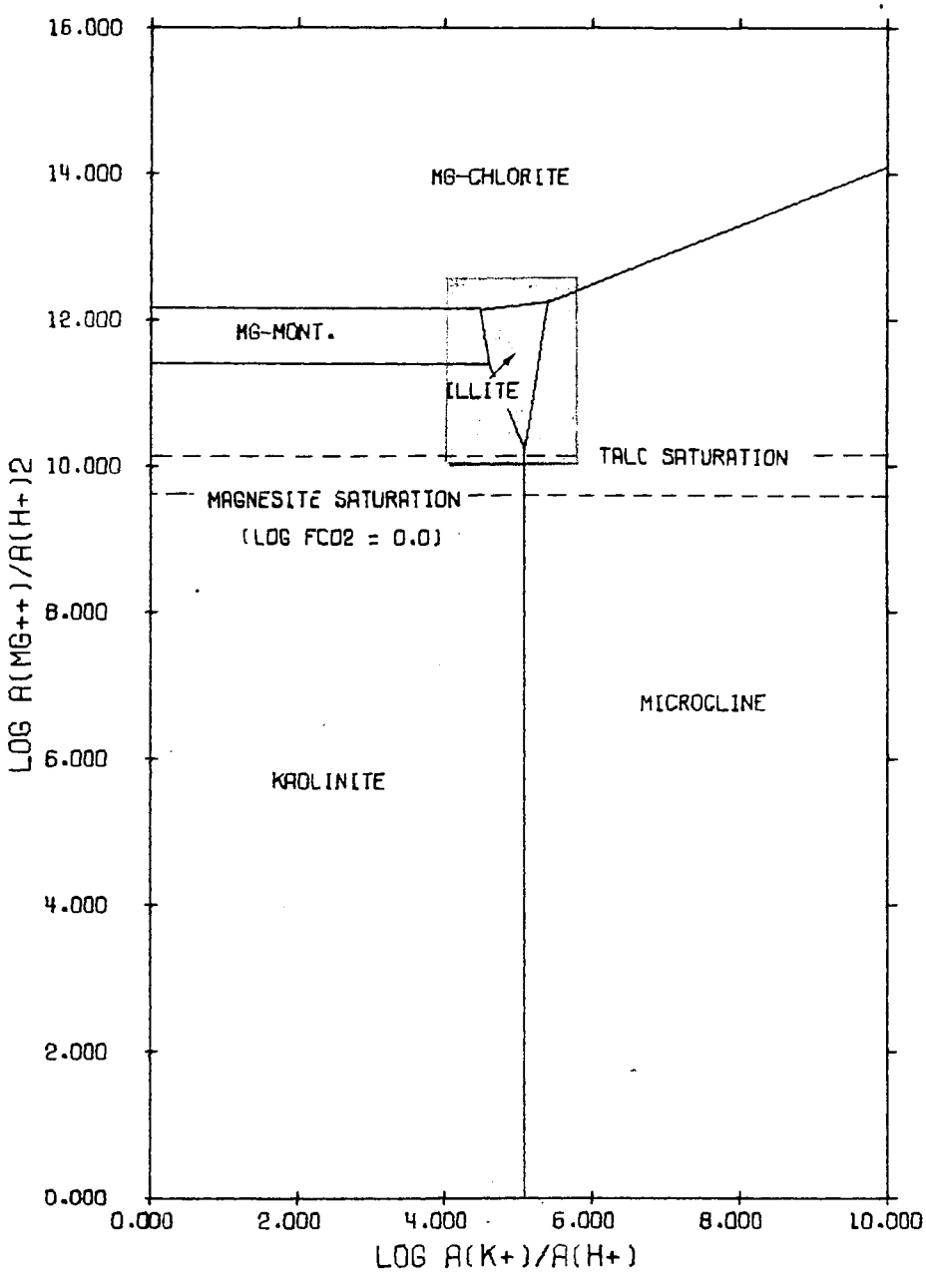

Figure 85. Activity Diagram for the System; $HCl-H_2O$ = $Al_2O_5-CO_2K_2O-Mg-SiO_2$ at 60°C; log a_{H_4} SiO_4 = - 3.52 = Quartz Saturation (from Helgeson, Brown and Teeper, 1969)

(Illite) (Chlorite)

$$3KAl_2AlSi_3O_{10}(OH)_2 + 10(Fe,Mg)^{2+} + 12H_2O \rightarrow 2Al(Mg,Fe)_5AlSi_3O_{10}(OH)_8 + 5Al^{3+} + 3Si(OH)_4 + 3K^+ + 2H^+$$ (Al-Shaieb, 1981)

As will be discussed in Chapter XII, the maximal temperature to which the Bartlesville Sandstone was subjected was up to 70°C. Figure 85, an activity diagram depicting chemical equilibria of the included minerals at one atmosphere of pressure and 60°C (Helgeson et al.,1969) gives a rough estimate of the ratio of $Mg^{2+}/H+$ and K+/H+ at the time the diagenetic reactions were taking place. The reactions show that kaolinite and illite will alter to chlorite and that microcline will alter to illite and kaolinite. These reactions should occur simultaneously. This suggests that pore water composition was probably located somewhere in the shaded area. While ferrous iron activity was probably of greater importance in the Bartlesville than the activity of Mg^{2+} (as iron chlorite is the dominant chlorite species), the similarities in behavior of Mg^{2+} and Fe^{2+} allows for substitution.

CHAPTER XIII

MECHANISMS

Three major groups of mechanisms have provided the drive behind the generation of hydrocarbons and diagenesis of the clays. These processes, depth of burial, local tectonics, and depositional environment, provided pore fluids with varying ionic species and in sufficient concentrations to create large amounts of secondary porosity and significantly alter the mineralogic composition of the original sandstone. This chapter endeavors to 1) explain how these three mechanisms have influenced the paragenetic history of the Bartlesville in the Cushing Field; 2) describe the relationship between depth of burial and the generation of hydrocarbons and diagnesis of clays, and 3) provide a real time framework for the sequence of events which influenced the diagenetic history of the Bartlesville Sandstone in the Cushing Field.

Depth of Burial

Increased temperatures and pressures in the Bartlesville caused by increased depth of burial ultimately resulted from the continuous subsidence of the Arkoma Basin and deposition of sediments throughout the middle Pennsylvanian and the early Permian. Maximal formation temperature is assumed to have occurred at the point of maximal burial. This assumption is based on the fact that throughout most of geologic history

the platform has been a tectonically stable region, free of volcanic activity and igneous intrusions. These events could have altered (increased) a "normal" geothermal gradient. Consequently, it was felt that the vitrinite reflectance of organic matter contained within the Cherokee Group in and around the thesis area could provide a reasonably accurate measure of the degree of thermal maturation, maximum temperature attained and ultimately the maximum depth of burial of the formation. Hood (1975, p. 988) states: "Probably one of the most useful measures of organic metamorphism is the reflectance of vitrinite." These data could then be used in conjunction with graphs by Hood to determine if hydrocarbons had been generated from Cherokee sediments.

Mean vitrinite reflectance values and correlative Level of Organic Metamorphism (LOM) (Figure 86) (Hood et al., 1975) of organic matter contained within the Bartlesville Sand in the Cushing Field are contained in Table II. As can be seen, values of LOM average roughly 7 for the Bartlesville. Figure 87 also incorporates effective heating time and maximum temperature and relates these to LOM. "Effective heating time" is defined by Hood (p. 990, 1975) as the "time during which a specific rock has been within 15°C (27°F) of its maximum temperature." Assuming a constant normal geothermal gradient of 1°C per 100 feet and that maximum depth of burial was attained in early to mid Permian times and maintained within 1,500 feet (15°C x /100 feet/1°C/ = 1,500 feet) the effective heating time roughly calculates to be 100 million years (M.Y.) or less. Using Figure 87, an LOM of 7 and a combined effective heating time of 100 M.Y. yields a maximum temperature up to 70°C or a maximum depth of burial of up to 7,000 feet (70°C x /100 feet/1°C/ = 7,000 feet) for the Bartlesville in the Cushing Field.

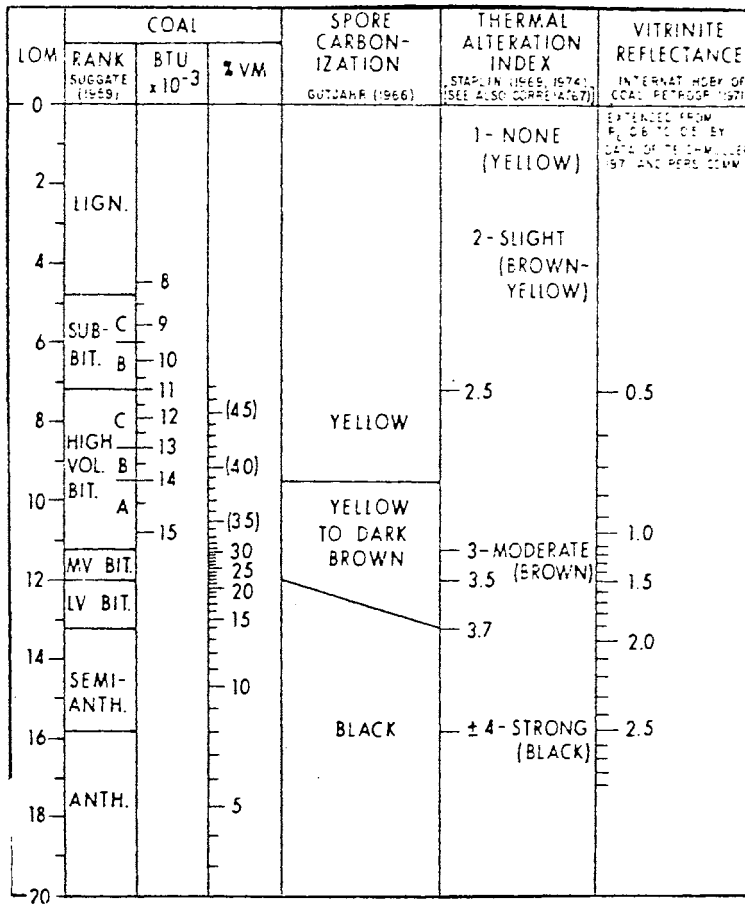

Figure 86. Comparison of Different Scales of Organic Metamorphism (from Hood, 1975)

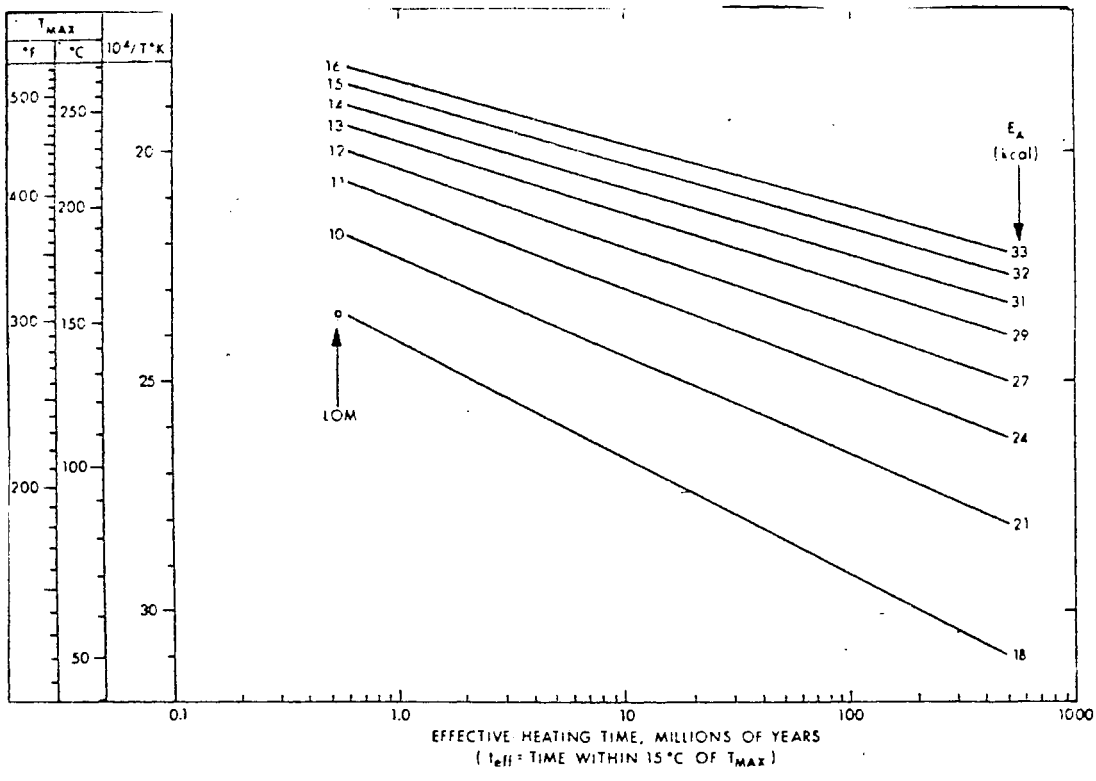

Figure 87. Relation of LOM to Maximum Temperature and Effective Heating Time (from Hood, 1975)

TABLE II

VITRINITE REFLECTANCE VALUES FROM THE BARTLESVILLE SANDSTONE IN THE CUSHING OIL FIELD, CREEK COUNTY, OKLAHOMA
(LOM values calculated from Hood, 1975)

Bartlesville		
Depth	Mean V.R.	LOM
2766	0.99	10.8
2741	0.56	7.9
2818	0.51	7.3
2600	0.93	10.5
2786	0.48	7.0

Note: (1) Mean Reflectance values at 2,766 and 2,600 feet are probably of recycled organic matter.
(2) Vitrinite Reflectance analysis was performed by Hagar Laboratories, Denver, Colorado.

The depth of burial and degree of thermal metamorphism show that the organic matter in the Cherokee Group was heated enough to generate hydrocarbons. Baker (1962) concluded upon examination of Cherokee sediments that organic matter contained in those sediments was the source of oil found in Cherokee reservoirs. Hatch and Leventhall (1982) arrived at the conclusion that the organic matter from black photostatic Cherokee shales is very similar to Cherokee crude oils, thus inferring Cherokee sediments were the source for oil found in Cherokee reservoirs (including the Bartlesville in the Cushing Field).

The significance of this is that migrating Cherokee pore fluids would tend to become more acidic in the presence of CO_2 gas, one of the by-products of the hydrocarbon generation process.

Local Tectonics

Faulting, fracturing and folding undoubtedly have played an important role in the initiation and duration of different diagenetic events. Large scale faulting has occurred along the Wilzetta Fault. Small scale faulting and fracturing is probably very common (and related to the extensive folding that has taken place) though difficult to detect in the subsurface. These faults and fractures provided conduits for pore waters. Additionally, the folding provided a geometry which would facilitate movement and mixing of pore waters.

Depositional Environment

Depositional environment appears to have influenced the diagenetic history of this region significantly. Somewhat distinct trends can be observed from the study of Figures 88, 89, and 90, plots of the

different constituents noted in thin sections. Grain size and detrital matrix are two indicators of depositional environment. Four general trends were recognized: 1) feldspar content increased as grain size decreased (Figure 90, 2,737' and 2,740'); 2) feldspar content increased as the amount of detrital matrix increased (Figure 90, 2,737', 2,740', and Figure 88, 2,420', 2,490', 2,439'); 3) amount of secondary porosity increased as the grain size increased and the amount of detrital matrix decreased (Figure 88, 2,662', 2,663', 2,692', 2,694', and Figure 90, 2,740', 2,744', 2746', 2,747', 2,760', 2,772'); 4) amount of secondary porosity increased as the amount of feldspar decreased.

The trends generally indicate that facies containing relatively large amounts of detrital matrix and finer grain sizes also contain higher percentages of feldspar and lower amounts of secondary porosity. The lower porosities combined with a high detrital matrix suggests that these fine-grained sediments also have low permeabilities. This relationship slowed the migration of pore fluids capable of dissolving feldspars. Less interaction between the pore waters and rock grains resulted in the inhibition of diagenetic reactions.

Depth of Burial/Clay Diagenesis and Hydrocarbon Generation

Hydrocarbon generation and clay diagenesis are the two most important processes providing for ionic enrichment of pore waters. With increased depth of burial, temperature increased. Eventually, organic matter became heated and resulted in the generation of hydrocarbons and CO_2. The CO_2 reacted with pore water to form carbonic acid which caused the dissolution and alteration of feldspar to kaolinite and

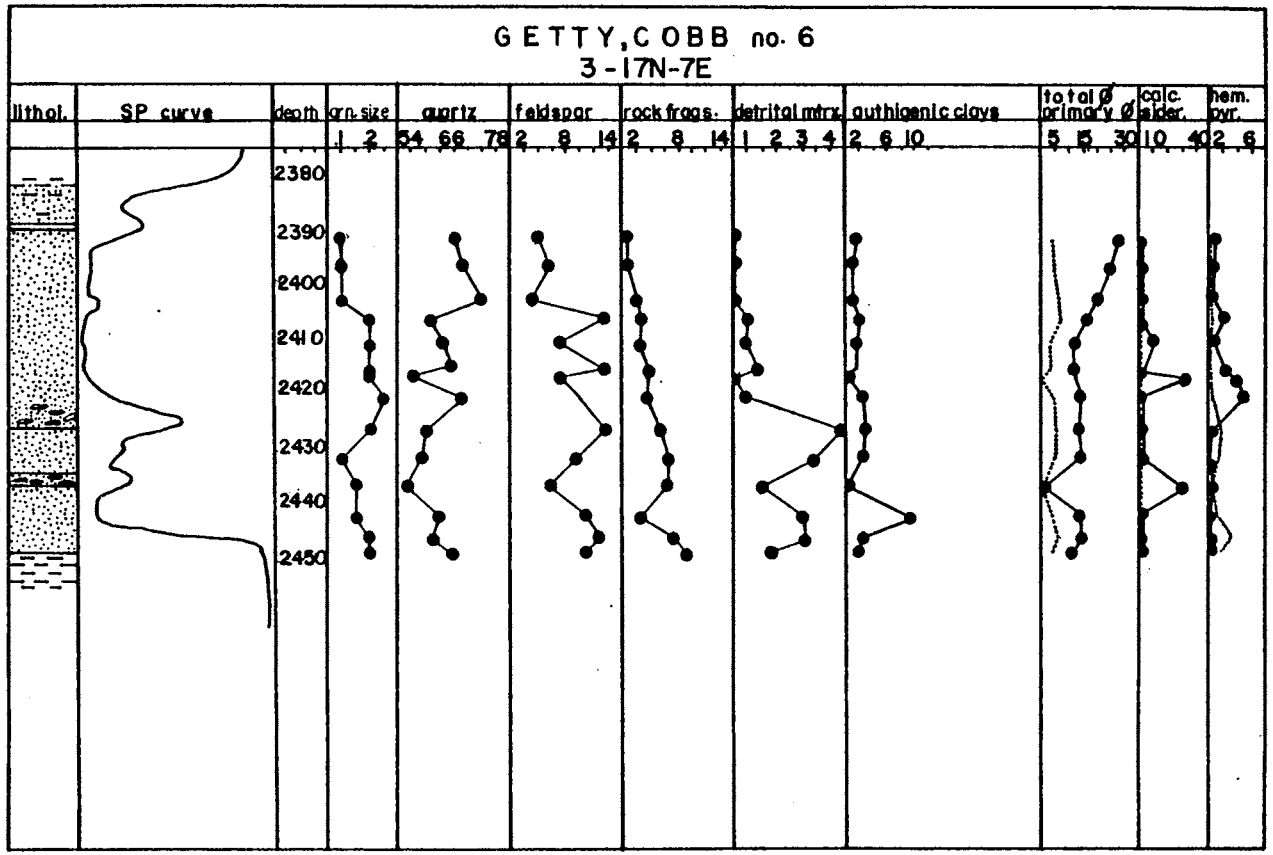

Figure 88. Synthesis of Information Gathered From the Getty, Cobb #6, Core

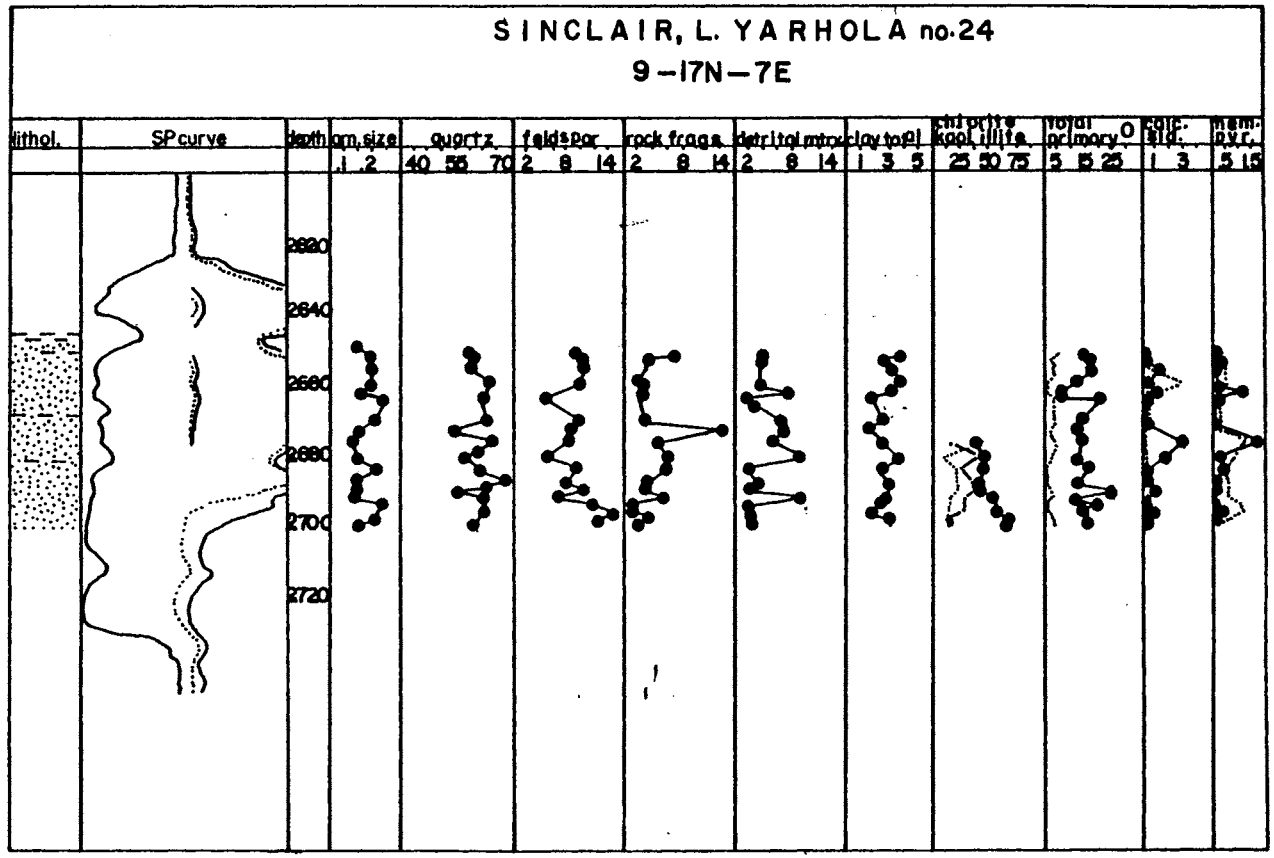

Figure 89. Synthesis of Information Gathered From the Sinclair, L. Yarhola #24 Core

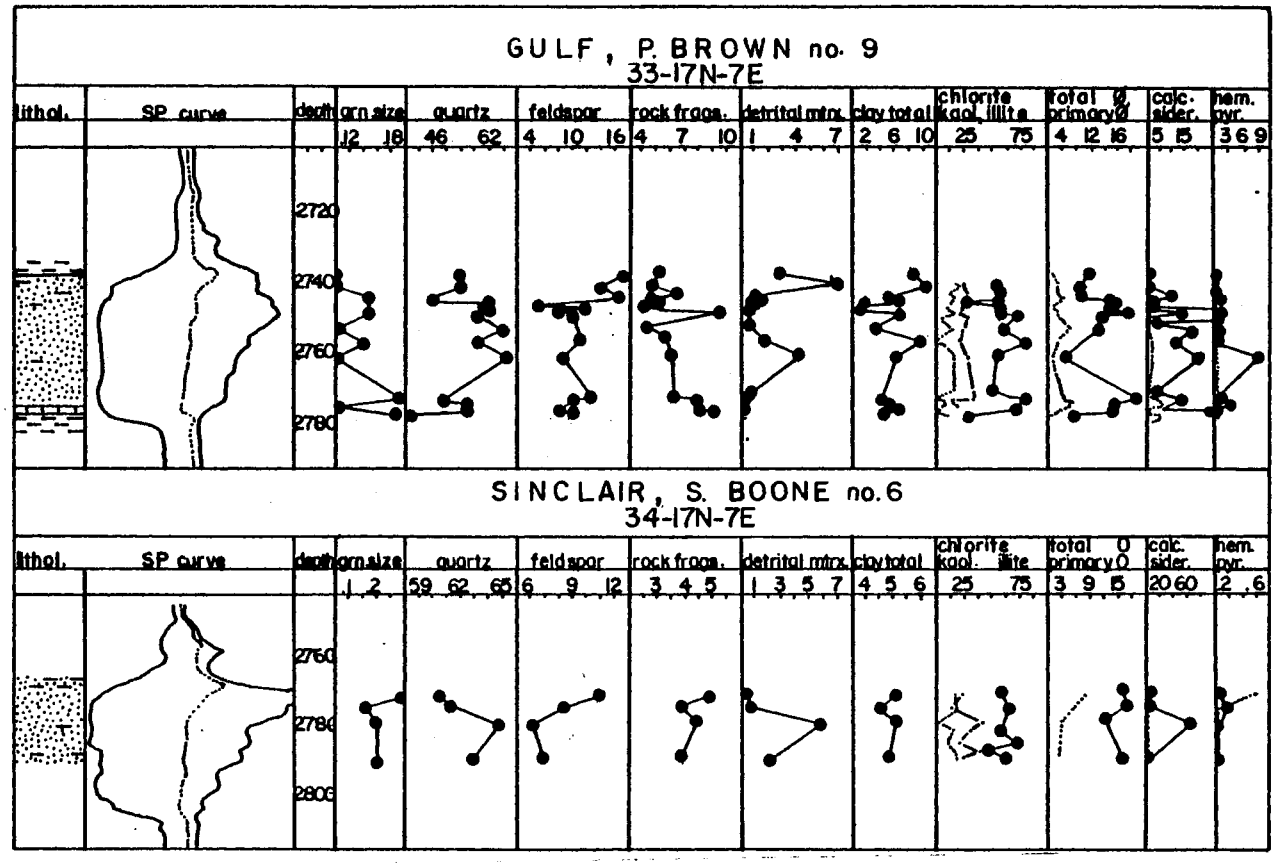

Figure 90. Synthesis of Data Gathered From the Gulf, P. Brown #9 Core, and the Sinclair S. Boone #6 Core

illite. As feldspars were dissolved and altered, the pore waters became enriched in Al^{3+} and Si^{4+} as well as Na^{+}, Ca^{2+}, K^{+}, Fe^{2+} and a host of other ions. The Si^{4+} was precipitated as different forms of quartz (megaquartz at first; chalcedony and microquartz later) as Si^{4+} activity increased.

Chloritization of kaolinite (Figures 42, 76) and illite resulted mainly from an increase in activities of Mg^{2+} and Fe^{2+} in pore waters with depth. The ionic activities of magnesium and iron increased due to the dissolution of magnesium and iron-rich minerals such as biotite and hornblende and the alteration of smectite to illite (Burst, 1969 and Hower, 1976).

Real-Time Model

Following deposition, the Bartlesville Sandstone was buried by late Desmoinesian, Missourian, Virgilian and probably even early Permian sediments. As discussed earlier, maximum depth of burial of the Bartlesville occurred during Permian times and was around 7,000 feet in the study area. This depth of burial is not quite great enough, assuming a geothermal gradient of $1^{o}C/100$ feet, to cause the generation of significant amounts of hydrocarbons and CO_2 gas. But it is felt that organic matter in lower Cherokee sediments to the west, southwest and south which were buried more deeply, underwent a greater degree of thermal alteration and generated large amounts of liquid and gaseous hydrocarbons and CO_2 gas. The CO_2 gas mixed with the pore water and created an acidic solution. These pore fluids migrated upslope, mixed with the original pore fluids in the Cushing anticline and initiated the diagenetic reactions. Feldspars were leached and

large amounts of secondary porosity created. Following this period of most active diagenesis, oil migrated up the shelf and accumulated in the anticline. An additional aid to the movement of oil was the regional tilt westward at the rate of about 50 feet per mile given to the entire region during Permian times.

The accumulation of oil in the Bartlesville in the Cushing Field in Permian times halted the diagenetic reactions that had been taking place and froze the morphology of the reservoir rock.

CHAPTER XIV

CONCLUSIONS

The following conclusions have been made from this study:

1. The Bartlesville Sandstone consists of four different sand bodies; the first deposited in a deltic distributionary channel, the second and third deposited in fluvial channels, and the fourth deposited at strandline sands of the advancing Cherokee sea.

2. Deposition was strongly influenced by the structural geology of the area as the Bartlesville thins over the crests of the domes.

3. Generation of the anticline was probably related directly to hypothesized strike-slip movement (dip-slip movement is also present) along the Wilzetta Fault which bounds the east side of the field. Movement along the fault took place throughout the Pennsylvanian and especially in Atokan and Desmoinesian times.

4. The Wilzetta Fault is a growth fault in this area. The stratigraphic section on the downthrown block is significantly thicker than that on the upthrown block.

5. Compositionally, the Bartlesville is classified as a subarkose. Plagioclase and microcline were common while rock fragments were rare.

6. Four major groups of diagenetic features were noted: dissolution features (mainly feldspars), precipitates (predominantly quartz overgrowths and authigenic clays), alteration features, replacement

features (calcite replacing feldspar and quartz).

7. Secondary porosity, as a result of partial to complete feldspar dissolution, is the predominant porosity type in this reservoir. Primary porosity is volumetrically unimportant.

8. Mean vitrinite reflectance of organic matter contained in the Bartlesville indicates that it was buried deeply enough and heated enough to generate hydrocarbons. These data, combined with data from studies by Baker (1962) and most recently by Hatch and Leventhal (1982) strongly suggest that oil in the Cushing Oil Field had a Pennsylvanian source.

9. Carbon dioxide gas, formed as a result of hydrocarbon generation process, reacted with pore water to form carbonic acid. This in turn lowered the pH of the pore water enough to dissolve feldspars and create large quantities of secondary porosity.

10. Generation of secondary porosity was related directly to the depositional environment. Secondary porosity was greatest in the coarser grained facies.

11. Secondary migration of hydrocarbons from the south, southwest and west into the anticline probably occurred in late Pennsylvanian and early Permian times. Later, tilting of the region to the west probably enhanced the rate of movement of the oil and gas. With the accumulation of oil in the sand, diagenetic reactions were halted.

REFERENCES

Al-Shaieb, Z. and Shelton, J. W., 1981, Migration of Hydrocarbons in Sandstones: Amer. Assoc. Petrol. Geol. Bull. Vol. 65, No. 11, pp. 2433-2436.

Al-Shaieb, Z., 1982, personal communication.

Baker, D. R., 1962, Organic Geochemistry of the Cherokee Group in Southeastern Kansas and Northeastern Oklahoma: Bull. Amer. Assoc. Petrol. Geol., Vol. 46, No. 9, pp. 1621-1641.

Bass, N. W., 1934, Origin of Bartlesville Shoestring Sands, Greenwood & Butler Counties, Kansas: Bull. Amer. Assoc. Petrol. Geol., Vol. 18, pp. 1333-1342.

Bass, N. W., Leathercock, C., Dillard, W. R., and Kennedy, L. E., 1937, Origin and Distribution of Bartlesville and Burbank Shoestring Oil Sands in Parts of Oklahoma and Kansas: Amer. Assoc. Petrol. Geol. Bull., Vol. 21, pp. 30-66.

Beal, C. H., 1917, Geologic Structure in the Cushing Oil and Gas Field, Oklahoma: U.S.G.S. Bulletin 658, 63 pp.

Bennison, A. P., 1979, Mobile Basin and Shelf Border Area in Northeast Oklahoma During Desmoinesian Cyclic Sedimentation: Tulsa Geol. Soc. Spec. Publication No. 1, pp. 283-294, 349-360.

Berg, O. R., 1966, Depositional Environment of a Portion of the Bluejacket Sandstone, Mayes County, Oklahoma: Shale Shaker, Vol. 16, No. 11, pp. 50-54.

Billings, M. P., 1972, Structural Geology: Prentice-Hall, Inc., Englewood Cliffs, New Jersey.

Boles, J. R. and Franks, S. G., 1979, Clay Diagenesis in Wilcox Sandstones of Southwest Texas: Implications of Smectite Diagenesis on Sandstone Cementation: Jour. Sed. Petrology, Vol. 49, No. 1, pp. 0055-0070.

Bosworth, T. O., 1920, Structure of the Cushing Oil Field, in Geology of the Mid Continent Oil Fields, Amer. Assoc. Petroleum Geologists Memoirs, pp. 169-183.

Branson, C. C., 1954, Marker Beds in the Lower Desmoinesian of northeastern Oklahoma: Oklahoma Academy of Science, Vol. 33, pp. 190-193.

Branson, C. C., 1962, Pennsylvanian History of Northeastern Oklahoma: Tulsa Geol. Soc. Digest, pp. 83-86.

Brown, T. H., Leeper, R. H., Helgeson, H. C., 1969, Handbook of Theoretical Activity Diagrams Depicting Chemical Equilibria in Geologic Systems Involving an Aqueous Phase at One Atmosphere and 0 to 300°C: Freeman, Cooper and Co., San Francisco, 253 pp.

Bullard, B. M., 1928, Cushing Oil Field, Oil and Gas in Oklahoma: Okla. Geol. Soc. Bull. 40, pp. 140-141.

Burst, J. F., 1969, Diagenesis of Gulf Coast Clayey Sediments and Its Possible Relation to Petroleum Migration: Amer. Assoc. Petrol. Geol. Bull., Vol. 53, pp. 73-93.

Buttram, F., 1914, The Cushing Oil and Gas Field, Oklahoma: Oklahoma Geol. Survey Bull. 18, 64 pp.

Clayton, J. M., 1965, Paleodepositional Environments of the "Cherokee" Sands of Central Payne County, Oklahoma: Shale Shaker, Vol. 15, No. 11, pp. 50-66.

Cole, G., 1969, Cherokee Group on the East Flank of the Nemaha Ridge, North Central Oklahoma: Shale Shaker, Vol. 19, pp. 134-146.

Dalton, D. V., 1960, The Subsurface Geology of Northeast Payne County, Oklahoma: Unpublished Master's Thesis, University of Oklahoma, Norman.

Dille, A. C. F., 1956, Paleotopography of the Precambrian Surface of Northeastern Oklahoma: Tulsa Geol. Soc. Digest, pp. 122-126.

Dogan, N., 1969, A Subsurface Study of Middle Pennsylvanian Rocks (from the Brown Limestone to the Checkerboard Limestone) in East Central Oklahoma: Master's Thesis, University of Tulsa, 67 pp.

Ebanks, W. J., 1979, Correlation of Cherokee (Desmoinesian) Sandstones of the Missouri-Kansas-Oklahoma Tri-State Area: in Pennsylvanian Sandstones of the Mid- Continent, Tulsa, Geol. Soc. Spec. Publication No. 1, pp. 295-313.

Fath, A. E., 1918, The Structure of the Northern Part of the Bristow Quadrangle, Creek County, Oklahoma, With Reference to Petroleum and Natural Gas: U. S. Geol. Survey Bull. 661, pp. 69-99.

Fath, A. E., 1921, The Origin of the Faults, Anticlines and "Buried Granite Ridge" of the Northern Part of the Mid Continent Oil and Gas Field: U.S. Geol. Survey Prof. Paper 128, pp. 75-84.

Fath, A. E., 1925, Geology of the Bristow Quadrangle, Creek County, Oklahoma: U. S. Geol. Survey Bull., 63 pp.

Foley, L. L., 1926, Origin of the Faults in Creek and Osage Counties, Oklahoma: Bull. Amer. Assoc. Petrol. Geol. Vol. 10, No. 3, pp. 293-303.

Foley, R. L. and Pittman, J. S., 1979, Length Slow Chalcedony: a New Testament for Vanished Evaporites: SEPM Reprint Series No. 8, pp. 59-73.

Ham, W. E., Dennison, R. E., and Merritt, C. A., 1964, Basement Rocks and Structural Evolution Southern Oklahoma, Okla. Geol. Survey Bull. 95, pp. 142-167.

Hanke, Harold W., 1967, Subsurface Stratigraphic Analysis of the Cherokee Group in North-Central Creek County, Oklahoma: Shale Shaker, No. 4, 1967, pp. 150-167.

Hatch, J. R. and Leventhal, J. S., 1982, Comparative Organic Geochemistry of Shales and Coals From Cherokee Group and Lower Part of Marmathon Group of Middle Pennsylvanian Age, Oklahoma, Kansas, Missouri, and Iowa: Bull. Amer. Assoc. Petrol. Geol. (Abst.), Vol. 66, No. 5, p. 579.

Hawisa, I., 1965, Dept. Environ. of the Bartlesville, the Red Fork, and the Tower Skinner Sandstones in Portions of Lincoln, Logan, and Payne Counties, Oklahoma: Master's Thesis, University of Tulsa, Oklahoma, pp. 1-34.

Heald, M. T. and Larese, R. E., 1973, The Significance of the Solution of Feldspar in Porosity Development, Jour. of Sed. Petrology, Vol. 43, No. 2, pp. 458-460.

Hood, A., Gutjahr, C. C. M. and Heacock, R. L., 1975, Organic Metamorphism and the Generation of Petroleum: Bull. Amer. Assoc. Petrol. Geol., Vol. 58, No. 6, pp. 986-996.

Howe, W. B., 1951, Bluejacket Sandstone of Kansas and Oklahoma: Bull. Amer. Assoc. Petrol. Geol. Vol. 35, p. 2092.

Howe, W. B., 1956, Stratigraphy of Pre-Marmaton Des Moinesian (Cherokee) Rocks in Southeastern Kansas: Kansas Geol. Survey Bull. 123, pp. 123-132.

Hower, J. et al., 1976, Mechanism of Burial Metamorphism of Argillaceous Sediments: I. Mineralogical and Chemical Evidence: Geol. Soc. Amer. Bull. Vol. 87, pp. 725-737.

Huffman, G. G., 1959, Pre-Sesmoinesian Isopachous and Palegeologic Studies in Central Mid-Continent Region: Bull. Amer. Assoc. Petrol. Geol. Vol. 43, No. 11, pp. 2541-2574.

Hulse, W. J., Depositional Environment of the Bartlesville Sandstone in the Sallyards Field, Greenwood County, Kansas: Tulsa Geol. Soc. Special Publisation No. 1, pp. 327-336, 349-360, 1979.

Jordan, L., 1959, Oil and Gas in Creek County, Oklahoma: in Geology of Creek County: Oklahoma Geol. Survey Bull., pp. 61-99.

Jordan, L., 1967, Geology of Oklahoma - A Summary: Oklahoma Geology Notes, Vol. 27, No. 12, pp. 215-228.

Kirk, M. S., 1957, A Subsurface Section From Osage County to Okfuskee County, Oklahoma: Shale Shaker, Vol. 7, No. 6, February, pp. 2-20.

Kittrick, J. A. and Hope, E. W., 1963, A Procedure for the Particle-Size Separation of Soils for X-Ray Diffraction Analysis: Sci. Paper No. 2261, Washington Agr. Expt. Sta. Project No. 1384, pp. 319-325.

Koff, L. R., 1978, Tectonics of the Oklahoma City Uplift: Master's Thesis, Oklahoma University, Norman, 64 pp.

Krauskopf, K. B., 1979, Introduction to Geochemistry, McGraw-Hill Book Company, New York, p. 206.

Krumme, G. W., 1975, Mid-Pennsylvanian Source Reversal on the Oklahoma Platform: Tulsa University Ph.D. Dissertation.

Leatherock, C. and Bass, N. W., 1937, Physical Characteristics of Bartlesville and Burbank Sands in Northeastern Oklahoma and Southeastern Kansas: Bull. Amer. Assoc. Petrol. Geol. Vol. 21, pp. 246-258.

Luza, K. V., and Lawson, J. E., 1981, Seismicity and Tectonic Relationship of the Nemaha Uplift in Oklahoma. III. Okla. Geol. Survey Bull. pp. 1-26.

McElroy, M. N., 1961, Isopach and Lithofacies Studies of the Des Moinesian Series of North Central Oklahoma: Shale Shaker Digest Vol. 12, No. 1, pp. 2-21.

McKeenry, J. W., 1953, Subsurface Geology of Northwestern Logan County, Oklahoma: Shale Shaker Digest Vol. 3, No. 6, pp. 6-35.

Merritt, J. W. et al., 1930, Oil and Gas in Oklahoma, Creek County: Oklahoma Geol. Survey Bull. 40, Vol. 3, pp. 1-43.

Moore, G. E., 1979, Pennsylvanian Paleography of the Mid-Continent: in Pennsylvanian Sandstones of the Mid-Continent: Tulsa Geol. Soc. Spec. Publication No. 1, pp. 2-12.

Morgan, J. T. and Gordon, D. T., 1970, Influence of Pore Geometry on Water-Oil Relative Permeability: Jour. of Petrol. Tech., No. 10, pp. 1199-1208.

Oakes, M. C., 1953, Krebs and Cabaniss Groups of Pennsylvanian Age in Oklahoma: Bull. Amer. Assoc. Petrol. Geol. Vol. 37, pp. 1523-1526.

Odom, I. E., Willand, T. N. and Lassin, R. J., 1978, Paragenesis of Diagenetic Minerals in the St. Peter Sandstone (Ordovician), Wisconsin and Illinois, in SEPM Special Publication No. 26, pp. 425-443.

Phares, R. S., 1969, Depositional Framework of the Bartlesville Sandstone in Northeastern Oklahoma: M.S. Thesis, University of Tulsa, Oklahoma, 59 pp.

Phipps, S., 1982, Personal Communication.

Pittman, E. D., 1979, Porosity, Diagenesis and Productive Capability of Sandstone Reservoirs: in Aspects of Diagenesis, Soc. Econ. Paleon, and Min. Spec. Publication No. 26, pp. 159-174.

Puckette, J., 1982, Personal Communication.

Pulling, D. M., 1979, Subsurface Stratigraphic and Structural Analysis, Cherokee Group, Pottawatomie County, Oklahoma: Shale Shaker, Vol. 29, pp. 124-137; 148-158.

Riggs, C. H. et al., 1958, History and Potentialities of the Cushing Oil Field, Creek County, Oklahoma: Bureau of Mines Report of Investigations 5415, pp. 1-73.

Saitta, S. B., 1968, Bluejacket Formation - A Subsurface Study in Northeastern Oklahoma: Master's Thesis, University of Tulsa, Oklahoma, 74 pp.

Sartin, J. P., 1958, A Cross-sectional Study of the Oil-producing Rocks of Des Moinesian Age in Northeastern Oklahoma: Unpublished Master's Thesis, University of Oklahoma, Norman, 75 pp.

Schmidt, V. and McDonald, D.A., 1979, Texture and Recognition of Secondary Porosity in Sandstones, in Aspects of Daigenesis, Soc. Econ. Paleon. and Min., Spec. Publication No. 26, pp. 208-226.

Scholle, P., 1979, Constituents, Textures, Cements and Porosities of Sandstones and Associated Rocks: AAPG Memoir No. 28, p. 201.

Shelton, J. W., 1973, Models of Sand and Sandstone Deposits: A Methodology for Determining Sand Genesis and Trend: Okla. Geol. Soc. Bull. 118, 122 pp.

Shelton, J. W., 1982, Personal Communication.

Shulman, C., 1966, Stratigraphic Analysis of the Cherokee Group in Adjacent Portions of Lincoln, Logan, and Oklahoma Counties, Oklahoma: Shale Shaker Digest, Vol. 16, No. 2, pp. 126-140.

Stewart, G., 1982, Personal Communication.

Surdam, R. C. and Boles, J. R., 1978, Hiagenesis of Volcanic Sandstones in Aspects of Diagenesis, SEPM Spec. Publication No. 26, pp. 227-243.

Verish, N. P., 1979, Reservoir Trends, Depositional Environments, and Petroleum Geology of Selected Cherokee Sandstones in T11-13N, R4-5E: Shale Shaker, Vol. 29, No. 9, pp. 209-236.

Visher, G., 1968, A Guidebook to the Bluejacket-Bartlesville Sandstone, Oklahoma: Oklahoma Geol. Soc., 72 pp.

Wardwell, D. P, Bradenthaler, R., Williams, W., and Van Dall, J., 1927, Water Problems in the North Part of the Cushing Field, Creek County, Oklahoma: U. S. Bureau of Mines (mimeographed report).

Weirich, R. E., 1929, Cushing Oil and Gas Field, Creek County, Oklahoma: Paper in Structure of Typical American Oilfields, Vol. 2-A Symposium, Amer. Assoc. Petrol. Geol., pp. 396-406.

Weirich, T. E., 1953, Shelf Principle of Oil Origin, Migration and Accumulation: Bull. Amer. Assoc. Petrol. Geol., Vol. 37, pp. 1017-1045.

Wickham, J. S., 1978, The Southern Oklahoma Aulacogen: in Structure and Stratigraphy of the Ouachita Mountains and Arkoma Basin, AAPG Field Guide.

APPENDIX

CORE DESCRIPTIONS

Petrologic Log

Company SINCLAIR OIL & GAS

Well Location L. YARHOLA No. 24, 9-17N-7E

GRAIN SIZE AVG \ MAX:

POROSITY
P PRIMARY
S SECONDARY
M MICROPOROSITY

CONSTITUENTS

QUARTZ
M Monocrystalline
P Polycrystalline
C Chert
O Other

FELDSPAR
P Plagioclase
O Other

ROCK FRAGMENTS
M Metamorphic
I Intrusive
V Volcanic

CLAY & CARBONATE
C Clay
Ca Carbonate

FOSSILS
Plant
C Carbonaceous Material
W Carbonized Wood

INVERBRATES & ALGAE
A Algae
Ar Arthropods
B Brachiopods
C Cephalopods
Co Corals
E Echinoderm
F Fusulina
G Gastropod
P Pelecypod
S Sponge

CLAY MINERALS
C Chlorite
H Halloysite
I Illite
K Kaolinite
S Smectite
Mi Mixed Layered
O Other

CARBONATE
C Calcite
Fe Ferroan Calcite
D Dolomite
Fe Ferroan Dolomite
S Siderite
O Other

SILICA
O Quartz Overgrowth
M Micro Quartz
Ch Chalcedony

SULFIDES
P Pyrite
O Other

SULFATES
G Gypsum
A Anhydrite
B Barite
O Other

MICA
M Muscovite
B Biotite
O Other

Lithology

- CLAY / CLAYSTONE
- SILTY CLAYSTONE / MUDSTONE
- SILT / SILTSTONE
- SAND / SANDSTONE
- INTERBEDDED SANDSTONE / MUDSTONE
- MUDDY SANDSTONE
- CONGLOMERATE
- LIMESTONE
- MARL
- DOLOMITE
- DOLOMITIC ROCKS
- GYPSUM / ANHYDRITE
- GYPSIFEROUS ROCKS
- HALITE
- CHERT
- CHERTY ROCKS
- COAL / LIGNITE
- VOLCANIC ROCKS
- INTRUSIVE ROCKS
- METAMORPHIC ROCKS

Bedding(B)-Laminae(L)

- MASSIVE
- HORIZONTAL
- INITIAL SLOPE / DIP
- GRADED
- CROSS BEDDING (DUNES WAVES)

*Surface-Features

- RIPPLE LAMINAE
- CURRENT SOLEMARKS
- *Surface-Related

Deformed Features

- FLOWAGE(F) FAULTED(Fa) LOAD(L)
- WATER ESCAPE
- DISRUPED

Organic

- BURROW TRACE FOSSIL
- BIOTURBATED
- ROOT TRACES

Chemical

- CONCRETIONS
- STYLOLITES

Contacts of Strata

- ABRUPT
- TRANSITIONAL
- EROSIONAL
- BORED
- DEFORMED

Cores

- CORED INTERVAL AND CORE NUMBER
- RECOVERY
- NO RECOVERY

Miscellaneous

- THIN SECTION
- P & P ANALYSIS
- SEM

Rock Classification

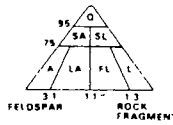

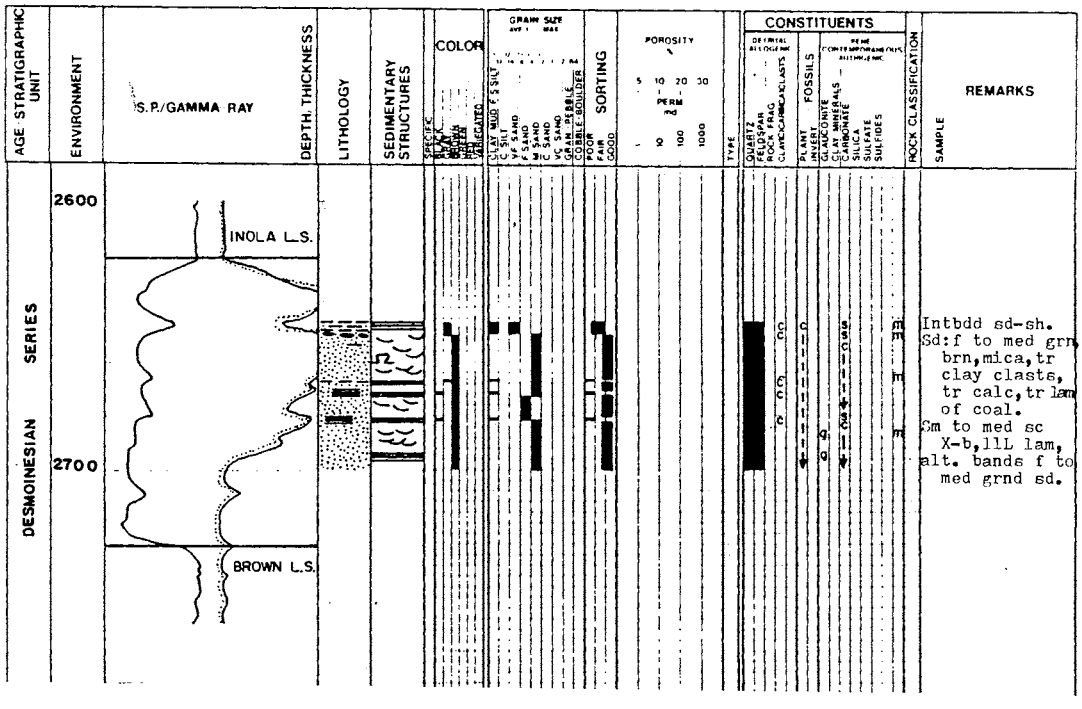

Petrologic Log

Company SINCLAIR OIL & GAS

Well Location S.BOONE No.6, 34-17N-7E

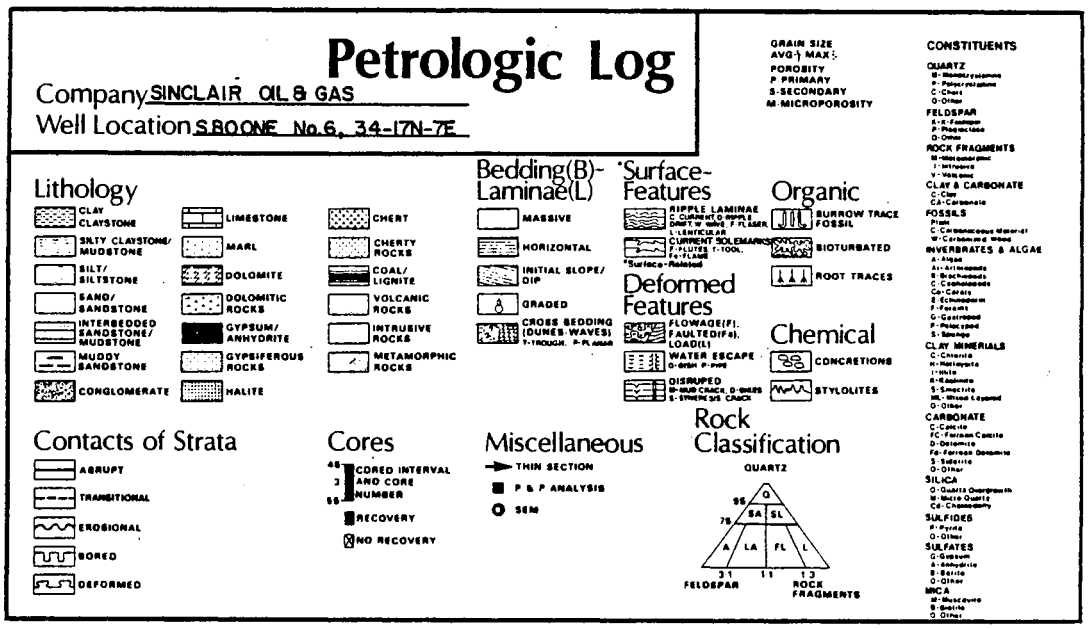

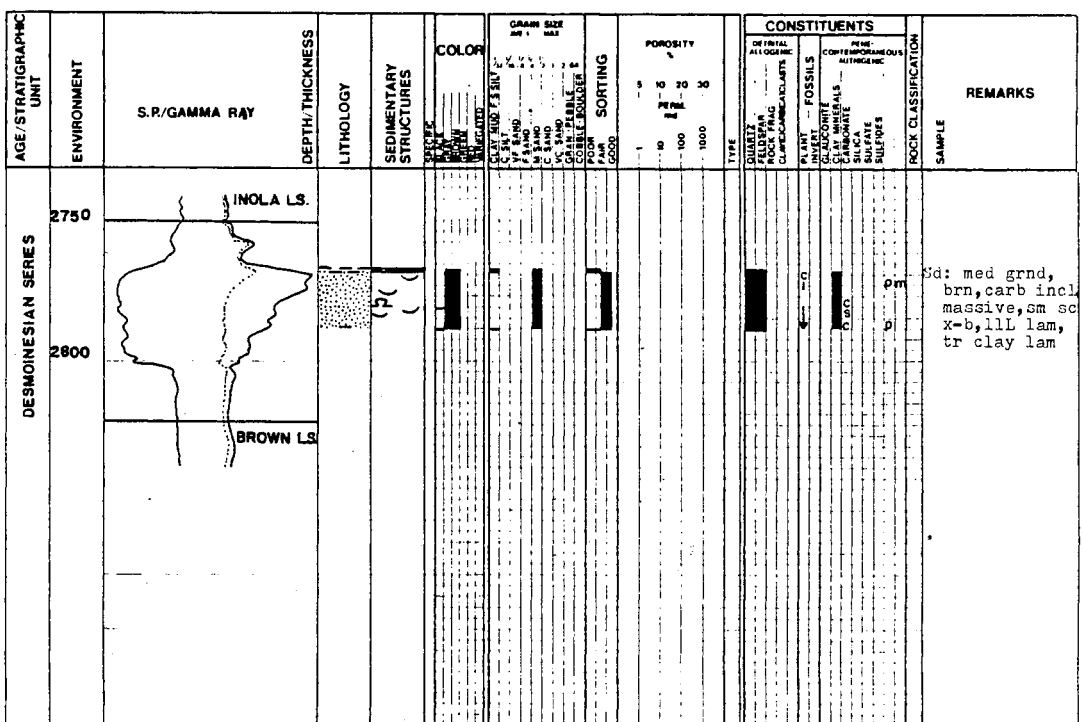

Petrologic Log

Company SINCLAIR OIL & GAS

Well Location B.B. JONES No. 21, 4-17N-7E

GRAIN SIZE
AVG \ MAX
POROSITY
P PRIMARY
S SECONDARY
M MICROPOROSITY

CONSTITUENTS
QUARTZ
FELDSPAR
ROCK FRAGMENTS
CLAY & CARBONATE
FOSSILS
INVERBRATES & ALGAE
CLAY MINERALS
CARBONATE
SILICA
SULFIDES
SULFATES
MICA

Lithology

- CLAY / CLAYSTONE
- SILTY CLAYSTONE / MUDSTONE
- SILT / SILTSTONE
- SAND / SANDSTONE
- INTERBEDDED SANDSTONE / MUDSTONE
- MUDDY SANDSTONE
- CONGLOMERATE
- LIMESTONE
- MARL
- DOLOMITE
- DOLOMITIC ROCKS
- GYPSUM / ANHYDRITE
- GYPSIFEROUS ROCKS
- HALITE
- CHERT
- CHERTY ROCKS
- COAL / LIGNITE
- VOLCANIC ROCKS
- INTRUSIVE ROCKS
- METAMORPHIC ROCKS

Bedding(B)-Laminae(L)

- MASSIVE
- HORIZONTAL
- INITIAL SLOPE / DIP
- GRADED
- CROSS BEDDING (DUNES WAVES)

Surface-Features

- RIPPLE LAMINAE
- CURRENT SOLEMARKS
- *Surface-Related

Deformed Features

- FLOWAGE(F) FAULTED(F) LOAD(L)
- WATER ESCAPE
- DISRUPED

Organic

- BURROW TRACE FOSSIL
- BIOTURBATED
- ROOT TRACES

Chemical

- CONCRETIONS
- STYLOLITES

Contacts of Strata

- ABRUPT
- TRANSITIONAL
- EROSIONAL
- BORED
- DEFORMED

Cores

- CORED INTERVAL AND CORE NUMBER
- RECOVERY
- NO RECOVERY

Miscellaneous

- THIN SECTION
- P & P ANALYSIS
- SEM

Rock Classification

QUARTZ — FELDSPAR — ROCK FRAGMENTS

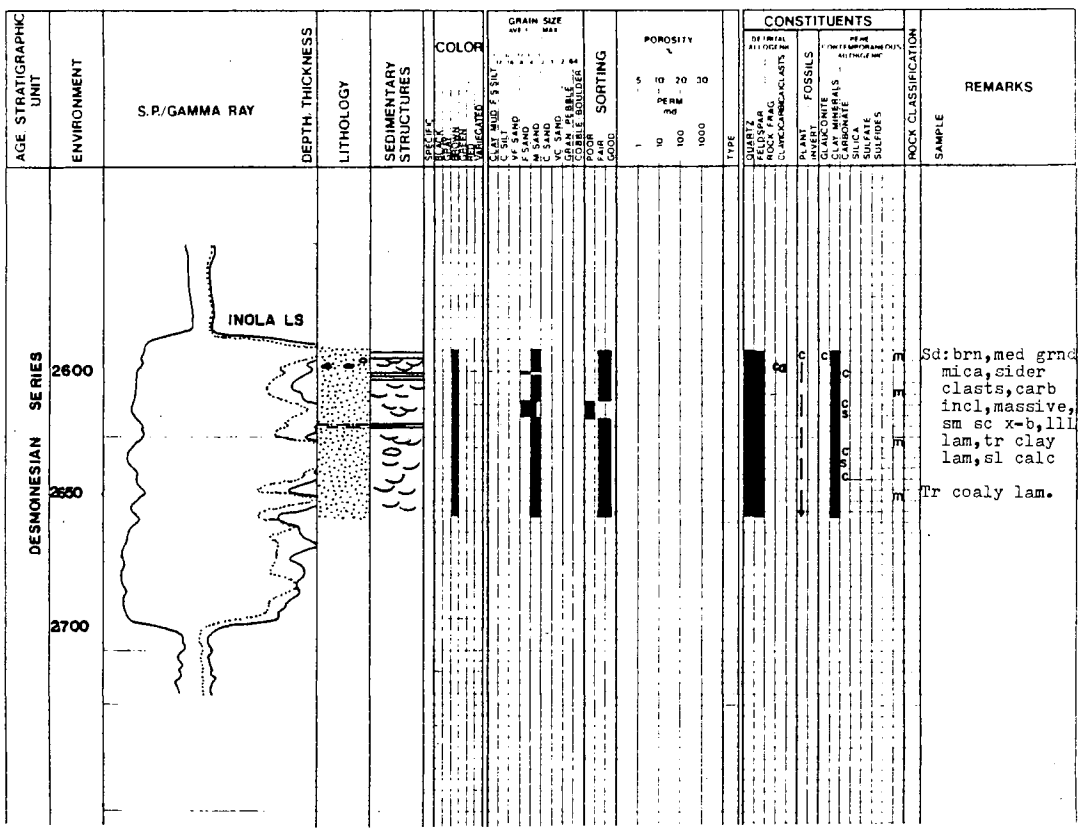

Petrologic Log

Company GETTY OIL Co.

Well Location COBB No.6, 3-17N-7E

GRAIN SIZE
AVG-) MAX-)
POROSITY
P PRIMARY
S SECONDARY
M MICROPOROSITY

CONSTITUENTS

QUARTZ
M Metamorphic
P Polycrystalline
C Chert
O Other

FELDSPAR
K K Feldspar
P Plagioclase
O Other

ROCK FRAGMENTS
M Metamorphic
I Intrusive
V Volcanic

CLAY & CARBONATE
C Clay
Ca Carbonate

FOSSILS
Plant
C Carbonaceous Material
W Carbonized Wood

INVERTEBRATES & ALGAE
A Algae
An Actinopoda
B Brachiopods
C Cephalopods
Co Corals
E Echinoderm
F Foram
G Gastropod
P Pelecypod
S Sponge

CLAY MINERALS
C Chlorite
H Halloysite
I Illite
K Kaolinite
S Smectite
ML Mixed Layered
O Other

CARBONATE
C Calcite
FC Ferroan Calcite
D Dolomite
Fd Ferroan Dolomite
S Siderite
O Other

SILICA
Q Quartz Overgrowth
M Micro Quartz
Ch Chalcedony

SULFIDES
P Pyrite
O Other

SULFATES
G Gypsum
A Anhydrite
B Barite
O Other

MICA
M Muscovite
B Biotite
O Other

Lithology

- CLAY / CLAYSTONE
- SILTY CLAYSTONE / MUDSTONE
- SILT / SILTSTONE
- SAND / SANDSTONE
- INTERBEDDED SANDSTONE / MUDSTONE
- MUDDY SANDSTONE
- CONGLOMERATE
- LIMESTONE
- MARL
- DOLOMITE
- DOLOMITIC ROCKS
- GYPSUM / ANHYDRITE
- GYPSIFEROUS ROCKS
- HALITE
- CHERT
- CHERTY ROCKS
- COAL / LIGNITE
- VOLCANIC ROCKS
- INTRUSIVE ROCKS
- METAMORPHIC ROCKS

Bedding(B)-Laminae(L)

- MASSIVE
- HORIZONTAL
- INITIAL SLOPE / DIP
- GRADED
- CROSS BEDDING (DUNES WAVES) T-THROUGH P-PLANAR

Surface-Features

- RIPPLE LAMINAE C-CURRENT O-WAVE I-ORIENTED T-TRACE F-FLASER L-LENTICULAR
- CURRENT SOLEMARKS F-FLUTES T-TOOL Fo-FLUTE
- *Surface-Related

Deformed Features

- FLOWAGE(F) FAULTED(Fa) LOAD(L)
- WATER ESCAPE D-DISH P-PIPE
- DISRUPED M-MUD CRACK D-DIKES S-SYNERESIS CRACK

Organic

- BURROW TRACE FOSSIL
- BIOTURBATED
- ROOT TRACES

Chemical

- CONCRETIONS
- STYLOLITES

Contacts of Strata

- ABRUPT
- TRANSITIONAL
- EROSIONAL
- BORED
- DEFORMED

Cores

- 45 CORED INTERVAL
- 3 AND CORE
- 55 NUMBER
- RECOVERY
- NO RECOVERY

Miscellaneous

- THIN SECTION
- P & P ANALYSIS
- SEM

Rock Classification

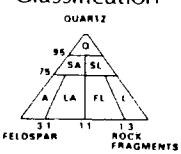

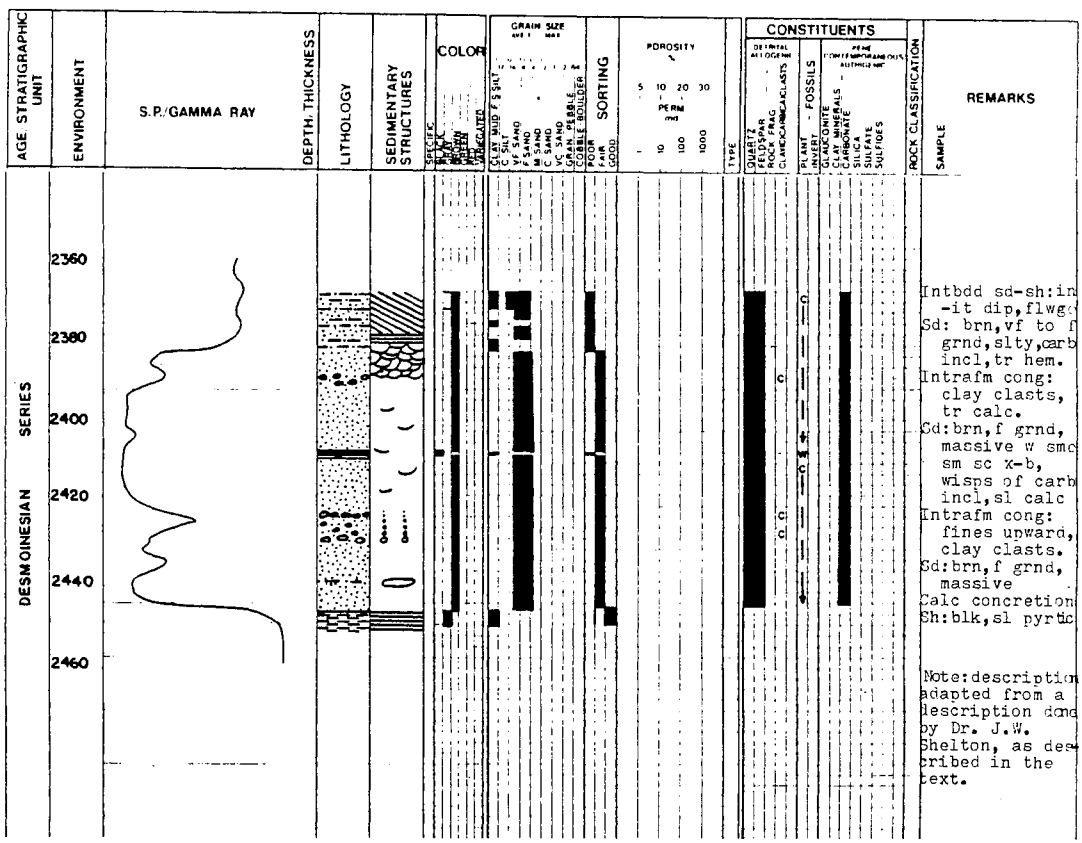

Petrologic Log

Company SINCLAIR OIL & GAS

Well Location L. KEYS, No. 46

GRAIN SIZE
AVG \ MAX
POROSITY
P PRIMARY
S SECONDARY
M MICROPOROSITY

CONSTITUENTS

QUARTZ
FELDSPAR
ROCK FRAGMENTS
CLAY & CARBONATE
FOSSILS
INVERBRATES & ALGAE
CLAY MINERALS
CARBONATE
SILICA
SULFIDES
SULFATES
MICA

Lithology

- CLAY / CLAYSTONE
- SILTY CLAYSTONE / MUDSTONE
- SILT / SILTSTONE
- SAND / SANDSTONE
- INTERBEDDED SANDSTONE / MUDSTONE
- MUDDY SANDSTONE
- CONGLOMERATE
- LIMESTONE
- MARL
- DOLOMITE
- DOLOMITIC ROCKS
- GYPSUM / ANHYDRITE
- GYPSIFEROUS ROCKS
- HALITE
- CHERT
- CHERTY ROCKS
- COAL / LIGNITE
- VOLCANIC ROCKS
- INTRUSIVE ROCKS
- METAMORPHIC ROCKS

Bedding(B)-Laminae(L)

- MASSIVE
- HORIZONTAL
- INITIAL SLOPE / DIP
- GRADED
- CROSS BEDDING (DUNES WAVES)

Surface-Features

- RIPPLE LAMINAE
- CURRENT SOLEMARKS
- *Surface-Related

Deformed Features

- FLOWAGE(F)
- FAULTED(F) LOAD(L)
- WATER ESCAPE
- DISRUPTED

Organic

- BURROW TRACE FOSSIL
- BIOTURBATED
- ROOT TRACES

Chemical

- CONCRETIONS
- STYLOLITES

Contacts of Strata

- ABRUPT
- TRANSITIONAL
- EROSIONAL
- BORED
- DEFORMED

Cores

- CORED INTERVAL AND CORE NUMBER
- RECOVERY
- NO RECOVERY

Miscellaneous

- THIN SECTION
- P & P ANALYSIS
- SEM

Rock Classification

QUARTZ

95 / 75

Q, SA, SL, A, LA, FL, L

FELDSPAR — ROCK FRAGMENTS

AGE STRATIGRAPHIC UNIT	ENVIRONMENT	S.P./GAMMA RAY	DEPTH, THICKNESS	LITHOLOGY	SEDIMENTARY STRUCTURES	COLOR	GRAIN SIZE	SORTING	POROSITY	CONSTITUENTS	ROCK CLASSIFICATION	SAMPLE	REMARKS
DESMOINESIAN SERIES		INOLA LS	2800										Intbdd sd-sh. Sd:brn,vf to f grnd,carb incl, mica,tr hem, sm to med sc x-b,lll lam. Intrafm cong: clay clasts
			2850										
		BROWN LS.											

Petrologic Log

Company ARCO

Well Location H. DUNSON No 42, 33-17N-7E

GRAIN SIZE
AVG) MAX
POROSITY
P PRIMARY
S SECONDARY
M MICROPOROSITY

CONSTITUENTS
QUARTZ
FELDSPAR
ROCK FRAGMENTS
CLAY & CARBONATE
FOSSILS
INVERBRATES & ALGAE
CLAY MINERALS
CARBONATE
SILICA
SULFIDES
SULFATES
MICA

Lithology

CLAY
CLAYSTONE
SILTY CLAYSTONE
MUDSTONE
SILT/
SILTSTONE
SAND/
SANDSTONE
INTERBEDDED
SANDSTONE/
MUDSTONE
MUDDY
SANDSTONE
CONGLOMERATE
LIMESTONE
MARL
DOLOMITE
DOLOMITIC
ROCKS
GYPSUM/
ANHYDRITE
GYPSIFEROUS
ROCKS
HALITE
CHERT
CHERTY
ROCKS
COAL/
LIGNITE
VOLCANIC
ROCKS
INTRUSIVE
ROCKS
METAMORPHIC
ROCKS

Bedding(B)-Laminae(L)

MASSIVE
HORIZONTAL
INITIAL SLOPE/
DIP
GRADED
CROSS BEDDING
(DUNES WAVES)

Surface-Features

RIPPLE LAMINAE
CURRENT RIPPLE
DRIFT W. WAVE
PLANAR
CURRENT
CURRENT SOLEMARKS
FLUTES
TOOL
FLAME
*Surface-Related

Deformed Features

FLOWAGE(F),
FAULTED(F),
LOAD(L)
WATER ESCAPE
DISRUPTED
MUDCRACK
DIKES
SYNERESIS CRACK

Organic

BURROW TRACE
FOSSIL
BIOTURBATED
ROOT TRACES

Chemical

CONCRETIONS
STYLOLITES

Contacts of Strata

ABRUPT
TRANSITIONAL
EROSIONAL
BORED
DEFORMED

Cores

CORED INTERVAL
AND CORE
NUMBER
RECOVERY
NO RECOVERY

Miscellaneous

THIN SECTION
P & P ANALYSIS
SEM

Rock Classification

QUARTZ
FELDSPAR
ROCK FRAGMENTS

AGE STRATIGRAPHIC UNIT	ENVIRONMENT	S.P./GAMMA RAY	DEPTH, THICKNESS	LITHOLOGY	SEDIMENTARY STRUCTURES	COLOR	GRAIN SIZE	SORTING	POROSITY	CONSTITUENTS	ROCK CLASSIFICATION	SAMPLE	REMARKS
			2750										Sd:brn, f to grnd,carb incl clay calsts, sm to med sc x-b
		ELECTRIC LOG UNAVAILABLE	2800		M								Sh:gry,slty lam d:brn,incr in clay clasts, tr sider clas mica,dd oil stn at base
			2850										

Petrologic Log

Company SINCLAIR OIL and GAS

Well Location CUSHING COOP S-1, 3-17N-7E

GRAIN SIZE
AVG-) MAX (-
POROSITY
P PRIMARY
S SECONDARY
M MICROPOROSITY

CONSTITUENTS
QUARTZ
FELDSPAR
ROCK FRAGMENTS
CLAY & CARBONATE
FOSSILS
INVERTEBRATES & ALGAE
CLAY MINERALS
CARBONATE
SILICA
SULFIDES
SULFATES
MICA

Lithology

- CLAY / CLAYSTONE
- SILTY CLAYSTONE / MUDSTONE
- SILT / SILTSTONE
- SAND / SANDSTONE
- INTERBEDDED SANDSTONE / MUDSTONE
- MUDDY SANDSTONE
- CONGLOMERATE
- LIMESTONE
- MARL
- DOLOMITE
- DOLOMITIC ROCKS
- GYPSUM / ANHYDRITE
- GYPSIFEROUS ROCKS
- HALITE
- CHERT
- CHERTY ROCKS
- COAL / LIGNITE
- VOLCANIC ROCKS
- INTRUSIVE ROCKS
- METAMORPHIC ROCKS

Bedding(B)-Laminae(L)

- MASSIVE
- HORIZONTAL
- INITIAL SLOPE / DIP
- GRADED
- CROSS BEDDING (DUNES WAVES)

Surface-Features

- RIPPLE LAMINAE
- CURRENT SOLEMARKS
- *Surface-Related

Deformed Features

- FLOWAGE(F) FAULTE DIF bl LOAD(L)
- WATER ESCAPE
- DISRUPTED

Organic

- BURROW TRACE FOSSIL
- BIOTURBATED
- ROOT TRACES

Chemical

- CONCRETIONS
- STYLOLITES

Contacts of Strata

- ABRUPT
- TRANSITIONAL
- EROSIONAL
- BORED
- DEFORMED

Cores

- CORED INTERVAL AND CORE NUMBER
- RECOVERY
- NO RECOVERY

Miscellaneous

- THIN SECTION
- P & P ANALYSIS
- SEM

Rock Classification

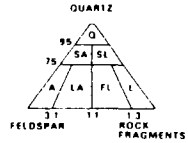

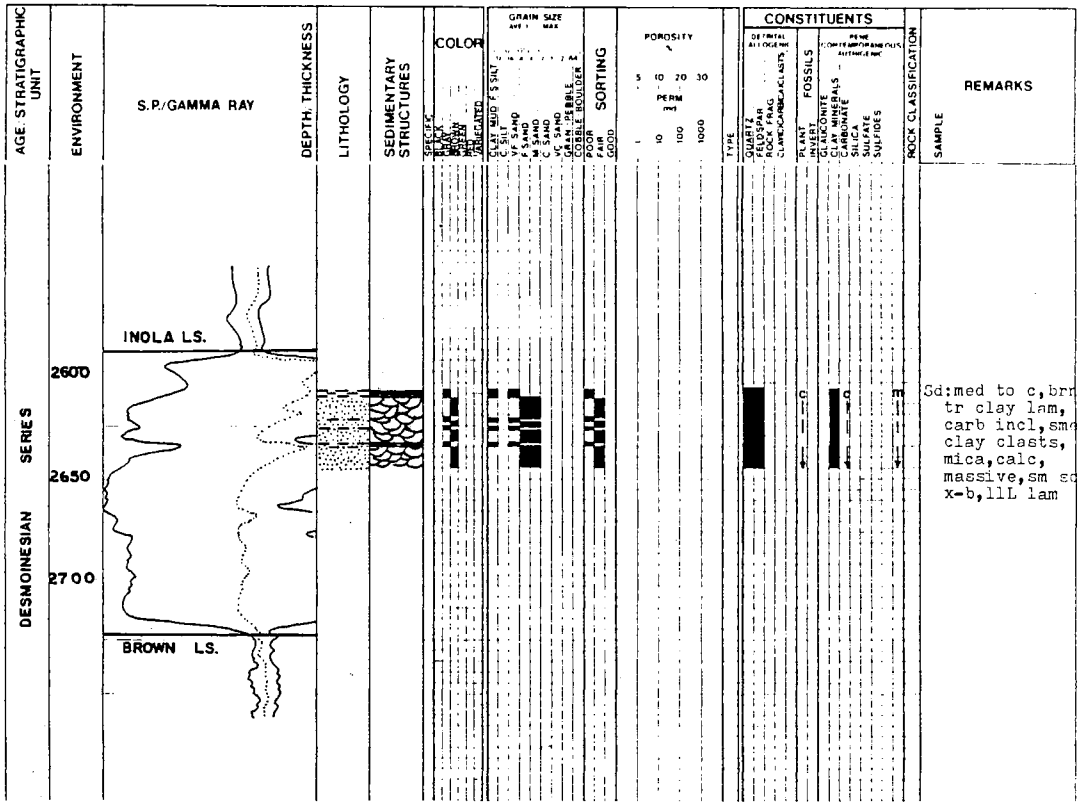

Petrologic Log

Company SINCLAIR OIL & GAS

Well Location P. BROWN No. 8, 34-17N-7E

GRAIN SIZE
AVG) MAX
POROSITY
P PRIMARY
S SECONDARY
M MICROPOROSITY

CONSTITUENTS
QUARTZ
FELDSPAR
ROCK FRAGMENTS
CLAY & CARBONATE
FOSSILS
INVERBRATES & ALGAE
CLAY MINERALS
CARBONATE
SILICA
SULFIDES
MICA

Lithology

CLAY / CLAYSTONE
SILTY CLAYSTONE / MUDSTONE
SILT / SILTSTONE
SAND / SANDSTONE
INTERBEDDED SANDSTONE / MUDSTONE
MUDDY SANDSTONE
CONGLOMERATE
LIMESTONE
MARL
DOLOMITE
OOLOMITIC ROCKS
GYPSUM / ANHYDRITE
GYPSIFEROUS ROCKS
HALITE
CHERT
CHERTY ROCKS
COAL / LIGNITE
VOLCANIC ROCKS
INTRUSIVE ROCKS
METAMORPHIC ROCKS

Bedding(B)-Laminae(L)

MASSIVE
HORIZONTAL
INITIAL SLOPE / DIP
GRADED
CROSS BEDDING (DUNES WAVES)

Surface-Features

RIPPLE LAMINAE
CURRENT SOLEMARKS
*Surface-Related

Deformed Features

FLOWAGE(F)
FAULTED(F)
LOADED
WATER ESCAPE
DISRUPED

Organic

BURROW TRACE FOSSIL
BIOTURBATED
ROOT TRACES

Chemical

CONCRETIONS
STYLOLITES

Contacts of Strata

ABRUPT
TRANSITIONAL
EROSIONAL
BORED
DEFORMED

Cores

CORED INTERVAL AND CORE NUMBER
RECOVERY
NO RECOVERY

Miscellaneous

THIN SECTION
P & P ANALYSIS
SEM

Rock Classification

QUARTZ
FELDSPAR
ROCK FRAGMENTS

AGE, STRATIGRAPHIC UNIT	ENVIRONMENT	S.P./GAMMA RAY	DEPTH, THICKNESS	LITHOLOGY	SEDIMENTARY STRUCTURES	COLOR	GRAIN SIZE	SORTING	POROSITY	CONSTITUENTS	ROCK CLASSIFICATION	SAMPLE	REMARKS
DESMOINESIAN SERIES		2750 INOLA LS. 2800											Sd:vf to f grn brn,carb incl tr clay lam, mica,tr hem, tr sider clasts,sl calc

Petrologic Log

Company SINCLAIR OIL & GAS

Well Location P. BROWN No. 9, 33-17N-7E

GRAIN SIZE
AVG \ MAX
POROSITY
P PRIMARY
S SECONDARY
M MICROPOROSITY

CONSTITUENTS
QUARTZ
FELDSPAR
ROCK FRAGMENTS
CLAY & CARBONATE
FOSSILS
INVERBRATES & ALGAE
CLAY MINERIALS
CARBONATE
SILICA
SULFIDES
SULFATES
MICA

Lithology

CLAY
CLAYSTONE
SILTY CLAYSTONE
MUDSTONE
SILT/
SILTSTONE
SAND/
SANDSTONE
INTERBEDDED
SANDSTONE/
MUDSTONE
MUDDY
SANDSTONE
CONGLOMERATE
LIMESTONE
MARL
DOLOMITE
DOLOMITIC
ROCKS
GYPSUM/
ANHYDRITE
GYPSIFEROUS
ROCKS
HALITE
CHERT
CHERTY
ROCKS
COAL/
LIGNITE
VOLCANIC
ROCKS
INTRUSIVE
ROCKS
METAMORPHIC
ROCKS

Bedding(B)-Laminae(L)

MASSIVE
HORIZONTAL
INITIAL SLOPE/
DIP
GRADED
CROSS BEDDING
(DUNES WAVES)

Surface-Features

RIPPLE LAMINAE
CURRENT SOLEMARKS
*Surface-Related

Deformed Features

FLOWAGE(F)
FAULTED(Fa)
LOAD(L)
WATER ESCAPE
DISRUPED

Organic

BURROW TRACE
FOSSIL
BIOTURBATED
ROOT TRACES

Chemical

CONCRETIONS
STYLOLITES

Contacts of Strata

ABRUPT
TRANSITIONAL
EROSIONAL
BORED
DEFORMED

Cores

CORED INTERVAL
AND CORE
NUMBER
RECOVERY
NO RECOVERY

Miscellaneous

THIN SECTION
P & P ANALYSIS
SEM

Rock Classification

QUARTZ
FELDSPAR
ROCK FRAGMENTS

AGE, STRATIGRAPHIC UNIT	ENVIRONMENT	S.P. GAMMA RAY	DEPTH, THICKNESS	LITHOLOGY	SEDIMENTARY STRUCTURES	COLOR	GRAIN SIZE	SORTING	POROSITY	CONSTITUENTS	ROCK CLASSIFICATION	SAMPLE	REMARKS
DESMOINESIAN SERIES	2700												Sh:gry,blk,fiss Sd: f to med grnd,carb incl mica,clay clasts,sm to med sc x-b, Calc concretion Sh:gry,blk,fiss
	2750												
	2800												

VITA

Erik Paul Mason

Candidate for the Degree of

Master of Science

Thesis: THE PETROLOGY, DIAGENESIS AND DEPOSITIONAL ENVIRONMENT OF THE BARTLESVILLE SANDSTONE IN THE CUSHING OIL FIELD, CREEK COUNTY, OKLAHOMA

Major Field: Geology

Biographical:

Personal: Born in Quincy, Illinois, the son of Paul and Pat Mason.

Education: Received Bachelor of Arts degree in Geology, December, 1976, from Principia College, Elsah, Illinois; completed requirements for the Master of Science degree at Oklahoma State University in December, 1982.

Professional Experience: Wellsite Geologist for Exploration Logging, Mid-Continent U.S.A. 1977-79. Pressure Detection Engineer for Exploration Logging (South America), 1979-81; Geologist, Union Oil Company of California (Oklahoma City), summer 1981.

STRUCTURAL CONTOUR MAP–TOP, INOLA LIMESTONE
CUSHING OIL FIELD
CREEK COUNTY, OKLAHOMA

R7E

T19N

T18N

T17N

T16N

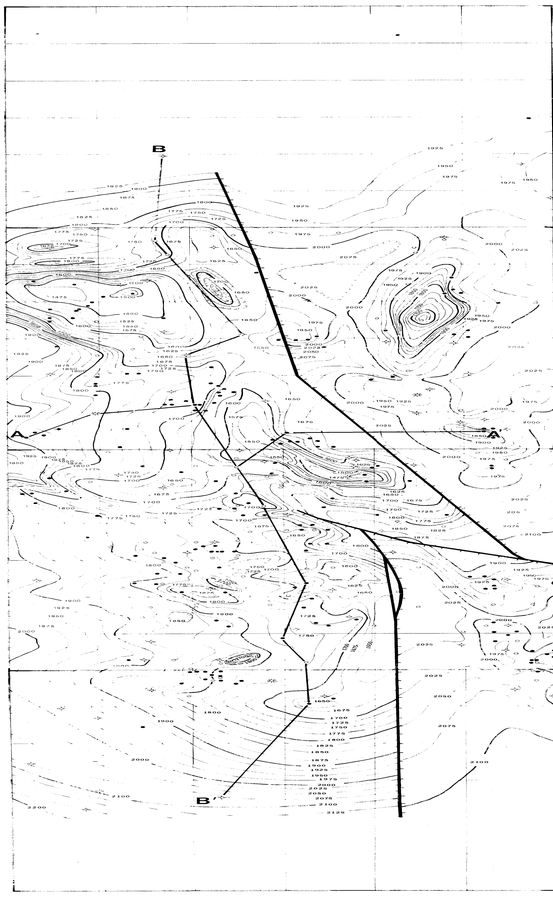

MAP SCALE : 2 INCHES=1 MILE

CONTOUR INTERVAL : 25 FEET

EAST-WEST STRATIGRAPHIC CROSS-SECTIONS
CC', DD', EE'
CUSHING OIL FIELD, CREEK COUNTY, OKLAHOMA

ERIK MASON M.S. THESIS 1982

LEGEND

● OIL ⊖ DRY and ABANDONED

✹ OIL and GAS ○ PRODUCTION INFORMATION UNAVAILABLE

SHALE SANDSTONE LIMESTONE

VERTICAL SCALE: 1 inch = 100 feet

HORIZONTAL SCALE: NONE

NOTE: Refer to index map for cross-section locations

DATUM — INOLA LIMESTONE

PLATE 2a

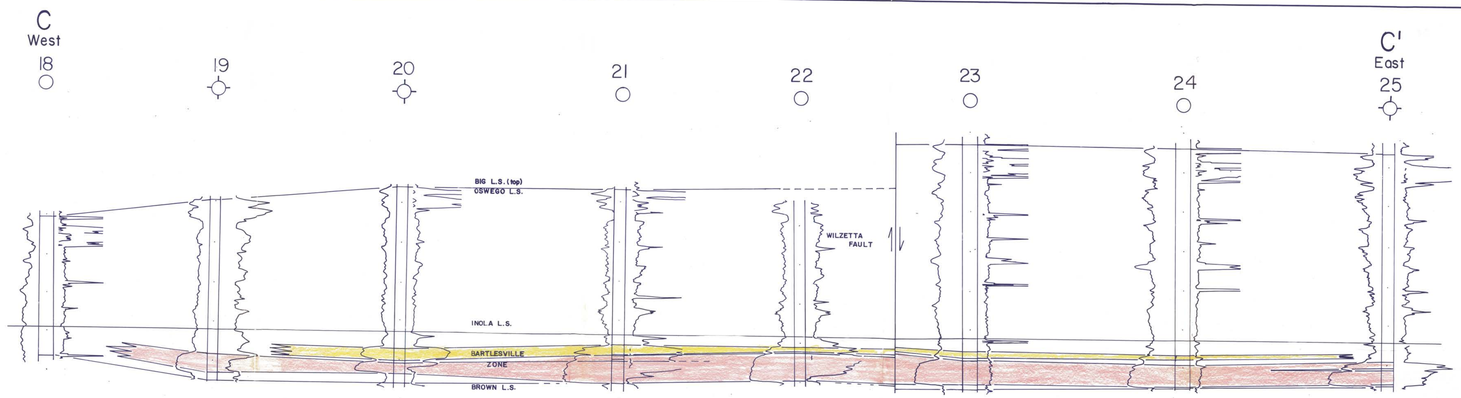

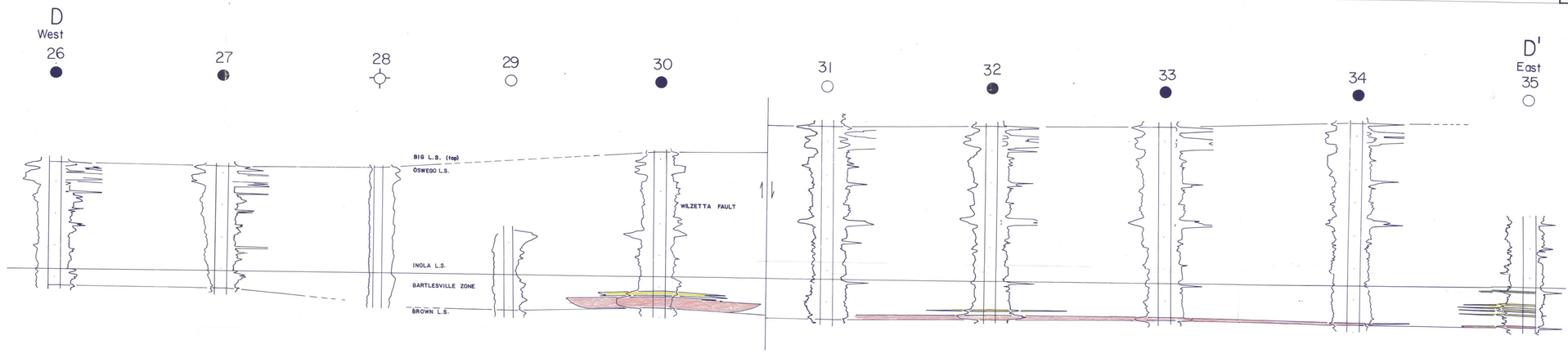

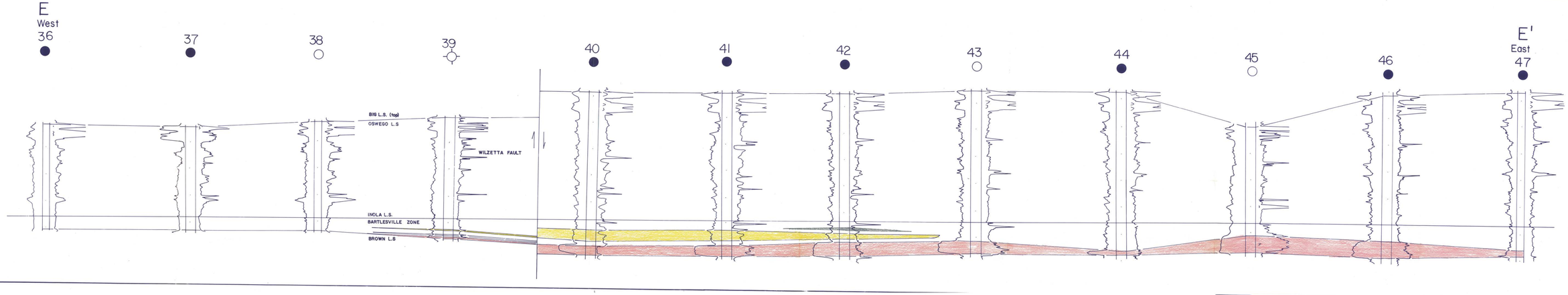

EAST-WEST STRATIGRAPHIC CROSS SECTIONS
FF', GG', HH'
CUSHING OIL FIELD, CREEK COUNTY, OKLAHOMA

ERIK MASON M.S. THESIS 1982

LEGEND

● OIL ⊹ DRY and ABANDONED

✹ OIL and GAS ○ PRODUCTION INFORMATION UNAVAILABLE

SHALE SANDSTONE LIMESTONE

VERTICAL SCALE: 1 inch = 100

HORIZONTAL SCALE: NONE

DATUM—INOLA LIMESTONE

NOTE: Refer to index map for cross-section locations

PLATE 2b

F West — F' East

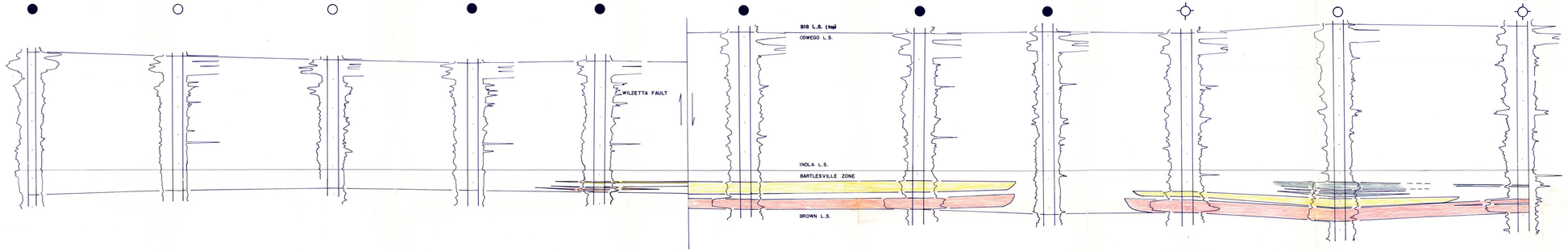

G West — G' East

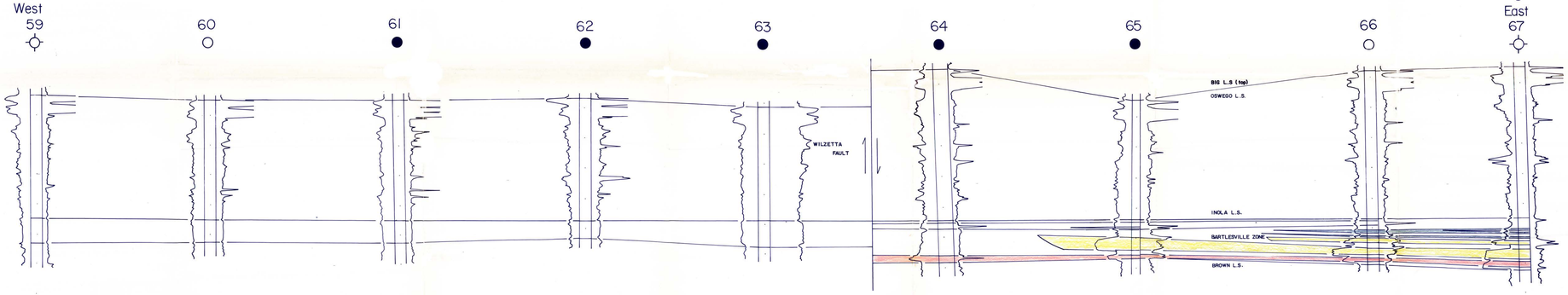

H West — H' East

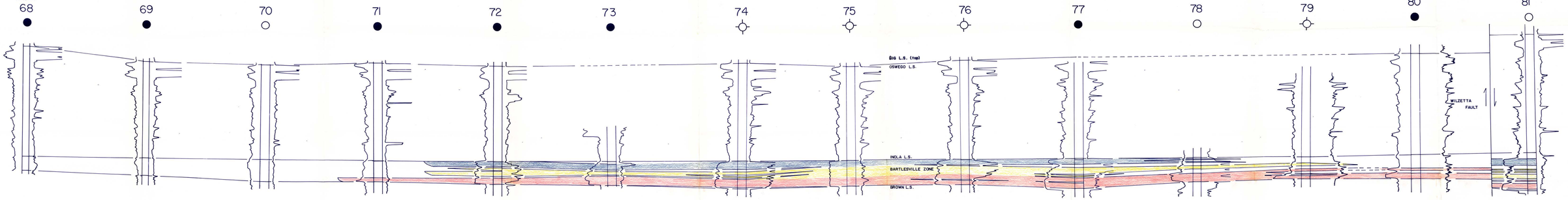

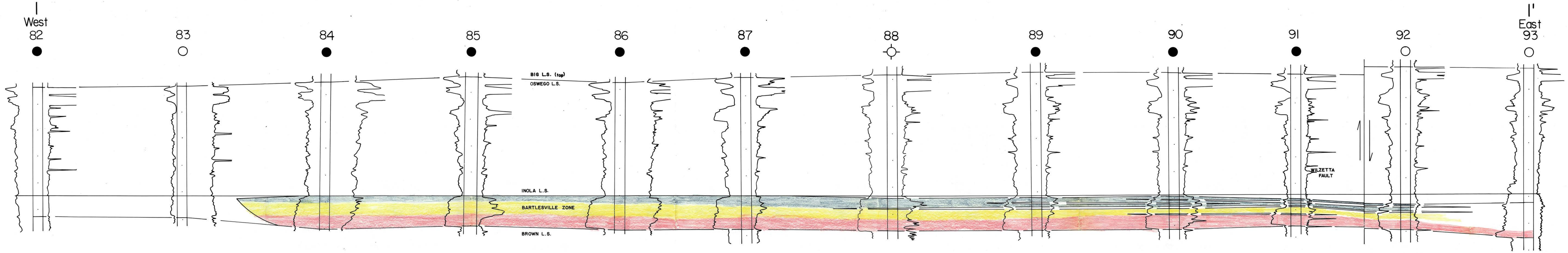

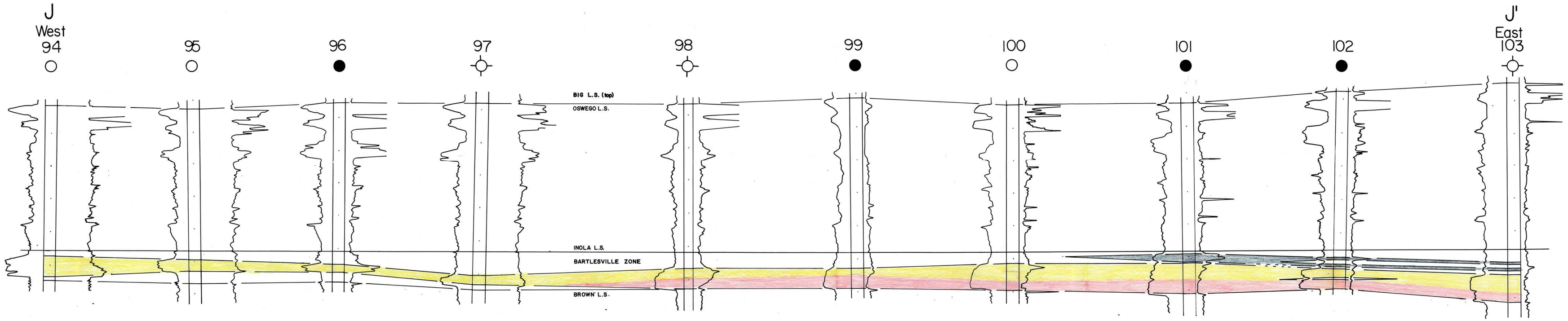

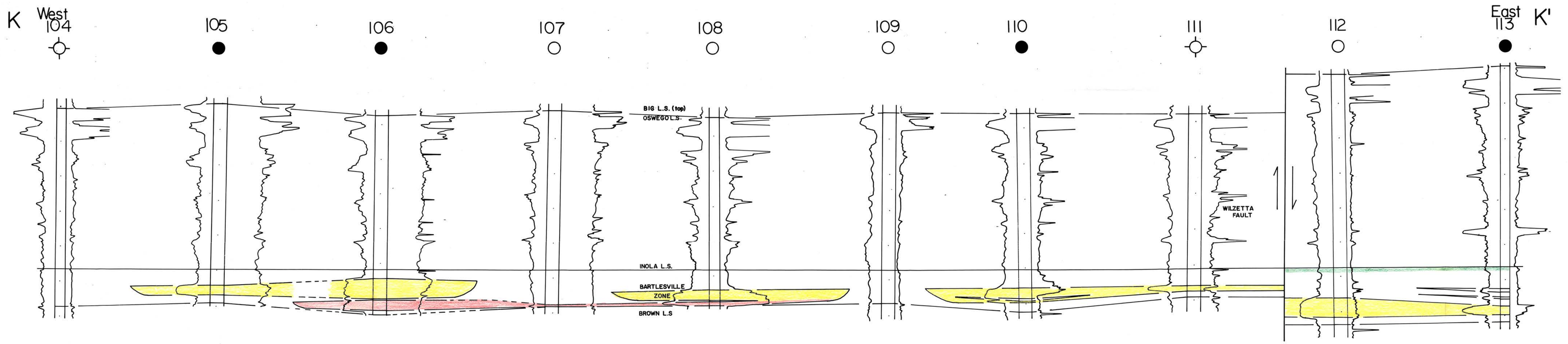

EAST WEST STRATIGRAPHIC CROSS SECTIONS
I I', J J', K K'
CUSHING OIL FIELD, CREEK COUNTY, OKLAHOMA

ERIK MASON M.S. THESIS 1982

LEGEND

● OIL ⊖ DRY and ABANDONED

✸ OIL and GAS ○ PRODUCTION INFORMATION UNAVAILABLE

SHALE SANDSTONE LIMESTONE

VERTICAL SCALE: 1 inch = 100 feet

HORIZONTAL SCALE: NONE

DATUM — INOLA LIMESTONE

NOTE: Refer to index map for cross section locations

PLATE 2c

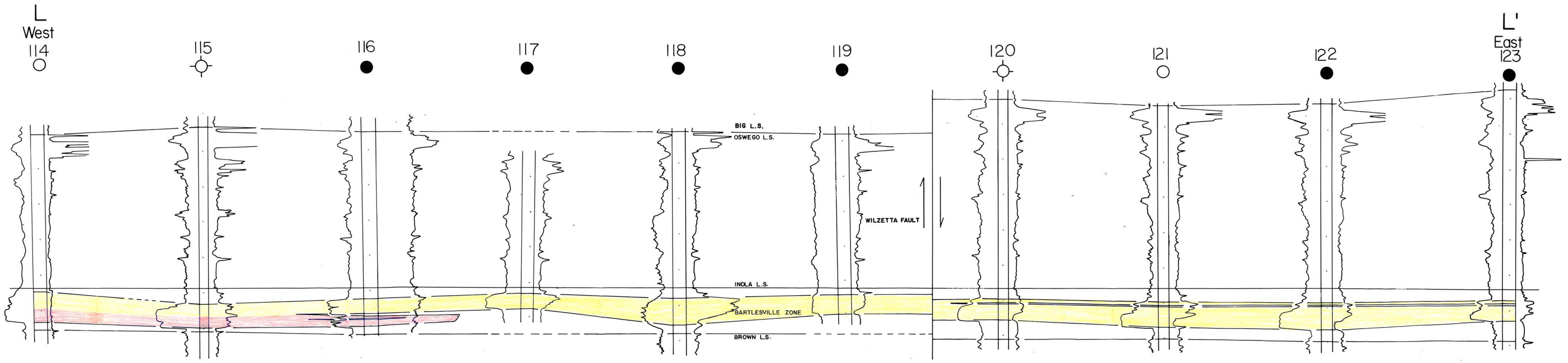

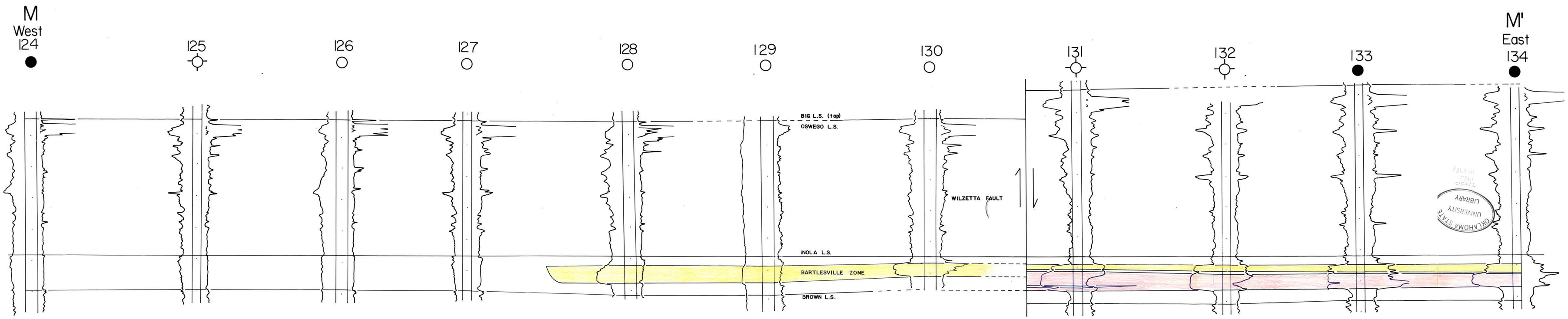

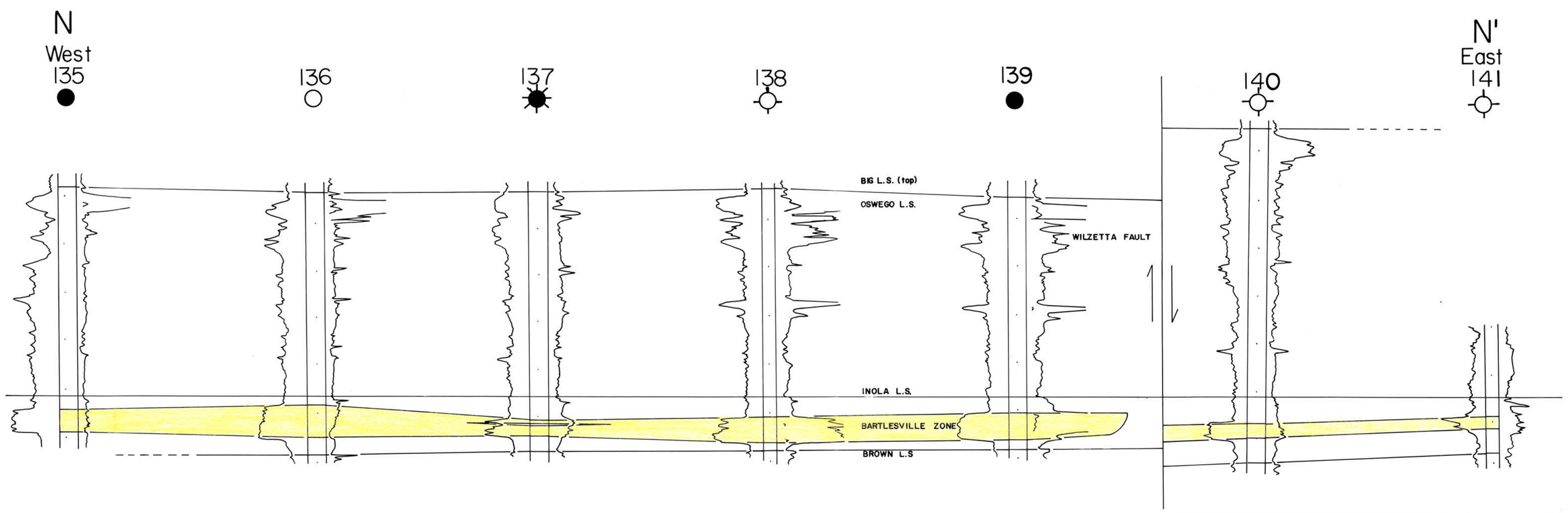

EAST WEST STRATIGRAPHIC CROSS SECTIONS
LL', MM', NN'
CUSHING OIL FIELD, CREEK COUNTY, OKLAHOMA

ERIK MASON M.S. THESIS 1982

LEGEND

● OIL ⊖ DRY and ABANDONED

✱ OIL and GAS ○ PRODUCTION INFORMATION UNAVAILABLE

SHALE SANDSTONE LIMESTONE

VERTICAL SCALE: 1 inch = 100 feet

HORIZONTAL SCALE: NONE

DATUM—INOLA LIMESTONE

NOTE: Refer to index map for cross section locations

PLATE 2d

NORTH - SOUTH STRUCTURAL CROSS-SECTION
CUSHING OIL FIELD, CREEK COUNTY
OKLAHOMA
PLATE 3a

B
North

B'
South

7 8 9 10 11 12 13 14 15 16 17

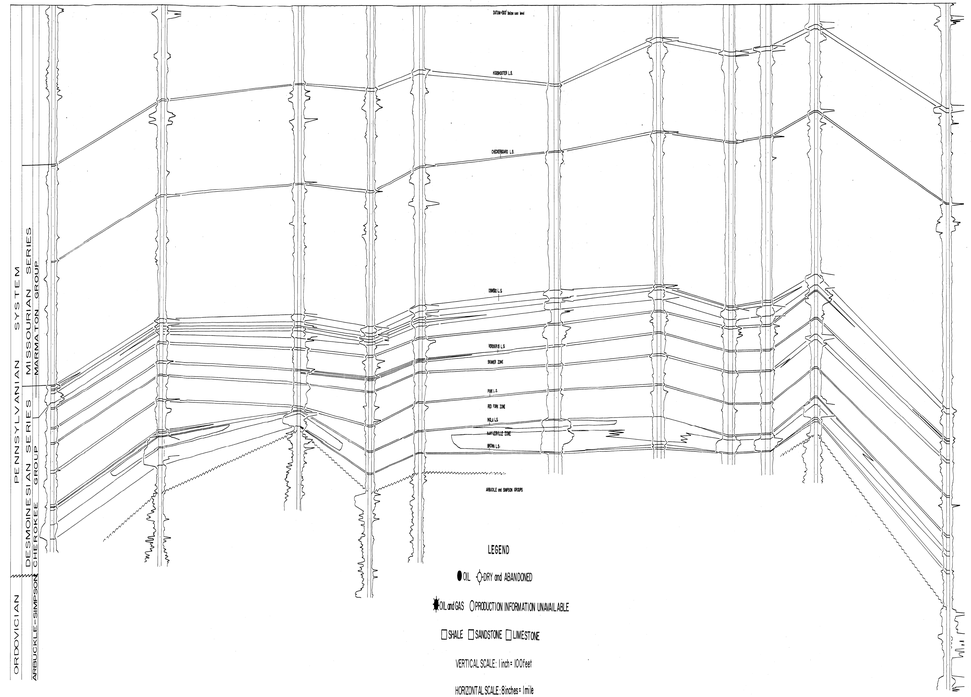

LEGEND

● OIL ◇ DRY and ABANDONED

✸ OIL and GAS ○ PRODUCTION INFORMATION UNAVAILABLE

□ SHALE □ SANDSTONE □ LIMESTONE

VERTICAL SCALE: 1 inch = 100 feet

HORIZONTAL SCALE: 8 inches = 1 mile

OFR 84228 K.S. 1983 BE

EAST - WEST STRUCTURAL CROSS SECTION

CUSHING OIL FIELD, CREEK COUNTY

OKLAHOMA

PLATE 3b

A

West

A'

East

1 2 3 4 5 6

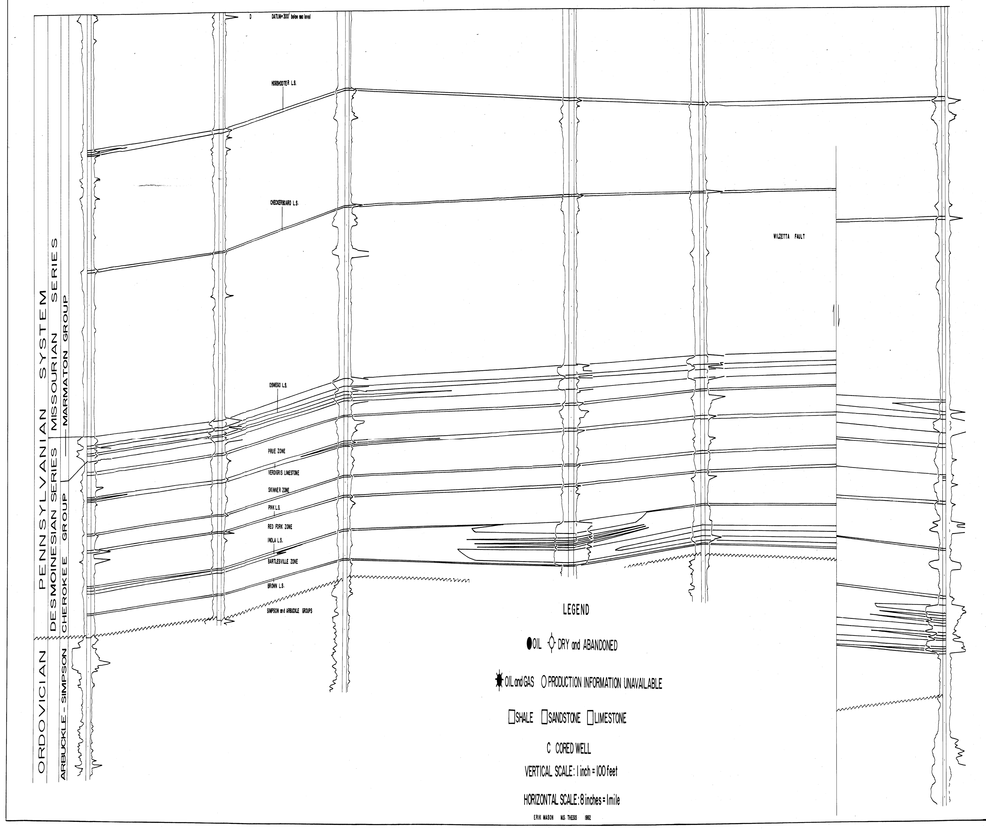

TOTAL ISOPACH, BARTLESVILLE ZONE *

CUSHING OIL FIELD
CREEK COUNTY, OKLAHOMA

R7E

T19N

T18N

T17N

T16N

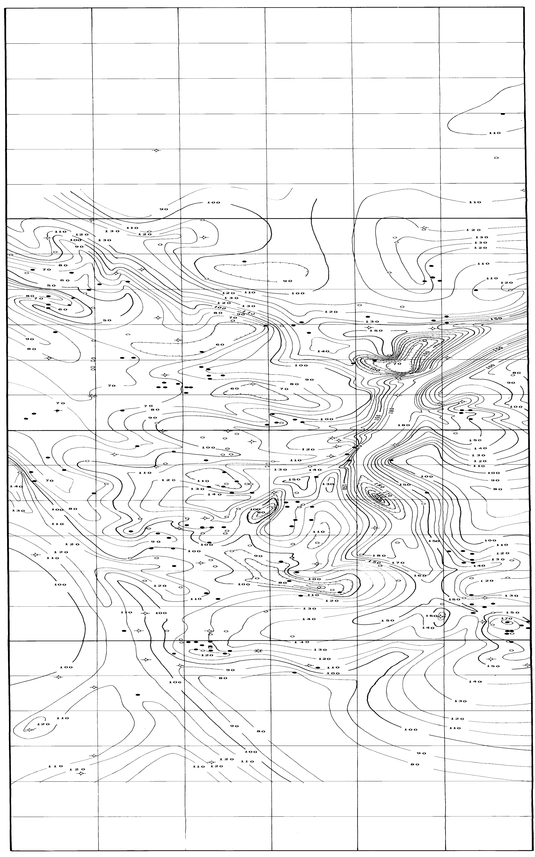

MAP SCALE: 2 INCHES = 1 MILE
CONTOUR INTERVAL : 10 FEET

* THE BARTLESVILLE SAND ZONE IS THE INTERVAL BETWEEN THE INOLA AND BROWN LIMESTONES.

NET SANDSTONE THICKNESS MAP
BARTLESVILLE ZONE *

CUSHING OIL FIELD
CREEK COUNTY, OKLAHOMA

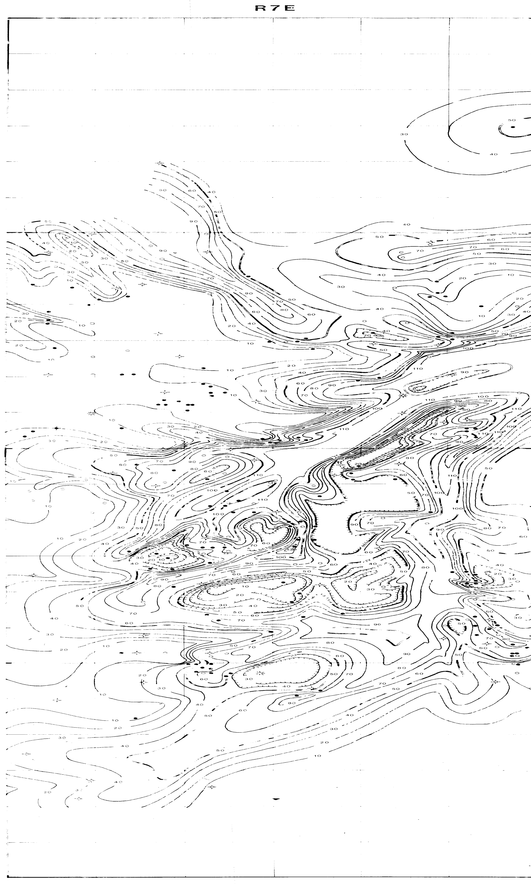

MAP SCALE: 2 INCHES = 1 MILE
CONTOUR INTERVAL: 10 FEET

* THE BARTLESVILLE SAND ZONE IS THE INTERVAL BETWEEN THE INOLA AND BROWN FORMATIONS.

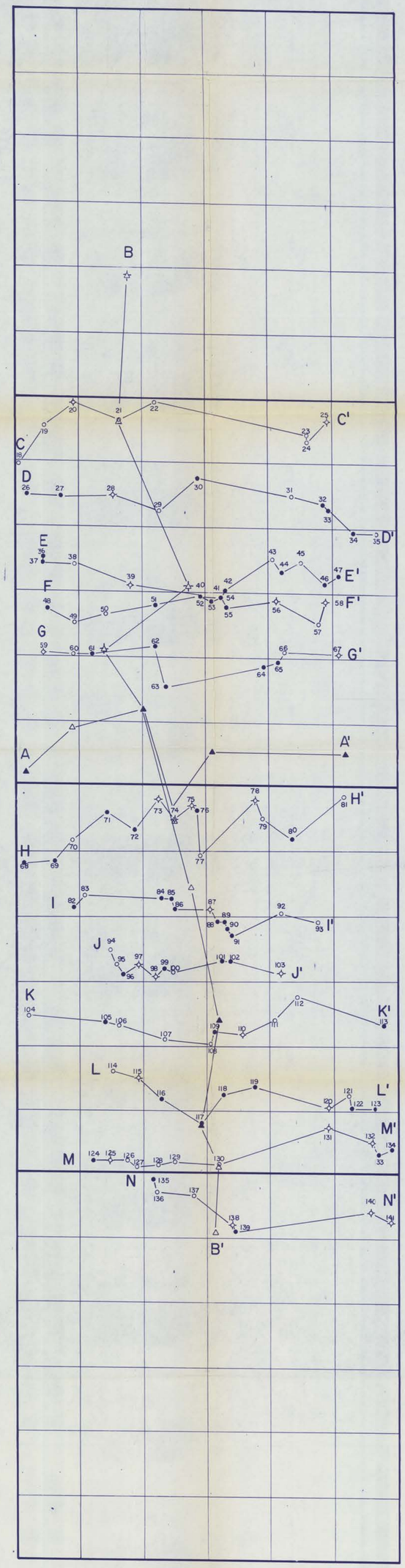

19N

18N

17N

16N

7E

Index map showing cross-section locations.

Legend

- dry hole (stratigraphic cross sections)
- ○ no data (" " ")
- ● oil well (" " ")
- dry hole (structural cross sections)
- △ no data (" " ")
- ▲ oil well (" " ")

Scale: 1 inch = .80 miles

ERIK MASON M.S. THESIS
1982